Tetraquarks in large-Nc QCD

Wolfgang Lucha, Dmitri Melikhov, Hagop Sazdjian

Version of Record: https://www.sciencedirect.com/science/article/pii/S0146641021000211
Manuscript_9039a65fe933d5acc72ca94f7ffa4d4c

Tetraquarks in large-N_c QCD

Wolfgang Lucha[a], Dmitri Melikhov[b,c,d], Hagop Sazdjian[e,*]

[a] *Institute for High Energy Physics, Austrian Academy of Sciences, Nikolsdorfergasse 18, A-1050 Vienna, Austria*
[b] *D. V. Skobeltsyn Institute of Nuclear Physics, M. V. Lomonosov Moscow State University, 119991 Moscow, Russia*
[c] *Joint Institute for Nuclear Research, 141980 Dubna, Russia*
[d] *Faculty of Physics, University of Vienna, Boltzmanngasse 5, A-1090 Vienna, Austria*
[e] *Université Paris-Saclay, CNRS/IN2P3, IJCLab, 91405 Orsay, France*

Abstract

The generalization of the color gauge group SU(3) to SU(N_c), with N_c taking arbitrarily large values, as had been proposed and developed by 't Hooft, has allowed for a decisive progress in the understanding of many qualitative, as well as quantitative, aspects of QCD in its nonperturbative regime. In particular, the notion of valence quarks receives there a precise meaning. The present work reviews the various aspects of the extension of this approach to the case of tetraquark states, which are a category of the general class of exotic states, also called multiquark states, whose internal valence-quark structure does not match with that of ordinary hadrons, and which have received, in recent years, many experimental confirmations. The primary question of describing, or probing, on theoretical grounds, multiquark states is first examined. The signature of such states inside Feynman diagrams in relation with their singularities is highlighted. The main mechanisms of formation of tetraquark states, provided by the diquark model and the molecular scheme, are considered together with their specific implications. The properties of tetraquark states at large N_c are analyzed through the Feynman diagrams that describe two-meson scattering amplitudes. It turns out that, in that limit, the possible formation of tetraquark states is mainly due to the mutual interactions of their internal mesonic clusters. These essentially arise from the quark-rearrangement, or quark-interchange, mechanism. In coupled-channel meson-meson scattering amplitudes, one may expect the occurrence of two independent tetraquark states, each having priviledged couplings with the two mesons of their dominant channel. The question of the energy balance of various schemes in the static limit is also analyzed. The clarification of the mechanisms that are at work in the formation of tetraquarks is the main outcome from the large-N_c approach to this problem.

Keywords: QCD, tetraquarks, large N_c, multiquark operators

Contents

*Corresponding author
Email addresses: wolfgang.lucha@oeaw.ac.at (Wolfgang Lucha), dmitri_melikhov@gmx.de (Dmitri Melikhov), sazdjian@ijclab.in2p3.fr (Hagop Sazdjian)

1. Introduction

The possibility of the existence of exotic hadrons, containing more valence quarks and antiquarks than a quark-antiquark pair for mesons and three quarks for baryons, had been considered since the early days of the quark model [1, 2]. The lack of experimental data about these hypothetical objects during the following decades has pushed them for a long time into a marginal situation. However, with the advent of Quantum Chromodynamics (QCD) as a theory of strong interactions, with the fundamental properties of asymptotic freedom and confinement [3–5], the road was open for detailed theoretical investigations on the subject [6, 7].

Progress has been achieved for the last two decades when several experiments have been able to detect, with sufficient precision, many candidates to represent exotic hadrons, the latter not being matched with the quantum numbers or the constituent content of the usual quark model [8–19]. These discoveries stimulated in turn vast theoretical investigations in order to understand and interpret the detailed dynamics that give rise to their existence. General accounts of them can be found in recent review articles [20–31].

While in the framework of QCD theory one explains in a satisfactory way the spectrum and transition properties of ordinary hadrons [32–42], the problem of exotic hadrons comparatively encounters additional difficulties. In QCD, which is a non-Abelian gauge theory, observable quantities must be color gauge invariant. This naturally explains why quarks and gluons, the building blocks of the theory, are not individually observed in nature; only color-singlet objects, actually represented by the ordinary hadrons, which are bound states of quarks and gluons, are detected as free particles. This property is commonly depicted by the term "confinement of quarks and gluons". It should be emphasized, however, that the term confinement has here a stronger meaning than the terms "color screening", also used in the literature. The bound states of quarks and gluons do not resemble the positronium- or hydrogen-like bound states of Quantum Electrodynamics (QED). Hadrons, which, in principle, are infinite in number, have masses squared that increase linearly with respect to their spin, lying along "Regge trajectories" [43–47]. This is due to the fact that the potential energy of the binding forces increases with respect to the mutual distances between quarks and/or gluons [48, 49]. However, the confining forces are only operative between colored objects or within color-singlet objects.

There are no confining or long-range van der Waals forces that would operate between hadrons. The latter mutually interact by means of short-range forces, represented by contact terms or meson-exchange terms[1].

The color gauge invariance principle should also apply to the constitution of exotic hadrons, also called "multiquark states". However, one realizes here that color-singlet multiquark states can easily be generated by products or combinations of products of free or interacting ordinary hadron states [50]. Since ordinary hadrons mutually interact by means of short-range forces (cf. footnote above), one should not find in that case spectra similar to that of the confining interactions found earlier in QCD. Rather, one would have loosely bound states, or corresponding resonances, typical of molecular or nuclear states, whose illustrated representative is the deuteron [51–54].

The existence of molecular-type exotic hadrons does not *a priori* exclude the formation of exotic hadrons by means of confining forces acting directly on the quarks and gluons. In such a case, one would expect to obtain bound states of compact size, due to the confining nature of all the operative forces. Such states are also designated as "compact exotic hadrons", in contradistinction to the "molecular states".

The eventual existence of compact multiquark states would implicitly mean that they are color or cluster irreducible, in the sense that they cannot be decomposed as combinations of products of simpler color gauge invariant states, which are the usual hadronic states. This basic property does not seem, however, realizable. When the multiquark generating operators or sources are expressed in local form, they can always be reexpressed, by means of Fierz rearrangements, as combinations of products of ordinary hadronic currents [50]. More generally, even when the multiquark operators take a multilocal form with the aid of gauge links, the color or cluster reducibility phenomenon continues to occur [55]. This means that, on formal grounds, compact multiquark states are not the most favored outcome of the exotic hadron construction. To ensure their existence on theoretical grounds, one should be able to find underlying dynamical mechanisms that ensure their stability against the natural forces of dislocation, represented by the formation of internal hadronic clusters.

The primary mechanism that might operate for the formation of compact multiquark states is the "diquark" one [7, 56], which has been first utilized in the study of baryon spectroscopy [57–59]. It is based on the observation that in SU(3), the color gauge group underlying QCD, the fundamental representation to which the quarks are belonging is the triplet **3**; therefore, two quarks belong either to the antitriplet representation $\overline{\mathbf{3}}$, which is antisymmetric, or to the sextet representation **6**, which is symmetric. The forces that act between the quarks are generally attractive in the $\overline{\mathbf{3}}$ representation and will have the tendancy to form bound states of diquarks, which, in the case of compact sizes, will behave as nearly pointlike antiquarks, thus in turn being attracted by a third quark.

The idea of the diquark mechanism has naturally been extended to the case of exotic hadrons [60–63], giving rise to detailed investigations [64–72]. This model, associated with approximate flavor symmetry and flavor independence of the confining forces, generally predicts, in the case of existence of exotic hadrons, several flavor multiplets of such states.

On the other hand, the effective forces that operate for the formation of molecular-type states are more dependent on the quark flavors and hence may not predict as many flavor multiplets as the diquark mechanism. One of the salient features of the molecular picture is its tendancy to predict bound states lying near the two-hadron threshold.

The difficulties encountered in clearly predicting the domains or conditions of existence of each category of exotic hadrons, compact or molecular, are intimately related to the fact that QCD theory is characterized by having a nonperturbative regime at large distances, which is not yet analytically solved. Efficient tools are provided through the recognition of approximate symmetries and the use of related effective field theories, among which one may quote chiral perturbation theory [73–76], heavy-quark effective theories [77–81] and effective theories involving nucleons [82–89]. Nonrelativistic effective field theories, aimed at studying bound-state properties, have been first developed in Ref. [90] and later completed under the name of "potential nonrelativistic QCD" in Ref. [91]. Other analytic approaches are forced to hinge on simplifying models, which in turn are subjected to theoretical debates.

For the time being, lattice theory remains one of the most powerful tools for the solution of QCD in its nonperturbative regime. It is essentially based on a numerical approach, discretizing the continuum of spacetime over

[1]The terms "long-range forces" and "short-range forces" are often used with different meanings in the literature. At the level of quark and gluon interactions, the long-range forces are represented by the confining forces and their residual van der Waals forces, while the short-range forces are those that operate by means of hadron exchanges or by contact interactions between hadrons. In the effective theories of hadrons, long-range forces are those that operate by meson exchanges (Yukawa-type forces), mostly by pion exchanges, while short-range forces are those resulting from contact interactions. We use, in the present work, the convention related to the quark and gluon interactions.

a euclidean finite-volume lattice [48, 92]. Lattice theory has also made decisive progress in the calculation of scattering amplitudes [93, 94]. Concerning the exotic hadrons, it has already provided many results, mainly in sectors containing two heavy quarks [95–109]. However, they are not all conclusive concerning the existence of tetraquarks. No evidence seems to be found, in general, in sectors with hidden or doubly-charm flavors [96–100, 105], except in [95, 107]. Open charm states are found in [108, 109]. The analysis of $bb\bar{b}\bar{b}$ systems does not seem conclusive [101, 106]. Evidence for deeply-bound states in doubly-bottom and open bottom-charm sectors with light quarks is found in [100, 102–104, 107]. (Other considerations for lattice theory calculations can be found in [110].)

Although the analyses of the internal structure of tetraquark candidates, found in lattice theory calculations, are not yet complete, a first-level information may be obtained from the overlap coefficients between the energy levels and the interpolating operators that are implemented. The fact that there is little overlap with tetraquark-like operators might suggest a larger size for the state. More precise information about the size of the observed states could be obtained from the calculation of appropriate form factors.

Among the approaches for the analysis of the nonperturbative properties of QCD, the large-N_c limiting method, originally introduced by 't Hooft [111–113], has been proven to be one of the most fruitful ones. It consists in generalizing the color gauge group SU(3) of QCD to the more general case of SU(N_c), with N_c considered as a parameter. It turns out that the large-N_c limit of the theory, associated with a scaling of the coupling constant as $g = O(1/\sqrt{N_c})$, has more simplifying features than in the finite-N_c case. The color-singlet parts of Feynman diagrams can then be classified according to their topological properties: it is the "planar" diagrams that are the dominant ones, while the other types of diagram can systematically be classified, according to their more complicated topology, within a perturbative expansion in $1/N_c$, as providing nonleading contributions.

This approach does not solve the theory, but allows, assuming that the large-N_c limit is a smooth one, a better understanding of some of its salient features. In this limit, the spectrum of the theory is essentially made of an infinite tower of free stable mesons, their mutual interactions occurring through nonleading effects in $1/N_c$ [114, 115]. This clearly shows that, in the hadronic world, the ρ-meson, for instance, is as elementary as the pion and could not be considered as a composite object of two pions [50]. Another outcome is a natural explanation of the OZI (Okubo, Zweig, Iizuka) rule [2, 116, 117], which asserts that leading strong interaction processes involving hadrons are those that have nonzero connecting quark lines between the initial and final states. Processes not satisfying this rule occur in nondominant orders of the $1/N_c$ expansion and are naturally subleading [114, 115]. The large-N_c limit brings also a natural explanation of the absence, at leading order, of the quark-antiquark sea inside hadrons and a theoretical support to Regge phenomenology [43–47], in which, in first approximation, hadronic processes are well described by tree diagrams with hadron exchanges [45].

The large-N_c approach to QCD has received much attention during the past decades in many phenomenological calculations related to hadronic physics. Its main virtue is to provide a theoretical basis for qualitative simplifications and for the understanding of the data.

The large-N_c limiting procedure has also been, over the last two decades, a decisive tool for new investigations in the search for possibly existing duality relations between gauge and string theories [118–124].

The purpose of the present article is to present a review of the main properties of the large-N_c approach, with emphasis put on its applications to exotic hadrons. Rather than focusing on particular candidates or particular data, our aim is to introduce the general aspects of the method, which might be applicable to a wide variety of situations.

The large-N_c analysis plays a crucial role in the recognition of those QCD Feynman diagrams that might contribute to the formation of exotic hadrons. It is in the large-N_c limit that the counting of the quark content of a hadronic state takes a systematic mathematical meaning, associated with the order of expansion with respect to $1/N_c$. However, a straightforward transposition to the case of exotic hadrons of results known from the large-N_c approach to ordinary hadrons might lead, in some cases, to wrong predictions. It is here that the analysis of the singularities of Feynman diagrams with respect to the quark content becomes of primary importance. This is usually done with the help of the Landau equations [125–127].

In summary, the large-N_c approach may be considered as one of the basic tools for a systematic investigation of the nonperturbative regime of QCD, with the objective of gaining complementary information with respect to other well-established approaches.

The paper is organized as follows. In Sec. 2, we present the general aspects of the large-N_c approach. Section 3 is devoted to a review of the various descriptions of exotic states by means of interpolating currents or multilocal operators. In Sec. 4, emphasis is put on the singularities of Feynman diagrams and the Landau equations for the

recognition of a possible presence of tetraquark states. Section 5 studies the properties of tetraquarks through the Feynman diagrams of meson-meson scattering amplitudes in terms of quark and gluon lines. Various cases of quark flavor contents are considered. In Sec. 6, some salient features of the molecular scheme, in relation with effective theories, are reviewed. In Sec. 7, the question of the reducibility of multiquark operators is considered and the energy balance of various configurations is studied in the static limit. The notion of geometric partitioning is introduced. A summary and concluding remarks follow in Sec. 8.

2. Large-N_c limit

2.1. General aspects

Quantum Chromodynamics is a non-Abelian gauge theory with the color gauge group SU(3), with three quark fields ψ^a ($a = 1, 2, 3$), belonging to the fundamental representation **3**, three antiquark fields $\overline{\psi}_b$ ($b = 1, 2, 3$), belonging to the antifundamental representation $\bar{\mathbf{3}}$ and eight gluon fields A^B_μ ($B = 1, \ldots, 8$), belonging to the adjoint representation **8** [3–5]. The primary, CP conserving, Lagrangian density, written in matrix form in color space and with N_f different quark flavors, reads

$$\mathcal{L} = -\frac{1}{2}\mathrm{tr}_c F_{\mu\nu}F^{\mu\nu} + \sum_{j=1}^{N_f} \overline{\psi_j}(iD_\mu\gamma^\mu - m_j)\psi_j, \tag{1}$$

where D is the covariant derivative, $D_\mu = 1\partial_\mu - igT^B A^B_\mu$, F is the field strength, $F_{\mu\nu} = (i/g)[D_\mu, D_\nu] = T^B F^B_{\mu\nu}$, g is the coupling constant and T^B are the generators of the gauge group in the fundamental representation, with normalization $\mathrm{tr}(T^A T^B) = (1/2)\delta^{AB}$. The quantization of the theory requires the introduction into the previous Lagrangian density of a gauge-fixing term together with a part containing auxiliary anticommuting scalar fields, the so-called Faddeev-Popov ghosts [127–131].

QCD has the property of asymptotic freedom, which asserts that the theory becomes almost free at short distances, or at high energies, while it becomes unstable at large distances, or at low energies. This is interpreted as the sign of a new regime, characterized by the confinement of the fundamental particles of the theory. One striking feature of the theory is that the coupling constant, which appears in the primary Lagrangian density (1), is not a free parameter: it is absorbed into the definition of the mass scale, usually denoted by Λ_{QCD} [132, 133], a phenomenon called "dimensional (or mass) transmutation". Actually, the mass of the proton is mainly determined by Λ_{QCD} and not by the masses of the quarks that enter into its constitution; even if the quarks were massless, the proton would continue having a mass of the order of its physical mass. This is in contrast to the behavior in the electroweak sector of the Standard Model, where the Higgs mechanism is at the origin of the mass scales. Therefore, the masses of the light quarks u, d, s do not play a major role in the theory and could, in many cases, be taken as zero.

The presence of a free parameter in a theory allows one to search for approximate solutions for some particular values of the parameter and then to apply perturbation theory around those values [134]. QED and the short-distance regime of QCD provide particular examples of this procedure, the expansion being realized around the free theory. 't Hooft observed that QCD possesses a hidden free parameter, represented by the dimension of the color gauge group SU(3), provided one considers it as part of the general class of non-Abelian gauge theories SU(N_c), with the particular physical value $N_c = 3$ of the parameter N_c [111]. He studied the limit of large values of N_c, with the quark fields belonging to the fundamental representation, which is of dimension N_c, and the gluon fields belonging to the adjoint representation, which is of dimension $(N_c^2 - 1)$, and showed that the theory in its nonperturbative regime becomes simplified in many instances.

A first glance of the effect of this limit can be taken at the level of the β-function, which displays the implicit mass-scale dependence of the coupling constant [4, 5, 135, 136] and which is a gauge and renormalization-group independent quantity up to two loops. At one-loop order it reads

$$\beta(g) \equiv \mu\frac{\partial g}{\partial \mu} = -\frac{1}{16\pi^2}\left(\frac{11}{3}N_c - \frac{2}{3}N_f\right)g^3, \tag{2}$$

where μ is the mass scale at which renormalization has been defined. Asymptotic freedom is realized for a negative value of β; this is indeed the case with the physical values $N_c = 3$ and $N_f = 6$. Taking now large values of N_c, while keeping N_f fixed, one notices that the negativity of β is strengthened. To ensure, however, a smooth limit, so that

$\Lambda_{\rm QCD}$ remains independent of N_c, one should admit that at the same time the coupling constant g scales with N_c like $N_c^{-1/2}$; the product $g^2 N_c$ then remains constant with respect to N_c:

$$g^2 N_c \equiv \lambda = O(N_c^0). \tag{3}$$

The corresponding β-function is, for large N_c,

$$\beta(\lambda) \equiv \mu \frac{\partial \lambda}{\partial \mu} = -\frac{11}{24\pi^2}\lambda^2 + O\Big(\frac{1}{N_c}\Big). \tag{4}$$

A similar conclusion is also obtained at the two-loop level.

Generally, the quark flavor number, N_f, manifests itself through quark-loop contributions. Equation (4) shows that in the large-N_c limit, with fixed N_f, the quark loop contributions are expected to be of nonleading order. This is one of the important qualitative simplifications that occur on practical grounds in the large-N_c limit.

Other types of large-N_c limits have also been considered in the past and presently for various purposes. The simultaneous limits of large values of N_c and N_f, with N_c/N_f fixed, has been considered by Veneziano [137]; it is evident, from the previous observation, that in that case the quark loops continue contributing to leading order. In another limiting procedure, one assumes that the quark fields belong to the second-rank antisymmetric tensor representation [138–141]; for $N_c = 3$, this representation is equivalent to the antitriplet one and therefore the physical content of actual QCD is not modified. For general N_c, the dimension of that representation is $N_c(N_c-1)/2$ and hence the number of degrees of freedom of the quark fields scale as N_c^2; this prevents the quark loops from disappearing from the leading order.

The above variants of the large-N_c limit have their own phenomenological advantages. We shall stick, however, in the present review, to the more traditional scheme developed by 't Hooft, because of its greater simplicity. Reviews about the large-N_c limit can be found in [23, 142–150].

2.2. Topological properties in color space

To study in more detail the properties of the theory in the large-N_c limit, it is advantageous to use a color two-index notation for the gluon fields [111]. Since they belong to the adjoint representation and the latter is contained in the direct product of the fundamental and antifundamental representations, one may represent the gluon fields with the notation $A^a{}_{b,\mu}$, its relationship with the conventional notation being the following:

$$A^a{}_{b,\mu} = (A^B_\mu T^B)^a{}_b, \qquad A^{a\dagger}{}_{b,\mu} = A^b{}_{a,\mu}, \qquad A^a{}_{a,\mu} = 0, \qquad a,b = 1,\ldots,N_c, \tag{5}$$

the third equation being a consequence of the property of the T's tracelessness. A similar notation can also be adopted for the ghost fields, which are introduced together with the gauge-fixing term in order to quantize the theory; however, for the simplicity of presentation, we shall not explicitly write down ghost fields in the remaining part of the paper, nor shall we draw the corresponding Feynman diagrams; their presence does not modify the main qualitative features that are drawn from the gluon fields.

With the above convention, the color contents of the quark and gluon propagators are

$$\langle \psi^a_{i,\alpha}(x)\overline{\psi}_{b,j,\beta}(y)\rangle = \delta_{ij}\delta^a{}_b S_{\alpha\beta}(x-y), \tag{6}$$

where i and j are flavor indices, α and β spinor indices, and S is the color-independent Dirac field propagator,

$$\langle A^a{}_{b,\mu}(x) A^c{}_{d,\nu}(y)\rangle = \Big(\delta^a{}_d\delta^c{}_b - \frac{1}{N_c}\delta^a{}_b\delta^c{}_d\Big) D_{\mu\nu}(x-y), \tag{7}$$

where D is the color-independent part of the gluon propagator. The term proportional to $1/N_c$ in the last equation ensures the traceless property of the gluon field. However, because of the factor $1/N_c$, it could be neglected in leading-order calculations; this amounts to replacing the gauge group SU(N_c) by U(N_c) and the (N_c^2-1) gluon fields by N_c^2 ones. The corresponding approximation is of order $1/N_c^2$ (cf. Ref. [142], Appendix C). This considerably simplifies the diagrammatic representation of the gluon propagator: as far as the color indices are concerned, the gluon propagates

Figure 1: The quark and gluon propagators in the conventional and the double-line representations, first and second columns, respectively. Lower indices are distinguished by bars.

as a quark-antiquark pair, which suggests a double-line representation for the gluon propagator. Figure 1 depicts, in two columns, the correspondence between the conventional and the double-line representations.

Concerning the interaction parts, they have structures of the following types: $\overline{\psi}_a \gamma^\mu A^a{}_{b,\mu} \psi^b$, $A^a{}_{b,\mu} A^b{}_{c,\nu} \partial^\mu A^{c,\nu}{}_a$, $A^a{}_{b,\mu} A^b{}_{c,\nu} A^{c,\mu}{}_d A^{d,\nu}{}_a$, quark flavor being conserved. One notices that a lower color index is always contracted with the upper index of a neighboring field and this ensures the continuity of lines arriving at a vertex and departing from it. The corresponding vertex diagrams are presented in Fig. 2 in both representations.

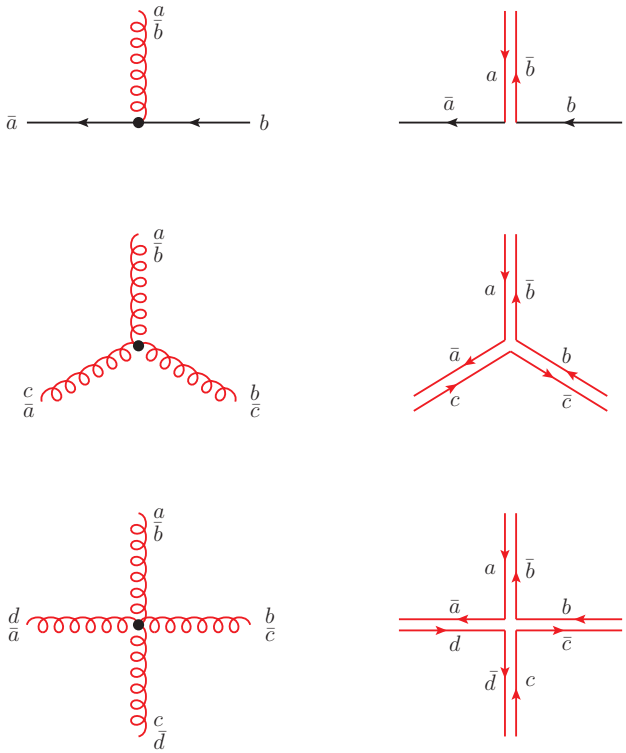

Figure 2: The quark-quark-gluon, three-gluon and four-gluon vertices in the conventional and the double-line representations, first and second columns, respectively. Lower indices are distinguished by bars.

The double-line representation allows a better control of the color flow inside Feynman diagrams. To have a first glance of it, we consider the two lowest-order contributions to the gluon self-energy, represented by a quark loop (Fig. 3a) and a gluon loop (Fig. 3b), respectively. Each color loop produces a factor N_c. The external gluon field color indices being fixed, diagram (a) does not have such a loop; furthermore, it contains two quark-quark-gluon vertices, each involving a coupling constant g; taking into account the large-N_c behavior of the latter [Eq. (3)], one finds that the

large-N_c behavior of diagram (a) is $O(N_c^{-1})$. On the other hand, diagram (b) contains one internal color loop, providing an additional factor N_c with respect to the previous diagram. Therefore, the large-N_c behavior of diagram (b) is $O(N_c^0)$. Thus, among the two diagrams of Fig. 3, it is diagram (b) which contributes to the leading-order behavior.

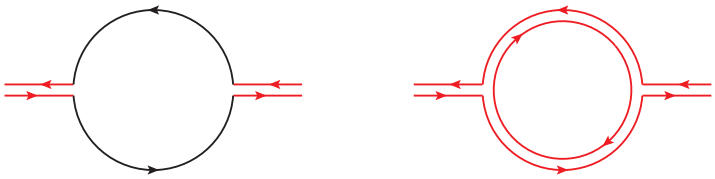

(a) $O(N_c^{-1})$ (b) $O(N_c^0)$

Figure 3: The lowest-order gluon self-energy contributions: (a) quark loop; (b) gluon loop. The corresponding orders in large-N_c behavior are also indicated.

The origin of the difference of contributions between the two diagrams can easily be understood: it is related to the distinct representations of the color group to which the quark and the gluon fields belong: one has N_c quarks in the fundamental representation against (N_c^2-1) gluons in the adjoint representation. At leading orders, internal gluon lines produce N_c times more contributions than quark lines, a feature that the double-line representation displays explicitly through the supplementary color loops. This means that, at leading orders, the quark loops, which actually are in N_f duplicates, can be neglected altogether, except when they appear as contractions of external quark lines. This is one of the main advantages of the large-N_c limiting procedure adopted by 't Hooft.

As a second example of the large-N_c counting rules, we consider, still in the gluon self-energy part, one-gluon exchange diagrams containing either a quark loop or a gluon loop (Fig. 4). Diagram (a) contains two color loops, producing a factor N_c^2, together with six vertices, producing a factor N_c^{-3} [Eq. (3)]. Its global behavior is therefore $O(N_c^{-1})$. Diagram (b) has one additional color loop and thus its behavior is $O(N_c^0)$. One again verifies the general property of the nonleading character of the internal quark loops.

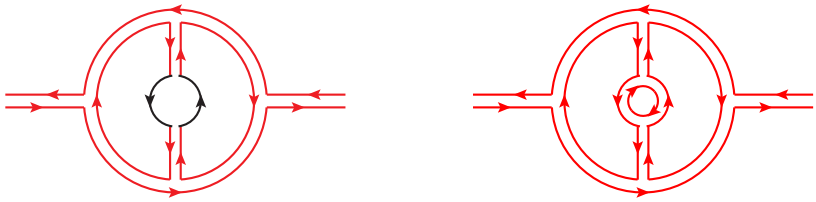

(a) $O(N_c^{-1})$ (b) $O(N_c^0)$

Figure 4: One-gluon exchange inside the gluon self-energy diagram: (a) including a quark loop; (b) including a gluon loop. The corresponding orders in large-N_c behavior are also indicated.

This second example outlines some other general features of the large-N_c behavior, that we would like to emphasize. The leading N_c-behavior of Fig. 4 is the same as in Fig. 3. This means that the large-N_c behavior does not follow the usual perturbative expansion in the coupling constant. The number of color loops may balance the occurrence of new vertices. The example of Fig. 4 may easily be generalized to more complicated types of diagram, where one finds again the same leading large-N_c behavior. The common feature of all these diagrams is that they can be mapped on a plane, and more generally on a two-dimensional surface, without allowing crossings of color lines. For this reason, they are called *planar diagrams*, which can be considered as belonging to a particular topological class in color space. It is to be emphasized that they are infinite in number.

On the other hand, the nonleading diagrams of Figs. 3 and 4, which contain the quark loops, could also be considered as planar. They, however, display an additional topological property, which is associated with the notion of a *hole*. Comparing diagrams (a) and (b) of both figures, one may distinguish figures (a) from figures (b) by the

occurrence in (a) of a hole in place of the internal color loop that exists inside the gluon loop in (b). Therefore, diagrams (a) above can be considered as planar, but with one hole inside the plane. It is evident that each occurrence of a hole produces a factor N_c^{-1} in the large-N_c counting rules.

The diagrams that do not fulfill the planarity condition are called *nonplanar*. They occur when, after their projection on a plane, some of the color lines cross each other. An example of such a case is provided by the two-gluon crossed-exchange diagram between two quark lines. Figure 5 displays a few Feynman diagrams occurring in the perturbative expansion of the two-point function of the color-singlet bilinear current $j_{\bar{k}\ell}$, $\langle j_{\bar{k}\ell}(x) j^{\dagger}_{\bar{k}\ell}(y)\rangle$, defined as

$$j_{\bar{k}\ell} = \overline{\psi}_{a,k}\psi^{a}_{\ell}, \tag{8}$$

where a is a color index and k and ℓ are fixed flavor indices; Dirac matrices and spinor indices have been omitted, as not being of primary importance in the present evaluation. Diagrams (a), (b) and (c) are planar and provide the leading large-N_c behavior. Diagram (d), representing the two-gluon crossed-ladder diagram, is nonplanar. One observes that it contains only one color loop, against the three color loops of the two-gluon ladder diagram (c). Its large-N_c behavior is therefore $O(N_c^{-1})$, against the $O(N_c^1)$ behavior of the three planar diagrams (a), (b) and (c).

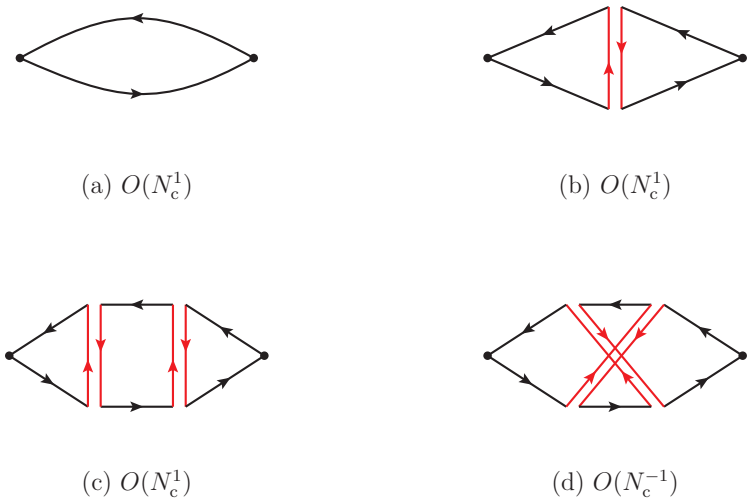

Figure 5: A few Feynman diagrams involved in the perturbative expansion of the correlation function $\langle j(x) j^{\dagger}(y)\rangle$. (a) A quark loop; (b) one-gluon exchange; (c) two-gluon ladder diagram; (d) two-gluon crossed-ladder diagram. The corresponding orders in large-N_c behavior are also indicated.

Nonplanar diagrams can be characterized by a specific topological invariant, the number of *handles*. Keeping in Fig. 5d one of the gluon propagators in space with respect to the projection plane, one observes that it plays the role of a handle of a two-dimensional surface. From the previous analysis, one deduces that each handle introduces a factor N_c^{-2} with respect to the planar diagram contribution.

The diagrams of Fig. 5 are examples of vacuum-to-vacuum diagrams corresponding to the connected part of correlation functions of gauge invariant local currents, each made of a quark and an antiquark field. Vacuum-to-vacuum diagrams can also be generated by gluon field currents, made of bilinear functions of gluon field strengths. An example is the current

$$G_{[\mu\nu][\eta\sigma]} = F^{A}_{\mu\nu}F^{A}_{\eta\sigma} = 2F^{a}{}_{b,\mu\nu}F^{b}{}_{a,\eta\sigma}. \tag{9}$$

The leading-order behavior of the corresponding two-point function is provided by the planar diagrams, two of which are represented in Fig. 6. Their large-N_c behavior is $O(N_c^2)$. Comparing this with the leading-order behavior of the quark bilinear case [Fig. 5], we observe that the latter can be deduced from the former by considering the external boundary quark loop as a hole inside the planar diagram topology.

We thus arrive at a general formula about the leading-order behavior of a diagram, characterized by the number of two topological invariants in color space, the hole, made of a color quark loop, and the handle, made of a gluon

(a) $O(N_c^2)$ (b) $O(N_c^2)$

Figure 6: Vacuum-to-vacuum planar diagrams made of gluon lines, corresponding to the two-point function of the gluonic current G [Eq. (9)].

propagator. Designating by B the number of holes and by H the number of handles, the power of the large-N_c behavior is

$$N_c^{2-B-2H} \equiv N_c^{\chi}, \tag{10}$$

where χ is called the Euler characteristic (cf. Ref. [142], Appendix A).

Planar diagrams without holes or with a number of holes determined by the external boundary color quark loops will provide the leading-order behavior at large N_c. The inclusion of handles and additional holes contributes to nonleading terms in $1/N_c$. Within this approach, $1/N_c$ appears as the effective perturbative expansion parameter of the theory. On the other hand, planar diagrams are infinite in number; this means that, even with the planarity approximation, one is not yet able to solve in a simple way the theory. Nevertheless, one hopes that the $1/N_c$ expansion will provide many qualitative simplifications and an improvement in the understanding of the dynamics of the theory.

2.3. Mesons

Properties of physical states can be investigated by considering correlation functions of gauge-invariant local currents, having the same quantum numbers. For mesons, the natural candidates are the quark bilinear currents, as defined in Eq. (8).

Considering the two-point function of such a current (generally, its connected part), typical Feynman diagrams of its perturbative expansion in the coupling constant have been presented in Fig. 5, where the first three, (a), (b) and (c), correspond to planar diagrams with leading-order behaviors in N_c. The most salient feature of these, and of all planar diagrams, is the fact that they contain only two quark lines (or propagators). A larger number of quark lines can appear only in nonleading diagrams, containing an additional number of holes. States characterized by a single quark-antiquark pair, as a leading descriptive element, correspond to the ordinary meson states. Therefore, the two-point function of the current, saturated by a complete set of hadronic intermediate states, reduces, at leading order in N_c, to a sum of meson poles:

$$\int d^4x e^{ip.x} \langle j(x) j^\dagger(0) \rangle = \sum_n \frac{iF_n^2}{p^2 - M_n^2 + i\epsilon} = O(N_c^1), \tag{11}$$

where F_n is defined as the matrix element of j between vacuum and the meson state $|n\rangle$:

$$\langle 0|j|n\rangle = F_n. \tag{12}$$

The number of meson states must be infinite. This is dictated by the asymptotic behavior of the left-hand side: because of asymptotic freedom, its high-energy behavior is known and contains logarithmic factors, which cannot be reproduced by a finite number of terms in the sum (11) [114]. This also entails a generic behavior at large N_c for each term of the series in connection with the behavior of the left-hand side ($O(N_c)$). The most natural solution is that the meson masses (for finite n) remain finite at large N_c, while the couplings F_n increase like $N_c^{1/2}$:

$$M_n = O(N_c^0), \qquad F_n = O(N_c^{1/2}). \tag{13}$$

From the complete decomposition of the two-point function into a series of poles [Eq. (11)], one also deduces that the meson states are stable at large N_c. If the mesons were unstable, they would have finite widths, manifested

as finite imaginary parts in the pole terms, which, in turn, would imply, through the unitarity property of the theory, the existence of unitarity cuts and the appearance of many-particle states; these would be manifested through the existence of more than two quark lines in the leading-order diagrams, which is not the case.

In obtaining Eq. (11), we have assumed that all planar diagrams containing two quark lines are perturbative representatives of single meson states. Since planar diagrams contain, in general, many gluon lines, the question arises as to whether such diagrams may also contain independent glueball states, which might be formed as gauge-invariant bound states of several gluon fields. This question is best analyzed through the study of the singularities and the imaginary part of the corresponding diagrams, by cutting them with a vertical line. An example of this is presented in Fig. 7. One observes that each gluon propagator, cut by the vertical line, is connected, with its

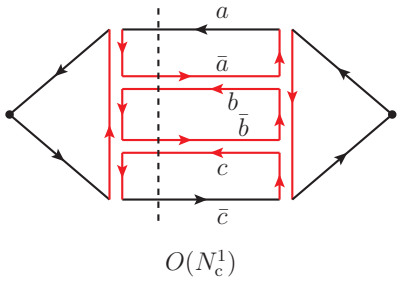

Figure 7: A planar diagram, contributing to the two-point function of the current j, with two gluon propagators submitted, together with the quark and antiquark propagators, to the vertical cut (dashed). The color indices of the various lines on the right of the vertical cut are explicitly indicated. Lower indices are distinguished by bars.

color indices, to the neighboring propagator, and nowhere a color-singlet gluonic cluster emerges. The set of the above gluon propagators belongs to the adjoint representation of the gauge group; on the other hand, the set of the quark and antiquark propagators belongs also to the adjoint representation. It is the connection of the two sets that produces a color-singlet representation. Therefore, the corresponding state is color-irreducible, in the sense that it is not decomposable into the product of other color-singlet representations. Hence, no independent glueball state may be generated from such a diagram. This property is very general for the two-point function and may be verified on more complicated planar diagrams.

Equation (11) can be diagrammatically described by representing the meson propagators by straight line segments and displaying the large-N_c behavior of the couplings [Eqs. (12) and (13)] (cf. Fig. 8, where the connected part of the two-point function is schematically represented in the form $\langle jj\rangle_c$).

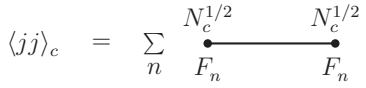

Figure 8: Equation (11) in diagrammatic form.

The study of the correlation functions of the currents j can be continued with the case of the three-point function $\langle jjj\rangle$, where j is a generic current, such that connections between three js are possible with quark lines. The simplest planar diagram, for the connected part, is presented in Fig. 9.

Cutting the diagram with a straight line in any direction and position, one meets always a pair of quark-antiquark lines, which means that the singularities of the diagram are located at meson poles[2]. These may be three or two in number. The first category involves, as a residue, the (amputated) vertex function of three meson sources, providing the three-meson coupling constant. The second category provides the coupling of a current j to two mesons. The corresponding equation is represented diagrammatically, together with the relevant large-N_c behaviors, in Fig. 10.

[2]The choice of the form and geometry of the cuts allows a selection of particular solutions of the Landau equations [125]; more generally, if p, q and r are the momenta associated with the external currents, then the singularities occur, according to the Landau equations, in the variables p^2, q^2 and r^2.

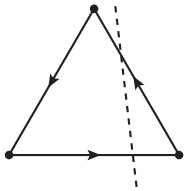

Figure 9: A planar diagram for the three-point function $\langle jjj\rangle_c$; here, the arrowed lines indicate quarks, whereas the dashed straight line indicates the cut.

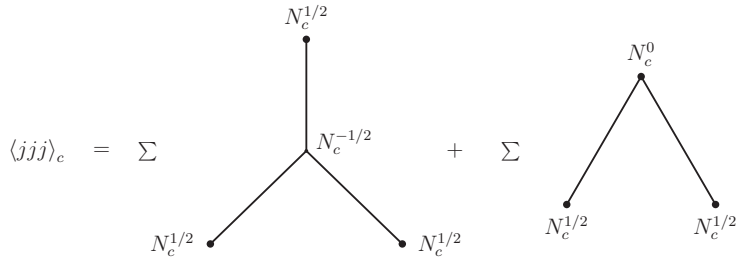

Figure 10: Diagrammatic representation of the three-point function $\langle jjj\rangle_c$ in terms of meson propagators and couplings, at leading order of N_c; here, the unarrowed lines indicate mesons. The large-N_c behaviors of the various couplings are explicitly indicated.

One finds that the three-meson couplings behave, at large N_c, as $N_c^{-1/2}$. This also determines the decay amplitude of mesons into two mesons, which vanishes at large N_c; the mesons are thus stable in this limit, a result that confirms the stability property already deduced from the decomposition of the two-point function [Eq. (11)]. The second type of diagram in Fig. 10 determines the coupling of the current j to two mesons, or, equivalently, to two pairs of quarks and antiquarks. Its behavior is N_c^0, a factor $1/N_c^{1/2}$ less than the coupling F_n [Eqs. (12) and (13)]. If one interprets these couplings as probability amplitudes of creating, by the current j, from the vacuum quark-antiquark pairs, one deduces that at large N_c mesons are made of one pair of quark-antiquark, while sea quarks, represented by additional quark-antiquark pairs, occur only as nonleading effects. This fact is a phenomenologically confirmed property, which is explained here in a natural way through the $1/N_c$ expansion method. This could also explain why meson-meson type interpolators are generally needed in lattice-QCD calculations in order to get the correct mass for states that couple strongly to these two mesons [108, 109].

We next consider four-point functions $\langle jjjj\rangle$ of generic currents j, such that connections between neighboring currents can be realized with quark lines. The simplest planar diagram, for the connected part, is presented in Fig. 11.

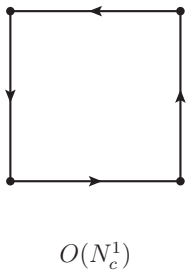

Figure 11: A planar diagram for the four-point function.

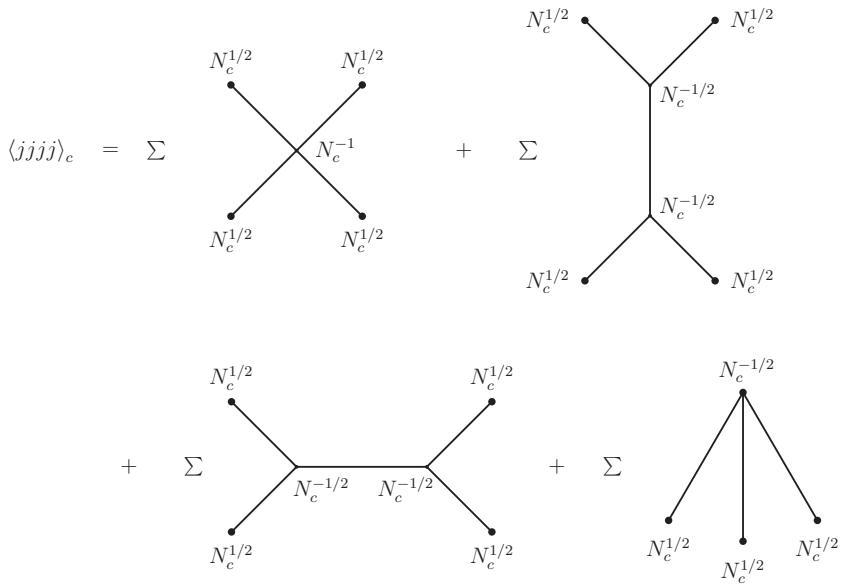

Figure 12: Diagrammatic representation of the four-point function $\langle jjjj\rangle_c$ in terms of meson propagators and couplings, at leading order of N_c. The large-N_c behaviors of the various couplings are explicitly indicated.

The singularities are again located at meson poles. The decomposition of the connected part of the four-point function in terms of meson propagators and couplings is diagrammatically presented, together with the relevant large-N_c behaviors of the couplings, in Fig. 12. One finds that the four-meson couplings are of order N_c^{-1}, smaller by a factor $1/N_c^{1/2}$ than the three-meson couplings. This, in turn, entails that the decay amplitudes of mesons into three mesons are also of order N_c^{-1}. The couplings of the currents j to three-meson states, or, equivalently, to three pairs of quarks and antiquarks, are of order $N_c^{-1/2}$.

Factoring out, in the above decomposition, the four meson propagators, together with their couplings to the external currents, one obtains the scattering amplitude of two mesons into two mesons, which is of order N_c^{-1}:

$$\mathcal{T}(MM \to MM) = O(N_c^{-1}). \tag{14}$$

It is worthwile noticing that, at that leading order, the scattering amplitude is expressed as a series of tree diagrams involving the infinite number of meson propagators and mutual couplings. This is in qualitative accordance with Regge phenomenology, where the dominant contributions come from tree diagrams of hadron exchanges and couplings [45], even though the Regge behavior itself cannot be demonstrated by the sole large-N_c limit.

The above procedure can be continued to higher numbers of currents. One particular outcome, as was already evident, is the relative decrease of the order in N_c-behavior of the meson couplings when the number of mesons increases. Thus, the n-meson couplings behave as $N_c^{1-n/2}$. One consequence of this property is that when a meson may decay into many mesons, it preferentially decays first into two mesons (or, possibly, into three mesons if there is a selection rule), which in turn decay into two or three mesons, and so forth. This is also a phenomenologically confirmed fact.

Another phenomenon occurring in hadron physics is related to the so-called OZI rule (after Okubo, Zweig and Iizuka) [2, 116, 117], which stipulates that, in the case of three light quarks, mesons generally are members of nonets of the flavor group U(3), rather than of separate octets and singlets of the group SU(3) (best illustrated by the $\varphi - \omega$ mixing)[3]. A violation of the rule concerns processes where the quark lines are completely disconnected between the initial and final states; such processes should be negligible. An example is illustrated by the two-point function $\langle j_{\bar{k}k}(x) j^\dagger_{\bar{\ell}\ell}(0)\rangle$, where k and ℓ are different fixed flavor indices. The two currents can mutually interact only through

[3]The pseudoscalar mesons are an exception, due to the chiral anomaly problem [75, 151]; however, the anomaly vanishes at large N_c.

gluon exchange. A planar diagram of the corresponding process is presented in Fig. 13. The diagram has two holes, due to the external color quark loop boundaries; its behavior at large N_c is $O(N_c^0)$, smaller by a factor $1/N_c$ with respect to the behavior of the planar diagrams of Fig. 5. Once again, the large-N_c limit provides a natural explanation of this qualitative effect, widely verified by experimental data.

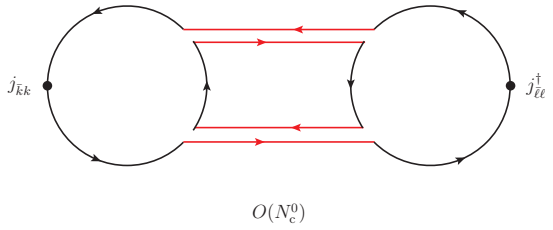

Figure 13: OZI-rule violating diagram: Two gluon propagators joining two quark loops with completely different flavor content. The order in large-N_c behavior is to be compared with the leading-order behaviors of Fig. 5.

To summarize, the large-N_c limiting procedure leads, according to the orders of N_c, to a hierarchical classification of the various processes that occur in QCD in its nonperturbative regime, providing a qualitative understanding of many typical phenomena that characterize the strong-interaction physics of hadrons. As far as the meson sector is concerned, at leading order in N_c, QCD reduces to a theory of an infinite number of free stable mesons, made of a quark-antiquark pair and of gluons, whose masses squared are expected to lie along Regge trajectories. At this level, all mesons are on equal footing; their differences arise only from their specific quantum numbers. The interactions among these mesons, which are responsible for their strong decays and nontrivial scattering processes, appear at nonleading orders of N_c. From this point of view, strong-interaction physics of mesons corresponds to a weakly interacting effective field theory, with an expansion parameter given by $1/N_c$, dominated by tree diagrams of meson exchanges and contact terms, as compared to the underlying strongly interacting theory, which is responsible for the confinement of quarks and gluons.

Studies of the influence of the large-N_c limit on meson properties can be found in Refs. [75, 152–158].

2.4. Baryons

One would like to complete the large-N_c approach by extending it to the physics of baryons. However, here, the method applied to the case of mesons turns out to be inapplicable.

The main reason of that difficulty is related to the description itself of baryonic states at large N_c. While for mesons, the change of the gauge group from SU(3) to SU(N_c) did not need any change in their description, characterized by their couplings to the local bilinear currents (8), baryons, and, more precisely, the currents to which they may couple preferentially, require a change of description. In SU(3), baryonic states are coupled to currents that are trilinear in quark fields and completely antisymmetric in color indices to ensure gauge invariance. A typical such current is:

$$j_B^{(3)}(x) = \frac{1}{3!}\epsilon_{abc}\psi^a(x)\psi^b(x)\psi^c(x), \tag{15}$$

where ϵ is the Levi-Civita symbol (a completely antisymmetric tensor) and, for simplicity, we have considered quarks with the same flavor and omitted the spin indices. In passing to SU(N_c), one has to generalize the above definition by using the Levi-Civita tensor in N_c dimensions, involving N_c indices, which, in turn, requires the use of N_c quark fields. The baryonic currrent then becomes:

$$j_B^{(N_c)} = \frac{1}{N_c!}\epsilon_{a_1 a_2 \cdots a_{N_c}}\psi^{a_1}\psi^{a_2}\cdots\psi^{a_{N_c}}. \tag{16}$$

Considering now the two-point function of this current, one can try to evaluate the N_c dependence of the corresponding Feynman diagrams, as was done in Fig. 5 for the mesonic currents. Typical diagrams are presented in Fig. 14.

Taking into account the normalization factor included in the definition of the current (16), the class of diagrams not containing gluon propagators [Fig. 14a] behaves as $O(N_c^0)$, which fixes the normalization for the other types of

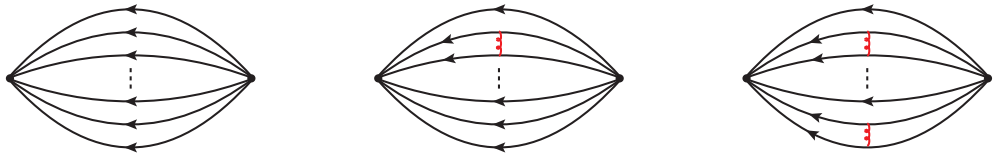

(a) $O(N_c^0)$ (b) $O(N_c^1)$ (c) $O(N_c^2)$

Figure 14: Typical Feynman diagrams of the two-point function of the baryonic current (16): (a) without gluon propagators; (b) with one gluon propagator (sample); (c) with two gluon propagators (sample). The order in large-N_c behavior of the contributions of all diagrams of each category is also indicated.

diagrams. A diagram containing one gluon propagator [Fig. 14b], joining two quark propagators, contains a damping factor $1/N_c$ coming from the coupling constant squared [Eq. (3)]. However, there are $N_c(N_c-1)/2 \sim N_c^2/2$ such diagrams; therefore the total contribution of this category of diagrams is $O(N_c^2/N_c) = O(N_c^1)$. A diagram containing two gluon propagators [Fig. 14c], joining different quark lines, contains the damping factor $1/N_c^2$ coming from the coupling constants at the vertices; this is to be multiplied by the total number of such diagrams, which is of the order of N_c^4; the total contribution of this category of diagrams is therefore $O(N_c^2)$. We observe that the perturbative expansion of the two-point function introduces at each order of the expansion a new factor N_c, which makes the corresponding series formally divergent at large N_c. Contrary to the case of the two-point functions of the mesonic currents, it is not possible here to group, in a stable way, elements of the perturbative series into topological classes having well-defined N_c behaviors.

Another complication arises from the fact that, inside baryons, the recognition of the color topological categories of diagrams is less evident than for mesons; the reason for this is related to the fact that, in baryons, all quark colors flow in the same direction, while in mesons the color of the antiquark flows in the opposite direction to that of the quark. We illustrate this phenomenon by focusing on the first gluon-exchange diagrams between two quark lines. They are presented, in the double-line representation, in Fig. 15.

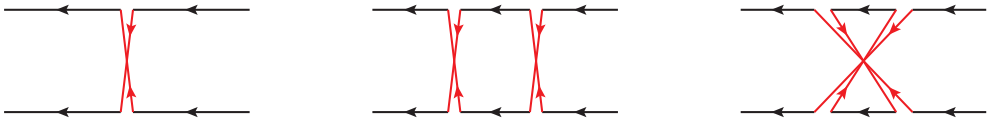

(a) $O(N_c^{-1})$ (b) $O(N_c^{-2})$ (c) $O(N_c^{-1})$

Figure 15: Gluon exchanges between two quark lines in the double-line representation: (a) one-gluon exchange; (b) two-gluon ladder exchange; (c) two-gluon crossed-ladder exchange. The order in large-N_c behavior of each diagram, with external color indices fixed, is also indicated.

Figure 15a corresponds to the one-gluon exchange diagram. We observe that, because of the similar directions of the quark color flows, the two color lines of the gluon propagator cross each other. As it stands, this diagram cannot be factorized in a plane, as in the planar-diagram case, into separate color flows without crossing. One could, of course, unfold one quark line, by inversing its drawing and flow, to make the diagram planar, however, this operation may, in general, be forbidden by the rest of the bigger diagram into which the above diagram is embedded. The behavior of the diagram, with fixed external color indices, is $O(N_c^{-1})$. Figure 15b corresponds to the ladder exchange of two gluon propagators. Here also, we meet the previous phenomenon. Contrary to the meson case, the diagram does not have any color loop and behaves at large N_c, with fixed external color indices, like $O(N_c^{-2})$, a factor $1/N_c$ less than in the case of mesons. Figure 15c corresponds to the crossed-ladder exchange of two gluon propagators. Here, the diagram contains an internal color loop and behaves like $O(N_c^{-1})$. It thus appears as the partner of the one-gluon exchange diagram for summation purposes. This property remains true for n-gluon exchange diagrams where each gluon line is crossed by the other $(n-1)$ gluon lines.

The above results seem to prevent the consideration, in a simple way, of the large-N_c limit in the sector of baryons, at least in a way that is parallel to that of mesons.

A way out of this difficulty was proposed by Witten [114]. He noticed that whereas the perturbative interaction between two quarks is small, of the order of $1/N_c$, it is the big number of quarks inside the baryons and the sum of the mutual interactions that are at the origin of the divergence. In such a case, diagrammatic considerations, which focus on the mutual interactions of a few neighboring quarks, are of little help. Every quark experiences a global strong force representing an average form of the sum of the forces exerted by the other quarks. One is then in a situation where a self-consistent mean-field approximation can be used. The problem simplifies further in the case of heavy quarks, where nonrelativistic theory applies in the form of the Hartree equations. Witten showed that these equations can be consistently solved, yielding a coherent description of the baryonic sector in the large-N_c limit.

The main property that characterizes these equations is that they globally scale as N_c at large N_c; this is due to the fact that each of their components – the total kinetic energy, the total potential energy and the mass of the baryon – has the same N_c-behavior. Therefore, N_c factors out of the equations, leaving N_c-independent equations, which ensure the stability of the result under perturbations with respect to $1/N_c$. In particular, the size and shape of the baryons turn out to be independent of N_c. The method is applied to the case of the ground state, as well as to the excited states, of baryons.

The above procedure is also applied to the study of processes like baryon-baryon, baryon-antibaryon and baryon-meson scatterings. All these processes have the property of leading to equations that globally scale like N_c, which is then factoured out.

The properties and dynamics of the baryons are thus mainly described, at large N_c, by semi-classical equations, rather than by microscopic quantum equations.

How to interpret the dissymmetry that emerges, at large N_c, between the mesonic and baryonic sectors? In this respect, Witten has made the following crucial observation [114]: The mesonic sector of QCD is described by a weakly interacting effective field theory, whose interaction scale is of the order of $1/N_c$. On the other hand, weakly coupled field theories often develop nonperturbative solutions, like solitons or monopoles [159–162], whose mass scale is governed by the inverse of the weak coupling. This is, in particular, the case for some electroweak theories with spontaneously broken symmetry, characterized, say, by a coupling constant squared α, which possess a magnetic monopole type solution, whose mass is of the order of $1/\alpha$ [159–161]. The structure of the monopole is determined, for small α, by solving classical equations, from which α drops out, the size and shape of the monopole then becoming independent of α. Similarly, the mass of the baryons in QCD is of the order of the inverse of the coupling $1/N_c$, i.e., of the order of $1/(1/N_c) = N_c$. Therefore, baryons can be considered as the QCD analogs of the solitons or magnetic monopoles, while mesons and glueballs are the analogs of ordinary particles.

More detailed investigations in the baryonic sector can be found in Refs. [144, 163–173].

2.5. Electric charges of quarks

We discuss, in this subsection, the generalization of the Standard Model (SM) to the case when the color subgroup of the SM symmetry group becomes $SU(N_c)$ instead of SU(3).

We first briefly recall the quantum numbers of the quark and lepton fields in the SM (see, e.g., [127, 129–131]). The SM of elementary particles is a gauge theory based on the spontaneously broken $SU_L(2) \times U_Y(1) \times SU(N_c)$ symmetry, where the $SU_L(2) \times U_Y(1)$ sector describes electroweak (EW) interactions of the fundamental fermion fields of the SM, quarks and leptons.

The SM contains three generations of fermion matter fields, quarks and leptons. In each generation, left-handed fermions compose doublets with respect to the $SU_L(2)$ group, whereas the right-handed matter fields are $SU_L(2)$ singlets. For instance, in the first generation, the SM contains two weak doublets

$$q_L = \begin{pmatrix} u_L \\ d_L \end{pmatrix}, \quad l_L = \begin{pmatrix} \nu_L \\ e_L \end{pmatrix}, \tag{17}$$

and four right-handed $SU_L(2)$ singlets (if one includes the Dirac right-handed neutrino field in the set of the SM fields):

$$u_R,\ d_R,\ e_R,\ \nu_R. \tag{18}$$

The quark and lepton doublets have the same $SU_L(2)$ charges: $+1/2$ for the upper components and $-1/2$ for its lower components. The right-handed quark and lepton singlets have zero $SU_L(2)$ charges. The $U_Y(1)$ quantum numbers – the weak hypercharges Y – for each $SU_L(2)$ multiplet are independent from each other (the upper and the lower components of any doublet have the same Y). In the SM one has

$$\begin{aligned} Y_L^l = -1, \quad Y_R^e = -2, \quad Y_R^\nu = 0, \\ Y_L^q = \tfrac{1}{3}, \quad Y_R^u = \tfrac{4}{3}, \quad Y_R^d = -\tfrac{2}{3}. \end{aligned} \tag{19}$$

The electric charge is related to the $SU_L(2)$ and $U_Y(1)$ quantum numbers by the Gell-Mann–Nishijima relation

$$Q = I_3 + Y/2, \tag{20}$$

where I_3 is the eigenvalue of the third component of the *weak isospin*. For the left-handed doublets, $I_3 = \pm 1/2$, for the right-handed singlets, $I_3 = 0$.

The SM is free from the chiral (axial) anomaly, since the quark-loop contribution to the anomaly cancels against the lepton-loop contribution. This happens since quark and lepton charges satisfy the relation

$$\sum_{\text{leptons}} Q^l + \sum_{\text{quarks}} Q^q = 0. \tag{21}$$

Quark fields belong to the fundamental representation of the SU(3) color group, so summation over quarks includes summation over color indices running from 1 to 3. Notice that the left-handed fermion fields and the right-handed fermion fields satisfy Eq. (21) separately.

When one generalizes the color group SU(3) to SU(N_c), the lepton quantum numbers remain unchanged, as leptons do not interact with the gluons, but the EW, i.e., $SU_L(2) \times U(1)$, quantum numbers of the quark fields should be changed. To obtain the electric charge and weak hypercharge of the quarks for arbitrary N_c, the following constraints are imposed: (i) The left-handed quark fields $\begin{pmatrix} u_L \\ d_L \end{pmatrix}$, $\begin{pmatrix} c_L \\ s_L \end{pmatrix}$ and $\begin{pmatrix} t_L \\ b_L \end{pmatrix}$ remain *weak isospin doublets* with $I_3 = \pm 1/2$, while the right-handed quark fields remain $SU_L(2)$ singlets. Electroweak quantum numbers of all quarks satisfy the Gell-Mann–Nishijima relation (20). (ii) The $SU_L(2)\times U(1)\times SU(N_c)$ Standard Model should be free of axial anomalies. Quark fields are in the fundamental representation of the $SU(N_c)$ color group, so there are N_c different quark colors. The anomaly cancellation condition requires that the sum of all electric charges (of leptons and quarks) vanishes.

In calculating the sum of charges in (21) for the left-handed particles, the terms $\pm 1/2$ in each left-handed doublet cancel out; the sum over quark colors gives a factor N_c and thus one comes to the following relation

$$Y_L^l + N_c Y_L^q = 0. \tag{22}$$

Taking into account that the hypercharge for the left-handed doublet remains the same as in the SM, $Y_L^l = -1$, one obtains $Y_L^q = \frac{1}{N_c}$. Proceeding in the same way for the right-handed particles, one finds

$$Y_L^l = -1, \quad Y_R^e = -2, \quad Y_R^\nu = 0, \tag{23}$$

$$Y_L^q = \tfrac{1}{N_c}, \quad Y_R^u = 1 + \tfrac{1}{N_c}, \quad Y_R^d = -1 + \tfrac{1}{N_c}. \tag{24}$$

The quark electric charges therefore become

$$Q_{u,c,t} = \frac{1}{2} + \frac{1}{2N_c}, \quad Q_{d,s,b} = -\frac{1}{2} + \frac{1}{2N_c}. \tag{25}$$

The electric charges of mesons are not changed compared to the case $N_c = 3$, since they contain one quark and one antiquark, whose Y-terms cancel each other. Masses of mesons, as quark-antiquark composites, remain finite, $O(N_c^0)$, at large N_c.

Baryons are bound states of N_c quarks. Their electric charges change compared to the SU(3) case and generally increase with N_c: for odd N_c their charges are integers, while for even N_c they are half-integers.

For the classification of baryons, one first uses *strong isospin*; this approximate symmetry of strong interactions is related to the smallness of the masses of the u and d quarks compared to Λ_{QCD} and to the values of the QCD

vacuum condensates. One may impose the conditions that, in the SU(N_c) theory, u and d quarks still form a doublet with $I_3 = +1/2$ and $-1/2$, respectively, while all other quarks are *strong isosinglets*, and that all quarks satisfy the Gell-Mann–Nishijima relation (20) for *strong hypercharges* of the quarks. For the light quarks u, d and s, one finds [174]:

$$Y_u = Y_d = \frac{1}{N_c}, \quad Y_s = -1 + \frac{1}{N_c}. \tag{26}$$

Baryons in large N_c have masses of $O(N_c)$. One then is entitled to use spin-flavor symmetry [166] and to classify baryons into spin-flavor representations at leading order in $1/N_c$. In general, the latter are decomposed into distinct flavor multiplets with increasing spins. It is then possible to assign the familiar baryons into representations where they keep the same values of spin, isospin, hypercharge and electric charge as in the SU(3) case. For instance, the proton is composed of $(N_c + 1)/2$ u quarks and $(N_c - 1)/2$ d quarks, N_c being now odd, and one may verify that its electric charge is +1. The reader may consult Ref. [174] for a more detailed account of the classification scheme of baryons.

2.6. Corrective effects

Let us briefly comment on the possible magnitude of the corrective factors in the $1/N_c$ expansion method in phenomelogical applications, where one has to use the physical value 3 of N_c.

The qualitative successes that the $1/N_c$ expansion method has obtained in QCD in the understanding of the hierarchy of various processes and phenomena brings an indirect or implicit justification of the validity of the method, which hinges, like other perturbative methods, on the smallness of the expansion parameter $1/N_c$. When the corrective factors to the leading terms are of order $1/N_c^2$, the latter become, for $N_c = 3$, of the order of 1/10, which is indeed a small quantity. For corrections of order $1/N_c$ (not to be confounded with leading terms of order $1/N_c$), one has a quantity of the order of 1/3, which is not fairly small. Generally, corrections of order $1/N_c$ come from internal quark loops, which, furthermore, are proportional to the flavor number N_f. Considering only the case of three light quarks (u, d, s), $N_f = 3$, one would have $N_f/N_c = 1$, which is not a perturbative parameter. Actually, it becomes important here to know about the size of the coefficient that accompanies the factor N_f/N_c. A hint about the latter coefficient is provided by the expression of the beta function, Eq. (2). Comparing both terms of the right-hand side of Eq. (2), one deduces that, for $N_f = 3$ and $N_c = 3$, the corrective term coming from the quark loops with respect to the leading term, is approximately equal to 0.18, which is a small quantity that might represent an acceptable value for an expansion procedure. In reality, on phenomenological grounds, the corresponding corrective factors, examples of which are provided by the quark-sea contributions inside hadrons (in the nonperturbative regime) and by the OZI-rule violations, are even much smaller, being of the order of a few percent.

Therefore, one may consider the perturbative expansion, in terms of $1/N_c$, at least for the first corrective terms, as a phenomenologically well-established procedure.

In conclusion, the large-N_c limit of QCD, proposed by 't Hooft and completed by Witten's proposal about baryons, leads to a consistent and simplified picture of the hadronic world and of its strong interaction dynamics.

2.7. The AdS/CFT correspondence

In this subsection, we briefly outline the role of the large-N_c limit in the correspondence established between string theories and quantum field theories, mostly known as the AdS/CFT correspondence [118–124]. This subject being out of the scope of the present review, we only focus here on the philosophy that has guided the related investigations. The interested reader is invited to consult the quoted references.

String theory has been present in hadronic physics from the early days of the discoveries of hadron resonances. The existence of a large number of hadron resonances, lying along Regge trajectories, was very suggestive of string theory spectra. Later, the advent of the quark model and of QCD introduced the concept of confinement of quarks and gluons, a property that is also shared by strings, at the endpoints of which are attached quarks. (For a review, cf., e.g., Ref. [175].)

It was noticed by 't Hooft, on the basis of the diagrammatic expansion in the large-N_c limit, that the resemblance between QCD theory in its nonperturbative regime and string theory is much enforced [111] in that limit. The spectrum of mesons is then very similar to that of free strings, whose coupling constant would be of the order of $1/N_c$. The

string picture is expected to be induced in QCD by the chromoelectric flux tubes and by the Wilson lines that ensure gauge invariance of multilocal operators. This suggests a correspondence between the two theories. However, flat-space string theories are consistently formulated in ten dimensions and the scales that they involve are of the order of the Planck scale, rather than of the hadronic scale [176–179]. The stringy behavior of QCD at large distances would then be understood as resulting from an effective field theory formulation [180–182].

On the other hand, the analysis applied to the large-N_c limit of QCD is rather general and could be applied to other gauge theories with different types of gauge symmetries. Duality relations could thus be searched for in a wider area of theories, general gauge field theories, on the one hand, and general string theories, on the other. The basic idea is that some physical theories might have two equivalent descriptions, each with different variables, such that the strong-coupling regime of one of them corresponds to the weak-coupling regime of the other. The corresponding investigations have been based on searches for theories having common global-symmetry properties, which survive the changes of description.

From the latter point of view, conformal invariance is the simplest symmetry that solves the problem. Conformal invariance requires the absence of any mass or energy scale in the theory. In four dimensions, where the gauge coupling constant is dimensionless, this amounts to the requirement that the latter be scale independent, which means that the β-function is null. It is only in supersymmetric theories that simple realizations of conformal invariance can be found. The most interesting example is provided by $\mathcal{N} = 4$ SU(N_c) super-Yang-Mills (SYM) theory, which involves four spinor supercharges. Another global symmetry, the R-symmetry, with the symmetry group SU(4), transforms the four supercharges into each other. The supersymmetry field content is then the following: the gluon fields belong to the singlet representation of the R-symmetry group, the fermion fields to the fundamental (**4**) representation and the scalar fields to the two-index antisymmetric (**6**) representation, all of them belonging to the adjoint representation of the color-gauge group.

If the above theory has a dual string theory, then its global invariance properties should be reflected by the latter. The conformal group is SO(2,4); locally, there is only one space with SO(2,4) isometries: five-dimensional anti-de Sitter space, or AdS_5. The SU(4) group of R-symmetry is equivalent to SO(6) and the latter is the symmetry group of a 5-sphere S^5. One therefore expects that the dual string theory should be formulated in a ten-dimensional space containing, at least in some regions, the product of the two previous spaces, $AdS_5 \times S^5$; notice that the total spacetime dimension precisely corresponds to the dimension in which flat-space string theory can be consistently formulated; in the present case, one should have a five-dimensional compactification into the 5-sphere and the introduction of a curvature through the anti-de Sitter space.

The link between string theory and gauge theory is realized by means of D-branes ("D" from Dirichlet) [183]. These are solitonic solutions of type-II strings and come out in various dimensionalities; Dp-branes have p spatial dimensions. In string perturbation theory, D-branes are defined as surfaces where open strings can end. The latter have massless modes representing gauge fields and their fermionic partners. If one has N_c coincident D-branes, open strings can start and end on two different branes; this implies labeling of the gauge fields and their fermionic partners with two different color indices, typical of the adjoint representation of an SU(N_c) gauge theory, which would then describe the low-energy dynamics of the theory.

The presence of D-branes changes the original flat-space metric to a curved one. D-branes, like black holes, contain event horizons. The low-energy limit of the new theory is represented by supergravity, itself containing classical brane-type solutions. Considering the case of N_c coincident $D3$-branes, appearing in type-IIB string theory ($p = 3$ being odd), one finds that the near horizon geometry is described by $AdS_5 \times S^5$. On the other hand, the low-energy limit of the dynamics in the worldvolume of the branes is described by $\mathcal{N} = 4$ SU(N_c) SYM theory. One thus obtains two different descriptions of the $D3$-branes at low energies, the first as a gravity theory in $AdS_5 \times S^5$ space, the second as an $\mathcal{N} = 4$ SU(N_c) SYM theory in four-dimensional Minkowski space. Designating the string theory coupling constant by g_s, its connection with 't Hooft's coupling constant λ [Eq. (3)] is $4\pi g_s = \lambda/N_c$. In the large-N_c limit, with λ fixed, g_s is generally small and the string theory is reduced, at leading order, to its classical limit. The precise outcome depends, however, on the domain of values of λ. When λ is sufficiently large, but finite, corresponding to the strong-coupling regime of the gauge theory, g_s is relatively large, but, however, the curvature radii of the AdS space and of the 5-sphere are also large, being proportional to $\lambda^{1/4}$. Then the dynamics is described by the $AdS_5 \times S^5$ near-horizon geometry, with small curvature, dominated by classical gravity. For small values of λ, it is the perturbative regime of the gauge theory that provides the simplest description. It was conjectured, on the basis of the property of the gauge theory being a unitary theory, that the gauge/gravity correspondence, demonstrated in

the supergravity approximation at large N_c, might go beyond that approximation and could be valid for the full string theory [118]. (Cf. also [123] for a detailed discussion of various aspects of this conjecture.)

Can one claim at this stage equivalence of gravitational theory and gauge theory? The question is pertinent, since the two theories live in different dimensions of spacetime. The gravitational theory is defined in ten-dimensional curved space, while the gauge theory is defined in four dimensions; the mapping between the degrees of freedom of the two theories does not seem trivial. A possible solution to this issue had been proposed by several authors, who had observed that the information carried by gravitational theories, defined in $(d + 1)$ dimensions, might be stored, according to a holographic principle, in a d-dimensional boundary region [184–187]. It is such a principle that is conjectured in the presently considered AdS/CFT correspondence, allowing the extension of the duality property away from the D-brane horizon region in AdS$\times S^5$ space [123].

In spite of this theoretical progress, the above duality relation does not directly apply to QCD theory, for several reasons. First, the latter theory is not conformally invariant; scale symmetry is broken by quantization and the bound-state spectrum displays there a mass gap with towers of discrete masses. Second, QCD is not supersymmetric. Third, quarks belong to the fundamental representation of the color group, while in $\mathcal{N} = 4$ SYM fermions belong, in four (identical) copies, to the (sole) adjoint representation with the six-fold presence of scalar partners. For these reasons, the treatment of QCD needs more elaborate pathways to establish the bridge to string theory [121]. The AdS/QCD correspondence remains, for the moment, at the level of phenomenological approaches or of model building [188–193].

3. How to describe multiquark states?

Properties of physical states are usually probed in quantum field theory by the study of Green's functions or correlation functions, using interpolating currents having nonvanishing couplings to them. This was the case for mesons [Eq. (8)] and baryons [Eq. (15)]. In the case of bound states, more detailed informations are obtained from the solution of bound-state equations, which generally require the use of multilocal operators as interpolating probes.

The problem is similar, in principle, in the case of exotic hadrons or multiquark states. One has to find appropriate interpolating currents to extract from correlation functions their specific properties. Here, however, additional complications arise. First, because of the increasing number of quarks in multiquark states, the number of the corresponding interpolating currents also increases and several combinations of them may be as good candidates as the individual ones. An optimal choice, for practical purposes, would be the one that would provide the strongest coupling to the state under study. However, the physical properties of the states are independent of the initial choice of interpolating currents, provided the latter have nonvanishing couplings to them. Second, in varying N_c, the definition of the multiquark state itself may change. An example of this phenomenon has been met with the ordinary baryons, for which the interpolating current had to be modified [Eq. (16)]. This phenomenon is rather general for multiquark states, in which case the large-N_c generalization of the interpolating currents is no longer unique: one has to deal with different schemes of well-known multiquark states of the case $N_c = 3$, such as tetraquarks, pentaquarks and hexaquarks.

We shall review, in this section, the various possibilities that one meets for the choice of interpolating currents and operators for the study of the properties of multiquark states. We shall first consider the case of the gauge group SU(3) and then its generalization to SU(N_c). For simplicity, we shall ignore spin/Dirac indices and concentrate on color and flavor indices. The inclusion of spin/Dirac indices can be done with the incorporation of appropriate Dirac matrices, taking into account the total spin and parity of the states.

3.1. SU(3)

We first consider the case of tetraquarks, which are mesons expected to be represented by two pairs of valence quarks and antiquarks[4]. To avoid mixing problems with ordinary meson states, we shall consider four different quark flavors, referred to by indices i, j, k, ℓ; color indices will be designated by $a, b, c, \ldots$.

Since the tetraquark is a color-singlet state, one has to find interpolating currents that are globally color singlets. As mentioned in the Introduction, an evident choice is the product of two mesonic color-singlet currents of the type

[4]For brevity, we shall often refer to them as four-quark states.

of Eq. (8). Designating by $T^{(1,1)}$ the tetraquark current, one has two different choices:

$$T^{(1,1)}_{\bar{i}j,\bar{k}\ell}(x) = j_{\bar{i}j}(x) j_{\bar{k}\ell}(x) = \Big(\overline{\psi}_{a,i}\psi^a_j\Big)(x)\Big(\overline{\psi}_{b,k}\psi^b_\ell\Big)(x), \tag{27}$$

$$T^{(1,1)}_{\bar{i}\ell,\bar{k}j}(x) = j_{\bar{i}\ell}(x) j_{\bar{k}j}(x) = \Big(\overline{\psi}_{a,i}\psi^a_\ell\Big)(x)\Big(\overline{\psi}_{b,k}\psi^b_j\Big)(x). \tag{28}$$

Another choice corresponds to the "diquark" combinations, by grouping the two quarks and the two antiquarks into antisymmetric or symmetric representations. In the first case, one obtains with the two quarks the antitriplet representation, $\bar{\mathbf{3}}$, and with the two antiquarks the triplet representation, $\mathbf{3}$; the two may then be combined into the singlet representation. In the second case, the two quarks are in the sextet representation, $\mathbf{6}$, and the two antiquarks in the antisextet representation, $\bar{\mathbf{6}}$, which also can be combined to yield the singlet representation. Designating by $T^{(\mp,\mp)}$ the corresponding currents, one has

$$T^{(-,-)}_{\overline{ik},j\ell}(x) = \frac{1}{2}\epsilon^{abc}\Big(\overline{\psi}_{a,i}\overline{\psi}_{b,k}\Big)(x)\epsilon_{dec}\Big(\psi^d_j\psi^e_\ell\Big)(x), \tag{29}$$

$$T^{(+,+)}_{\overline{ik},j\ell}(x) = \frac{1}{4}\Big(\overline{\psi}_{a,i}\overline{\psi}_{b,k} + \overline{\psi}_{b,i}\overline{\psi}_{a,k}\Big)(x)\Big(\psi^a_j\psi^b_\ell + \psi^b_j\psi^a_\ell\Big)(x), \tag{30}$$

where ϵ is the Levi-Civita tensor, already introduced in Eq. (15). The two currents $T^{(\mp,\mp)}$ are not independent of the two former currents $T^{(1,1)}$. By using in Eq. (29) the relation

$$\epsilon^{abc}\epsilon_{dec} = \delta^a{}_d\delta^b{}_e - \delta^a{}_e\delta^b{}_d, \tag{31}$$

and grouping in Eq. (30) the quark fields in bilinear current forms, one finds

$$T^{(-,-)}_{\overline{ik},j\ell} = -\frac{1}{2}(T^{(1,1)}_{\bar{i}j,\bar{k}\ell} + T^{(1,1)}_{\bar{i}\ell,\bar{k}j}), \qquad T^{(+,+)}_{\overline{ik},j\ell} = -\frac{1}{2}(T^{(1,1)}_{\bar{i}j,\bar{k}\ell} - T^{(1,1)}_{\bar{i}\ell,\bar{k}j}). \tag{32}$$

Clearly, one can also reexpress the currents $T^{(1,1)}$ as combinations of the currents $T^{(\mp,\mp)}$.

Finally, one can also choose tetraquark currents made of products of bilinear currents in the octet representation, $\mathbf{8}$:

$$T^{(8,8)}_{\bar{i}j,\bar{k}\ell}(x) = \Big(\overline{\psi}_{a,i}(T^A)^a{}_b\psi^b_j\Big)(x)\Big(\overline{\psi}_{c,k}(T^A)^c{}_d\psi^d_\ell\Big)(x), \tag{33}$$

$$T^{(8,8)}_{\bar{i}\ell,\bar{k}j}(x) = \Big(\overline{\psi}_{a,i}(T^A)^a{}_b\psi^b_\ell\Big)(x)\Big(\overline{\psi}_{c,k}(T^A)^c{}_d\psi^d_j\Big)(x), \tag{34}$$

where the T^As are the generators of SU(3) in the fundamental representation. By using the relation

$$(T^A)^a{}_b(T^A)^c{}_d = \frac{1}{2}\Big(\delta^a{}_d\delta^c{}_b - \frac{1}{N_c}\delta^a{}_b\delta^c{}_d\Big), \tag{35}$$

with $N_c = 3$, one can reexpress these currents in terms of the currents $T^{(1,1)}$:

$$T^{(8,8)}_{\bar{i}j,\bar{k}\ell} = -\frac{1}{2}\Big(\frac{1}{3}T^{(1,1)}_{\bar{i}j,\bar{k}\ell} + T^{(1,1)}_{\bar{i}\ell,\bar{k}j}\Big), \qquad T^{(8,8)}_{\bar{i}\ell,\bar{k}j} = -\frac{1}{2}\Big(T^{(1,1)}_{\bar{i}j,\bar{k}\ell} + \frac{1}{3}T^{(1,1)}_{\bar{i}\ell,\bar{k}j}\Big). \tag{36}$$

Therefore, only two currents are independent for the probe of tetraquarks with four different quark flavors. Their specific choice is a matter of taste or practical usefulness and does not prejudge in any way the physical structure of the tetraquark. It is the calculation of their couplings to the latter which ultimately may provide the physical information.

The above procedure of construction of currents can readily be generalized to other multiquark states. We briefly sketch some of them.

Pentaquarks are expected to be dominated by four valence quarks and one valence antiquark. We consider the case of four different flavors for the quarks, the antiquark having one of these flavors. A pentaquark current is most easily constructed as a product of a bilinear mesonic current [Eq. (8)] and of a trilinear baryonic current [Eq. (15)], an example of which is

$$P^{(1,1)}_{\bar{i}j,ik\ell}(x) = j_{\bar{i}j}(x) j_{B,ik\ell}(x) = \Big(\overline{\psi}_{a,i}\psi^a_j\Big)(x)\frac{1}{3!}\epsilon_{bcd}\Big(\psi^b_i\psi^c_k\psi^d_\ell\Big)(x). \tag{37}$$

Other currents commonly used are based on the diquark antisymmetric representation:

$$P^{(\bar{3},-,-)}_{\bar{i},ij,k\ell}(x) = \frac{1}{4}\epsilon^{abc}\overline{\psi}_{a,i}(x)\epsilon_{bde}\left(\psi^d_i\psi^e_j\right)(x)\epsilon_{cd'e'}\left(\psi^{d'}_k\psi^{e'}_\ell\right)(x). \tag{38}$$

Hexaquarks are dominated by six valence quarks (or by three quarks and three antiquarks, a case that we omit below). Their currents can commonly be represented as products of two baryonic currents or products of three antisymmetric diquark currents (here considered with four different quark flavors):

$$\begin{aligned} H^{(1,1)}_{ijk,ij\ell}(x) &= j_{B,ijk}(x)j_{B,ij\ell}(x) \\ &= \frac{1}{3!}\epsilon_{abc}\left(\psi^a_i\psi^b_j\psi^c_k\right)(x)\frac{1}{3!}\epsilon_{a'b'c'}\left(\psi^{a'}_i\psi^{b'}_j\psi^{c'}_\ell\right)(x), \end{aligned} \tag{39}$$

$$H^{(-,-,-)}_{ij,ik,j\ell}(x) = \frac{1}{8}\epsilon^{abc}\epsilon_{aa_1a_2}\left(\psi^{a_1}_i\psi^{a_2}_j\right)(x)\epsilon_{bb_1b_2}\left(\psi^{b_1}_i\psi^{b_2}_k\right)(x)\epsilon_{cc_1c_2}\left(\psi^{c_1}_j\psi^{c_2}_\ell\right)(x) \tag{40}$$

(no summation over repeated flavor indices).

3.2. SU(N_c)

In passing to SU(N_c), nontrivial modifications occur in the definitions of the interpolating currents that we met in the case of SU(3). This is related to the fact that these currents are generally defined as products of irreducible tensors and with the increase of N_c the number of such tensors increases in turn. Adopting the notation of irreducible representations based on Young tableaux (see, e.g., Ref. [194]), $[\ell_1, \ell_2, \cdots]$, where the nonincreasing integers ℓ_i ($i = 1, 2, \ldots$) denote the number of boxes in each column, the defining fundamental representation to which belongs the quark field is simply [1], while the antifundamental representation to which belongs the antiquark field is $[N_c - 1]$. When $N_c = 3$, the latter reduces to [2], which implies that a two-index antisymmetric tensor of quark fields belongs to the antitriplet representation $\bar{\mathbf{3}}$. When $N_c > 3$, one has $(N_c - 2)$ distinct antisymmetric irreducible representations, which generalize the case of $N_c = 3$. The two-index antisymmetric representation is then [2], while the two-index symmetric representation is [1, 1].

To construct the generalized antisymmetric multiquark representations, we introduce (generally colored) tensor currents, made of $(N_c - J)$ quark fields, or $(N_c - J)$ antiquark fields, where $J = 0, 1, 2, \ldots, (N_c - 1)$, combined together with the antisymmetric ϵ tensor, which now contains N_c indices:

$$j^{(J,-)}_{a_1a_2\cdots a_J} = \epsilon_{a_1a_2\cdots a_Jb_1b_2\cdots b_{N_c-J}}\psi^{b_1}\psi^{b_2}\cdots\psi^{b_{N_c-J}}, \tag{41}$$

$$\overline{j}^{\,a_1a_2\cdots a_J}_{(J,-)} = \epsilon^{a_1a_2\cdots a_Jb_1b_2\cdots b_{N_c-J}}\overline{\psi}_{b_1}\overline{\psi}_{b_2}\cdots\overline{\psi}_{b_{N_c-J}}, \tag{42}$$

flavor indices being ignored. The case $J = 0$ reproduces, up to a multiplicative constant, the baryonic color singlet current (16).

The equivalent forms of representation (29) are then

$$T^{(J,-)} = \frac{1}{(N_c - J)!}\,\overline{j}^{\,a_1a_2\cdots a_J}_{(J,-)}\,j^{(J,-)}_{a_1a_2\cdots a_J}, \qquad J = 1, 2, \ldots, (N_c - 2). \tag{43}$$

The choice $J = (N_c - 2)$ reproduces the antisymmetric representation of Eq. (32). The choice $J = 1$ corresponds to the grouping of the quark fields into the antifundamental representation.

The above currents do not exhaust all the possibilities of constructing interpolating currents. One still has the possibility of incorporating symmetric representations, as in Eq. (30), which we omit here for simplicity.

Other types of representation are the products of ordinary mesonic currents, like in Eqs. (27) and (28). Using in Eqs. (43) contractions of the two ϵ tensors, as in Eq. (31), which are present in j and $\overline{j}$, one can reexpress the antisymmetric-type tensor currents as combinations of products of such mesonic bilinear currents, as in Eq. (32). (In the case of one quark flavor, these reduce to powers of a single current.) The same result is also obtained with the

symmetric representations. We notice, in particular, that the simplest quadrilinear currents of the types of Eqs. (27) and (28), met in the SU(3) case, may continue playing the role of interpolating currents in the SU(N_c) case, corresponding to the choice $J = N_c - 2$ in the antisymmetric representation (43) and in the corresponding symmetric one.

It is the calculation of the couplings of the above currents to the hypothetical tetraquark state that may provide an indication about its internal structure. In the case of dominance of the currents of the types (27)–(30), the tetraquark will have a very similar structure as in the SU(3) case. In the case of dominance of the currents of the other extreme cases, like in (43) with J close to 1, the tetraquark will have a many-body structure, as in the case of baryons[5].

The fact that all tetraquark currents can be reexpressed as combinations of products of ordinary mesonic currents is an indication that they are color-reducible, unlike the currents of ordinary mesons and baryons. This has the consequence, that, at large N_c, the leading behavior of their correlation functions is given by that of products of correlation functions of ordinary mesonic currents, representing disconnected propagation of free mesons and not of tetraquarks [50, 114, 142]. We consider here, as an example, the case of the two-point function of the current (27). At large N_c, it behaves at leading order as

$$\langle T^{(1,1)}_{\bar{i}j,\bar{k}\ell}(x) T^{(1,1)\dagger}_{\bar{i}j,\bar{k}\ell}(0)\rangle \underset{N_c\to\infty}{=} \langle j_{\bar{i}j}(x) j^{\dagger}_{\bar{i}j}(0)\rangle \langle j_{\bar{k}\ell}(x) j^{\dagger}_{\bar{k}\ell}(0)\rangle = O(N_c^2), \tag{44}$$

where the N_c-behavior is obtained from Fig. 5a. This means that the search for tetraquark states in correlation functions has to go beyond the leading order [195].

For pentaquarks, the currents constructed as products of a mesonic and a baryonic current are still valid, provided one uses for the latter its expression of SU(N_c) [Eqs. (16) and (41)]:

$$P^{(1,1)}(x) = j(x) j^{(0,-)}(x). \tag{45}$$

Generalizations of the antisymmetric tensor currents (38) are:

$$\begin{aligned} P^{(J,K,-)} &= \overline{j}^{\,a_1\cdots a_J, b_1\cdots b_K}_{(J+K,-)} \, j^{(J,-)}_{a_1 a_2\cdots a_J} \, j^{(K,-)}_{b_1 b_2\cdots b_K}, \\ & \qquad J, K = 1, 2, \ldots, (N_c - 2), \quad (J + K) \le (N_c - 1). \end{aligned} \tag{46}$$

For hexaquarks, the analogs of representations (39) are

$$H^{(1,1)}(x) = j^{(0,-)}(x) j^{(0,-)}(x). \tag{47}$$

For the generalizations of the antisymmetric representations (40), we display here only the two extreme cases of interest:

$$H^{(1,1,\ldots,1,-)} = \epsilon^{a_1 a_2\cdots a_{N_c}} j^{(1,-)}_{a_1} j^{(1,-)}_{a_2} \cdots j^{(1,-)}_{a_{N_c}}, \tag{48}$$

$$H^{(1,1,N_c-2,-)} = \epsilon^{a_1 a_2\cdots a_{N_c}} j^{(1,-)}_{a_1} j^{(1,-)}_{a_2} j^{(N_c-2,-)}_{a_3\cdots a_{N_c}}. \tag{49}$$

Like the tetraquark currents, pentaquark and hexaquark currents are decomposable along combinations of products of ordinary hadronic currents; their two-point functions satisfy properties similar to that of Eq. (44).

Graphical representations of the currents introduced in the present subsection will be presented in Sec. 3.3, in the more general case of multilocal operators.

Multiquark-state currents of the types introduced above have been considered and studied in Refs. [196, 197].

3.3. Multilocal operators

The description of multiquark states may also necessitate in some instances the use of more general probes than local currents. Bound-state equations require the use of multilocal fields. Lattice gauge theory, which works in a discretized spacetime, is another instance where the theory is formulated from the start by means of such operators. It is therefore necessary to find the corresponding generalizations of the various currents that we met in our previous study. We shall focus our attention on representations that preserve the gauge invariance of the theory.

[5]For simplicity of language, we shall continue using for the exotic states the same names as in SU(3), independently of their internal structure.

Gauge-invariant operators are constructed by using path-ordered gluon-field phase factors [198–201], also called gauge links or Wilson lines, having the form

$$U^a{}_b(C_{yx}) = \left(P e^{\,ig \int_{C_{yx}} dz^\mu T^B A^B_\mu(z)} \right)^a{}_b, \tag{50}$$

where C_{yx} is an oriented curve going from x to y and P represents the path-ordering of the gluon fields according to their position on the line C_{yx}; the integration goes from x to y along that line. The phase factors $U(C_{yx})$ are the color parallel transporters along the lines C_{yx} [202].

The color-trace operation on a phase factor taken along a closed contour C_{xx} defines a gauge-invariant operator, called the Wilson loop. Its vacuum expectation value plays an important role in defining gauge-invariant static potential energies [48, 49, 92].

Gauge-invariant operators coupling to mesons and baryons (here for the group SU(3)) are[6]

$$M = \overline{q}_a(y) U^a{}_b(C_{yx}) q^b(x), \tag{51}$$

$$B = \frac{1}{3!} \epsilon_{abc}\, U^a{}_d(C_{xy}) q^d(y)\, U^b{}_e(C_{xt}) q^e(t)\, U^c{}_f(C_{xz}) q^f(z), \tag{52}$$

where flavor and spin indices have been omitted. A pictorial representation of them, with phase factor lines chosen along straight line segments, is given in Fig. 16. Meson and baryon local currents [Eqs. (8) and (15), respectively] are obtained (up to the defining multiplicative constants) by concentrating the quark and antiquark coordinates at single points and by shrinking in the latter expressions the phase factors to 1.

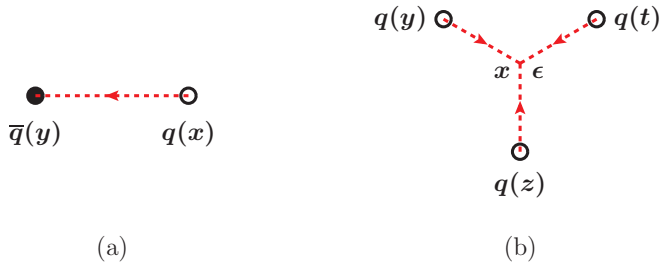

Figure 16: Pictorial representation of the gauge-invariant meson (a) and baryon (b) operators; in the baryon case, ϵ is the completely antisymmetric Levi-Civita tensor, indicating the antisymmetric property of the three-line vertex.

As a general remark, let us emphasize that physical properties of states should be independent of the shape of the lines C_{yx}, provided they are continuous and smoothly varied upon deformations from straight lines. The latter are generally chosen for their simplicity and for their adequacy in lattice calculations [48]. The above property can be verified in the case of bound-state energies, which are obtained from the behavior of Wilson-loop vacuum averages at large time separations. In QCD, the Wilson-loop vacuum average is expected to satisfy in that limit the area law and, more generally, the minimal surface property [48, 203, 204]. Smooth deformations of the phase-factor lines inside the bound-state definition do not change its energy, but only affect the expression of the wave function (cf. Sec. 7.2 below and Ref. [204], Appendix A).

Similar constructions can also be applied to the multiquark states. They were promoted in the past by Rossi and Veneziano [205, 206] and are called "string-junction" or "Y-shaped-junction" type representations. They are mainly considered for the antisymmetric representations, typical of the diquark picture [60–62], in which the interquark forces are expected to be attractive, leading to the emergence of multiquark bound states. Pictorial representations of these are given in Fig. 17. The local multiquark antisymmetric representation currents [Eqs. (29), (38) and (40)] are obtained (up to the defining multiplicative constants) by concentrating quark and antiquark coordinates at single points and by shrinking the phase factors to 1.

[6] In this and the following subsections, for ease of pictorial representations, the quark fields are designated by the notation q, rather than ψ.

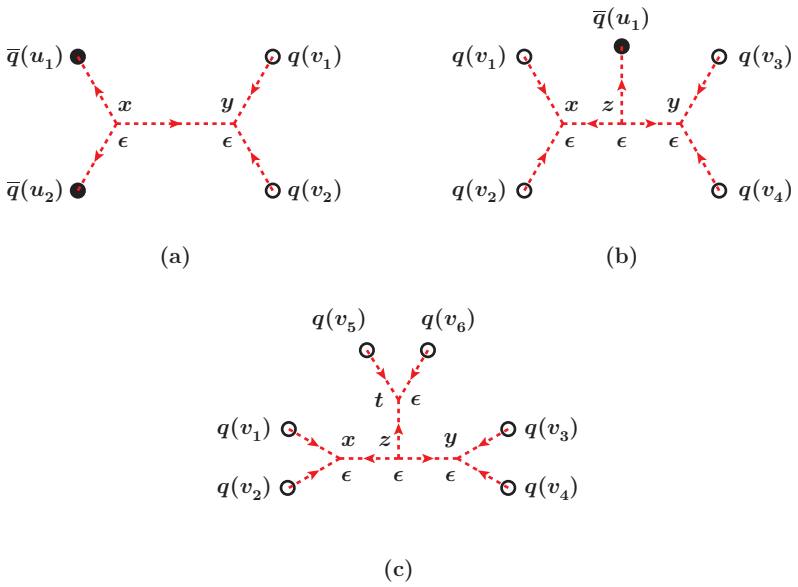

Figure 17: Pictorial representation of the gauge-invariant (a) tetraquark, (b) pentaquark, and (c) hexaquark operators.

Generalizations of the previous operators to the SU(N_c) case are straightforward, following the constructions of the corresponding local currents [Eqs. (8), (16), (43), (46), (48) and (49)]. The case of mesons and baryons is displayed in Fig. 18.

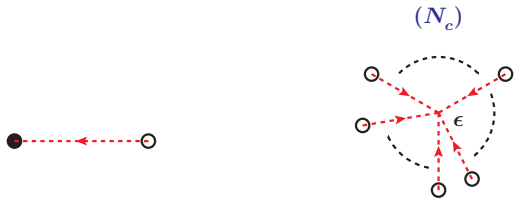

Figure 18: Meson and baryon operators in the SU(N_c) case.

Tetraquark, pentaquark and hexaquark operators are graphically represented in Figs. 19, 20 and 21.

In summary, multiquark states can generally be described, or theoretically probed, by several operators, each highlighting a particular aspect of the state under study. In passing to large N_c, the number of these operators increases and the structure of the multiquark states may become more complicated. One however hopes that only few of them will represent the dominant representative scheme, which might correspond to the outcome of more dynamical investigations.

4. Singularities of Feynman diagrams connected with multiquark states

While the large-N_c limit approach is a method aiming to explore the properties of the theory in its nonperturbative regime, here, for QCD, in its confining regime, it still hinges, as we have seen in Sec. 2, on the analysis of Feynman diagrams, which are representative of the perturbative regime of the theory. Although this might seem contradictory, it should be emphasized that one is not considering a single or a finite number of Feynman diagrams, but rather classes of Feynman diagrams which are distinguished by their topological properties in color space. Thus, in Fig. 5, the diagrams (a), (b) and (c) are parts of the same class of planar diagrams, depicting the two-point correlation function of meson currents, having the same large-N_c behavior. This class contains an infinite number of other diagrams,

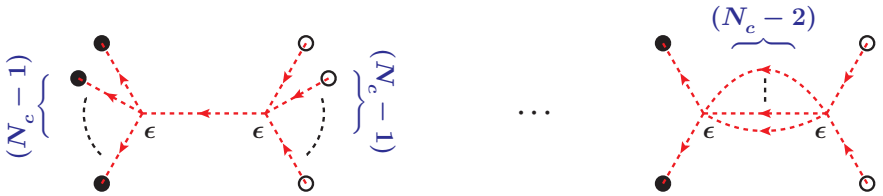

Figure 19: Tetraquark operators in the SU(N_c) case. The two extreme cases, with $J = 1$ and $J = (N_c - 2)$, corresponding to Eq. (43), are displayed. The first diagram contains $(N_c - 1)$ quarks and $(N_c - 1)$ antiquarks, with a single link between the two string junctions. The last diagram contains two quarks and two antiquarks, with $(N_c - 2)$ links between the string junctions.

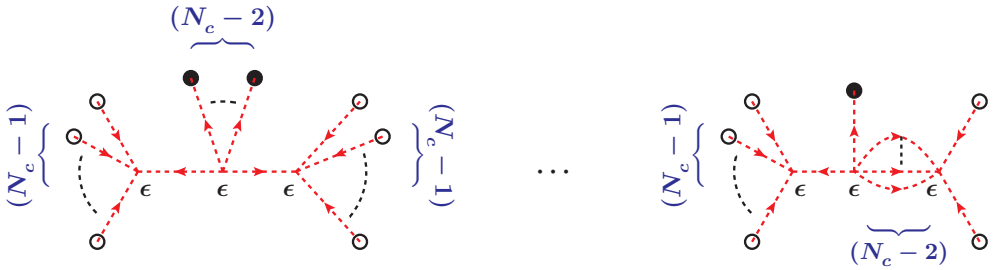

Figure 20: Pentaquark operators in the SU(N_c) case. Two extreme cases, with $J = 1$, $K = 1$ and $J = 1$, $K = (N_c - 2)$, corresponding to Eq. (46), are displayed. The first diagram contains $2(N_c - 1)$ quarks and $(N_c - 2)$ antiquarks. The last diagram contains $(N_c - 1) + 2$ quarks and one antiquark.

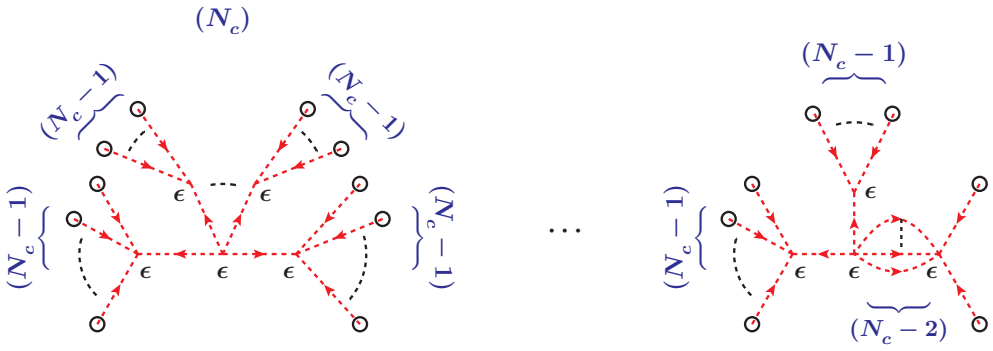

Figure 21: Hexaquark operators in the SU(N_c) case. Two extreme cases, corresponding to Eqs. (48) and (49), are displayed. The first diagram contains $N_c(N_c - 1)$ quarks. The last diagram contains $2(N_c - 1) + 2$ quarks.

involving many-gluon exchanges, but the same number (viz., two) of quark lines. The large-N_c approach assumes that the infinite sum of diagrams contained in this topological class produces the bound states of mesons and maintains the confining property of the theory [111, 114, 142].

Each Feynman diagram participating in the above summation process, though not explicitly displaying confining properties or bound-state attributes, should carry a minimum amount of common qualitative features with the other diagrams in order to produce at the end the desired nonperturbative effects. In the example of the two-point function of the meson currents given above, it is the number of quark lines which is common to all the summed diagrams. It is this number that allows the introduction of the notion of valence quarks. This is then manifested in each Feynman diagram through the singularity structure in momentum space, represented by a discontinuity in the total invariant mass squared, the so-called Mandelstam s-variable, starting from the two-quark threshold and going to infinity. The summation of diagrams transforms this singularity into a series of meson poles.

The same procedure also applies to the two-point functions of the baryonic currents. For $N_c = 3$, it is the Feynman diagrams with three quark lines which should be representative of the leading valence-quark structure. When the large-N_c limit is taken, the number of valence quarks for baryons increases with N_c, however, the singularity content of each diagram should remain, in that a threshold singularity in the s-variable should be present and should lead after summation to a series of baryon poles.

In passing to the case of exotic (multiquark) states, one expects a generalization of the above phenomenon. An exotic state with a number A of valence quarks should be represented, at leading order in N_c, by diagrams containing a number A of quark lines. Here, however, two kinds of difficulties emerge, which were not present in the case of ordinary hadrons. First, Feynman diagrams with A quark lines may contain color-singlet disconnected pieces; this is a consequence of the fact that the multiquark currents are generally expressible as combinations of products of ordinary currents (cf. Sec. 3, Eqs. (27), (28), (37), (39) and (44)). Such diagrams, which represent propagation of free particles, cannot participate in the formation of bound states and hence should not be taken into account. Second, there are still connected Feynman diagrams, having A quark lines, which do not possess singularities in the s-variable. Their singularities concern the u- or t-variables and therefore cannot not participate in the multiquark pole production process and should not be considered.

In summary, the counting of quark lines in a given Feynman diagram is no longer sufficient for its consideration in the formation process of the multiquark bound state. A more precise criterion, based on the analysis of the singularity structure in the s-variable, is necessary. This criterion is provided by the Landau equations [125, 127], which allow one to analyze in more detail the singularity properties of Feynman diagrams. We shall briefly sketch below the Landau equations and shall consider a few typical examples which will be helpful in the analyses of multiquark-state properties.

According to its quark-flavor structure (if one quark and one antiquark are of the same flavor), a multiquark state may have a mixing with an ordinary meson or baryon state. It is understood that to receive the multiquark label, the multiquark component having A valence quarks is part of the N_c-leading components of the total state. Otherwise, any ordinary hadron state has multiquark-type components, due to the sea quarks, which are parts of the N_c-subleading components. Therefore, independently of possibly existing mixings with ordinary hadron states, it is the structure of the multiquark component, assumed to provide, at least partly, the N_c-leading behavior of the state, which is the key ingredient of the present analysis.

A generic expression of a Feynman diagram is

$$I(p) = \int \prod_{\ell=1}^{L} \frac{d^4 k_\ell}{(2\pi)^4} \prod_{i=1}^{I} \frac{1}{(q_i^2 - m_i^2 + i\epsilon)}, \tag{53}$$

where p represents a collection of external momenta and q_i (I in number) are linear functions of the ps and of the loop variables k_ℓ (L in number).

The Landau equations are

$$\lambda_i (q_i^2 - m_i^2) = 0, \qquad i = 1, \ldots, I, \tag{54}$$

$$\sum_{i=1}^{I} \lambda_i q_i \cdot \frac{\partial q_i}{\partial k_\ell} = 0, \qquad \ell = 1, \ldots, L, \tag{55}$$

where the λs are Lagrange multipliers to be determined. Some of the parameters λ may vanish or may be compatible with vanishing values.

We are mainly interested in the location of the singularities produced by the quark propagators. Gluons being massless, the singularities of their propagators generally start at the same positions as those produced by the quark propagators. We therefore shall not consider, in general, gluon propagators in the Landau equations as independent sources of singularities; this is realized by putting, from the start, the corresponding λs equal to zero. However, gluon lines may participate in the production of quark singularities through the momentum they carry.

Since multiquark states are expected to decay into ordinary hadrons, or to have couplings with them in the case of bound states, it is easier to study their properties through the scattering amplitudes of ordinary hadrons and the corresponding Feynman diagrams.

We consider, for definiteness, the case of tetraquarks made of four quarks with different flavors; the quarks will be designated by indices 1 and 3 and the antiquarks by indices $\overline{2}$ and $\overline{4}$. As we have seen in Sec. 3.2, such a description still remains valid for general N_c, although in the latter case other representations also emerge (cf. Fig. 19). Within the present representation, the tetraquark may couple to two mesons and therefore may be probed in two-meson scattering processes. Using the bilinear currents defined in Eq. (8), one may consider, in momentum space, Fourier transforms of the correlation functions

$$\Gamma_{D1} \equiv \langle j_{\bar{2}1}(x) j_{\bar{4}3}(y) j^{\dagger}_{\bar{4}3}(z) j^{\dagger}_{\bar{2}1}(0)\rangle, \quad \Gamma_{D2} \equiv \langle j_{\bar{4}1}(x) j_{\bar{2}3}(y) j^{\dagger}_{\bar{2}3}(z) j^{\dagger}_{\bar{4}1}(0)\rangle, \tag{56}$$

$$\Gamma_{R1} \equiv \langle j_{\bar{2}1}(x) j_{\bar{4}3}(y) j^{\dagger}_{\bar{4}1}(z) j^{\dagger}_{\bar{2}3}(0)\rangle, \quad \Gamma_{R2} \equiv \langle j_{\bar{4}1}(x) j_{\bar{2}3}(y) j^{\dagger}_{\bar{2}1}(z) j^{\dagger}_{\bar{4}3}(0)\rangle, \tag{57}$$

where the subscript D refers to direct-channel processes and the subscript R to quark recombination or rearrangement channel processes.

We first consider two typical diagrams of the direct channel 1 process – a disconnected diagram and a connected one – represented in Figs. 22a and b, respectively. (The diagram with one-gluon exchange between the two disconnected color-singlet diagrams is zero.) The total conserved momentum of the two-meson processes is designated by P, with the usual definition $s = P^2$.

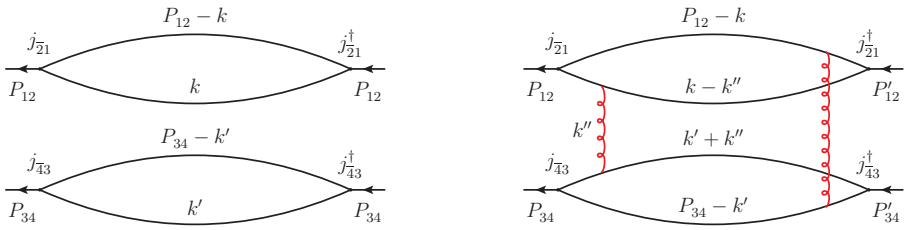

(a) $O(N_c^2)$ (b) $O(N_c^0)$

Figure 22: Disconnected (a) and connected (b) diagrams in the direct channel $M_{\bar{2}1} M_{\bar{4}3} \to M_{\bar{2}1} M_{\bar{4}3}$ of the meson-meson scattering amplitude.

The Landau equations of the disconnected diagram are themselves separable into two independent subsets, leading to the physical singularities $P_{12}^2 = (m_1 + m_2)^2$ and $P_{34}^2 = (m_3 + m_4)^2$, which do not involve s. These singularities refer to the internal structure of each meson, which propagates freely and independently from the other. It is evident that this diagram cannot be involved in the formation of a bound state or of a resonance. One can also consider all other planar diagrams which include the gluon exchanges inside each quark loop, associated with the above disconnected diagram, still finding the same singularities as above, confirming the fact that gluon propagators generally do not modify the location of singularities found with the sole quark propagators.

For the connected diagram of Fig. 22, it is sufficient to consider a vertical cut passing between the two gluon lines. The Landau equations are then:

$$\begin{aligned} &\lambda_1((P_{12} - k)^2 - m_1^2) = 0, \qquad \lambda_2((k - k'')^2 - m_2^2) = 0, \\ &\lambda_3((k' + k'')^2 - m_3^2) = 0, \qquad \lambda_4((P_{34} - k')^2 - m_4^2) = 0, \end{aligned} \tag{58}$$

$$-\lambda_1(P_{12}-k)+\lambda_2(k-k'')=0,\quad -\lambda_2(k-k'')+\lambda_3(k'+k'')=0,\quad \lambda_3(k'+k'')-\lambda_4(P_{34}-k')=0. \tag{59}$$

The following definitions hold:

$$P=P_{12}+P_{34}=P'_{12}+P'_{34},\quad s=P^2,\quad t=(P_{12}-P'_{12})^2,\quad u=(P_{12}-P'_{34})^2. \tag{60}$$

The system of equations (58) and (59) can be solved, leading to the physical singularity at $s=(\sum_{i=1}^4 m_i)^2$. The fact that the four quark masses are present means that we have four-quark intermediate states, which, together with the contributions of other diagrams involving more gluon lines, will generate two-interacting-meson states and possibly tetraquark states.

We next consider, in Fig. 23, two diagrams of the recombination channel 1. Here, the following definitions hold:

$$P=(P_{12}+P_{34})=(P'_{14}+P'_{23}),\quad s=P^2,\quad t=(P_{12}-P'_{14})^2,\quad u=(P_{12}-P'_{23})^2. \tag{61}$$

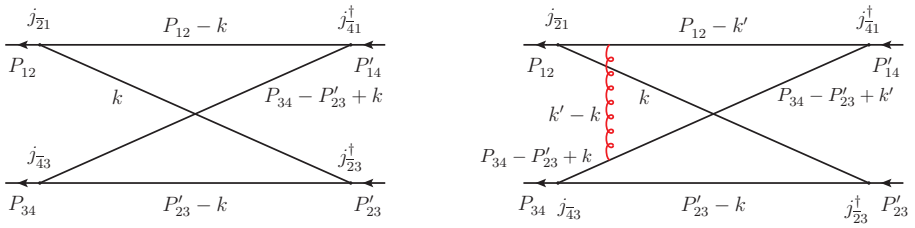

(a) $O(N_c)$ (b) $O(N_c)$

Figure 23: Diagrams in the quark-rearrangement channel $M_{\bar{4}1}M_{\bar{2}3}\to M_{\bar{2}1}M_{\bar{4}3}$ of the meson-meson scattering amplitude, not concerned, at large N_c, with tetraquark states.

The Landau equations of diagram (a) have several subsets of physical solutions: $t=(m_2+m_4)^2$, $u=(m_1+m_3)^2$, $P_{12}^2=(m_1+m_2)^2$, etc., but no singularities in s are found. The t- and u-channel singularities will be saturated, with similar diagrams involving gluon lines, by one-meson states. The singularities in the external momenta squared are those that are present in the external meson propagators. The Landau equations of diagram (b) also lead to the same sets of singularities as diagram (a). Therefore, the diagrams of Fig. 23, which apparently display four quark lines, do not participate in the formation of two-meson interacting systems, nor to possibly existing tetraquark states. Nevertheless, they produce, in the mesonic world, contact-type interactions, as well as one-meson exchange diagrams.

One may have another view of the preceding results, by referring to the topological properties of the diagrams in color space. The latter are planar diagrams and can be unfolded, as suggested in Ref. [207], to make explicit the color flow. The unfolded plane corresponds now to the (u,t) plane (Fig. 24). The t- and u-channel singularities are obtained by cutting the box diagrams by horizontal and vertical lines, respectively. It is evident, here, that the corresponding singularities are two-quark singularities, typical of one-meson states. The s-channel singularities are obtained by cutting the box diagrams by oblique and curved lines passing through the four quark propagators. However, when the diagram is color-planar, as is the case here, the cuts produce disconnected singularities, concentrated at opposite corners and corresponding to radiative corrections of external-meson propagators or of current vertices. s-channel singularities may arise only when the diagram is color-nonplanar.

A typical color-nonplanar diagram, which contributes to the s-channel singularities, is presented in Fig. 25, together with its unfolded form, where the nonplanarity is manifest.

The efficient Landau equations are obtained by cutting the diagram (a) of Fig. 25 by a vertical line passing between the two gluon lines. One now finds a physical singularity in the s-channel at the position $s=(\sum_{i=1}^4 m_i)^2$, as in the case of Fig. 22b. Therefore, this diagram, together with other diagrams of the same color-topological class, will contribute to the formation of two-meson interacting states and eventually to that of tetraquark states.

It is worthwhile noticing the difference of behavior in N_c of the diagram (b) of Fig. 22 and the diagram (a) of Fig. 25 – $O(N_c^0)$ for the first and $O(N_c^{-1})$ for the second – contributing to the formation of tetraquarks in the direct

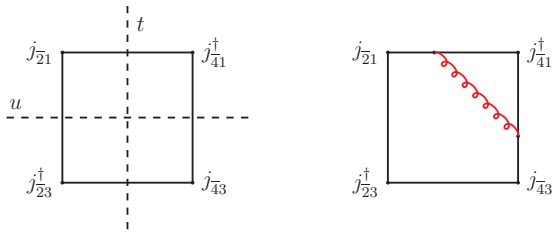

(a) $O(N_c)$ (b) $O(N_c)$

Figure 24: Diagrams of Fig. 23 in unfolded form.

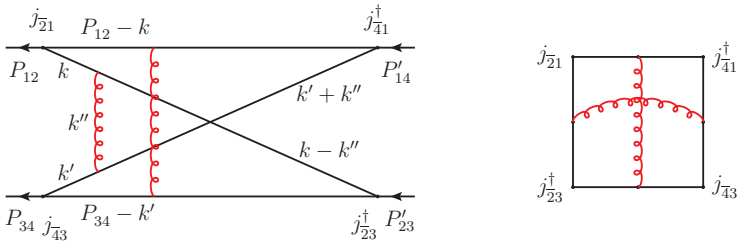

(a) $O(N_c^{-1})$ (b) $O(N_c^{-1})$

Figure 25: (a) Diagram in the quark-rearrangement channel $M_{\bar{4}1}M_{\bar{2}3} \to M_{\bar{2}1}M_{\bar{4}3}$ of the meson-meson scattering amplitude, participating, at large N_c, in the formation of possible tetraquark states. (b) The same diagram in the unfolded (u,t) plane, displaying its color-nonplanar character.

and recombination channels, respectively. This outlines the color-topological difference that exists between them: the former is planar, while the latter is nonplanar, a feature that may have consequences for the various couplings of tetraquarks to two-meson states.

Other examples or details of Landau equations can be found in Ref. [208].

5. Tetraquarks at large N_c

This section is devoted to a detailed study of some of the properties of tetraquarks at large N_c. We have seen, in Secs. 3.2 and 3.3, that tetraquarks at large N_c may be described by (N_c-2) inequivalent classes of operators having different numbers of valence quarks [Eq. (43)], generically each having (N_c-J) valence quarks and (N_c-J) valence antiquarks, where J takes values from 1 to (N_c-2). In multilocal form, they are pictorially represented, for the antisymmetric representation, in Fig. 19. For $J=(N_c-2)$, the representation is similar, in local form, to that of SU(3): the tetraquark continues to be described by two pairs of valence quarks and antiquarks. In particular, the local currents (27), (28) and (32) continue representing sources of tetraquarks. This situation is very similar to that of ordinary mesons, for which the extension of the gauge group to SU(N_c) does not change their description. For the representations with $1 \le J \le (N_c-3)$, one has new descriptions and, for values of J close to 1, the latter become similar to the description found for baryons: the number of valence quarks and antiquarks grows with N_c and presumably also the mass of the tetraquarks. Here, the tetraquark becomes rather a many-body object, requiring a different type of treatment. It is not clear, for the time being, which representation provides the most faithful description in the limit $N_c=3$. The most general situation would correspond to a mixture of all the above representations. Since, however, the representation with $J=(N_c-2)$ does not require any modification of treatment, it remains the most practical one from the mathematical and phenomenological viewpoints. This is why we shall concentrate, in the present section and review, on this representation. The reader may consult Refs. [196, 197] for a detailed account of the properties of tetraquarks in higher representations.

One particular feature of tetraquark and multiquark currents, met in Sec. 3, is their decomposition property into combinations of products of ordinary mesonic or baryonic currents, reflecting their color reducibility. At large N_c, two-point functions of tetraquark currents are dominated by the contributions of their disconnected parts [Eq. (44)]. This fact has led Witten and Coleman to conclude that multiquark states should not exist in QCD, at least as confined states [114, 142]. Actually, as was emphasized by Weinberg [195], the situation may be more complex. Dynamical effects may still be at work, preventing the multiquark states from being dissociated into their elementary mesonic or baryonic clusters. In such a case, the multiquark state will appear as a pole, or a narrow resonance, in nonleading terms of the $1/N_c$ expansion. Contrary to the case of ordinary mesons and baryons, in order to detect the conditions in which multiquark states may appear, one has to go, in the $1/N_c$ expansion of correlation functions of currents, beyond the leading orders. Studies in this line of approach can be found in Refs. [207–214].

Since the tetraquark state can couple, in the present representation, to two mesonic currents, it can naturally be probed in meson-meson scattering amplitudes, appearing as a possible pole or a resonance. We therefore shall study the tetraquark properties at large N_c through the N_c-leading or subleading typical Feynman diagrams that may contribute to its emergence. We shall first concentrate, in the following, on the case of fully exotic tetraquarks, containing four different quark flavors. This has the advantage of excluding mixings with ordinary mesons, which often may prevent one from drawing a clear conclusion. The case of cryptoexotic tetraquarks will be considered afterwards.

In searching for tetraquark poles, the following features should also be taken into account. Tetraquark poles in the s-channel may emerge in two different ways. The first possibility may take place within a class of diagrams having the same N_c-leading behavior, that is, belonging to the same color-planarity, an example of which is the class of planar diagrams. Here one sums a series of gluon propagators which might produce the expected pole. Such a mechanism would be representative of the production of a bound-state spectrum through the confining forces, as is already at work for the case of ordinary mesons. One important property of this mechanism is that, once the global N_c-dependence of the diagrams has been factorized, the bound-state equation becomes N_c-independent (at leading order), implying N_c-independence of the corresponding masses.

The second type of mechanism is related to the summation of diagrams not having the same N_c-leading behaviors. This happens when one considers, as a starting point, diagrams not having four-quark s-channel singularities, eventually having t- and u-channel singularities, representing ordinary-meson exchanges, or, in the simplest cases, four-meson contact terms. Examples of these cases are presented in the forthcoming Figs. 26 and 27. Such diagrams play the role of kernels in bound-state equations and generate, with the aid of the four quark propagators, a series of diagrams whose summation may lead to the emergence of poles. There are, however, two main differences with respect to the first type of mechanism outlined above: First, these kernels, as can be checked from Figs. 26 and 27, are of order $O(N_c^{-2})$ or $O(N_c^{-1})$; therefore, their iteration generates diagrams with lower N_c-dependences. An immediate consequence of this is that the resulting bound-state equation would have an N_c-dependent interaction kernel (generally vanishing when $N_c \to \infty$), whose effect would be that the mass of the possibly existing bound state or resonance either approaches the two-meson threshold or disappears at infinity with increasing N_c. The second difference is that the above kernels are of short-range type, since they involve either meson contact terms or meson exchanges; therefore, this mechanism is typical of the production of bound states or resonances in the molecular-type scheme, where the effective degrees of freedom are ultimately reduced to those of mesons.

In our subsequent analyses of Secs. 5.1, 5.2 and 5.3 we shall be primarily interested in the first type of mechanism, searching for the conditions of emergence of tetraquark poles from confining forces. The second type of mechanism, in relation with QCD Feynman diagrams, will be considered in Sec. 5.4 and, in a more general framework, in Sec. 6.

5.1. Fully exotic tetraquarks

Most of the material needed for this study has been already introduced in Sec. 4. We consider two pairs of quarks and antiquarks, with four different flavors, which we distinguish by the labels 1 and 3 for the quarks and $\overline{2}$ and $\overline{4}$ for the antiquarks. We then consider the four-current correlation functions (56) and (57), describing two direct channels and two quark-recombination channels, designated by $D1$, $D2$, $R1$ and $R2$, respectively.

We first consider the direct channels. The corresponding leading disconnected and connected diagrams, for channel $D1$, have been given in Fig. 22. It is understood that each such diagram is accompanied by an infinite number of other diagrams with many-gluon exchanges belonging to the same color-topology class (here, planar). It is only the

connected part of the correlation function that may provide information about the corresponding scattering amplitude. To isolate the latter, one has to factorize in the connected part of the correlation function the external meson propagators, together with the meson couplings [Eqs. (12) and (13)]. These diagrams, as has been shown by Eqs. (58)–(60), have four-quark singularities in the s-channel and hence may participate in the formation, as intermediate states, of two-meson states, as well as of possible tetraquark states, the latter henceforth being designated by T.

One then obtains the leading large-N_c behaviors for the two-meson scattering amplitudes in channels $D1$ and $D2$ and the corresponding transition amplitudes through two-meson and tetraquark intermediate states, respectively:

$$A(M_{\bar{2}1}M_{\bar{4}3} \to M_{\bar{2}1}M_{\bar{4}3}) \sim A(M_{\bar{2}3}M_{\bar{4}1} \to M_{\bar{2}3}M_{\bar{4}1}) = O(N_c^{-2}), \tag{62}$$

$$A(M_{\bar{2}1}M_{\bar{4}3} \to MM \to M_{\bar{2}1}M_{\bar{4}3}) \sim A(M_{\bar{2}3}M_{\bar{4}1} \to MM \to M_{\bar{2}3}M_{\bar{4}1}) = O(N_c^{-2}), \tag{63}$$

$$A(M_{\bar{2}1}M_{\bar{4}3} \to T \to M_{\bar{2}1}M_{\bar{4}3}) \sim A(M_{\bar{2}3}M_{\bar{4}1} \to T \to M_{\bar{2}3}M_{\bar{4}1}) = O(N_c^{-2}). \tag{64}$$

We next consider the recombination channels (57). Typical N_c-leading and -subleading diagrams have been shown in Figs. 23 and 25. Only diagrams of the type of Fig. 25 do have s-channel four-quark singularities and hence may participate in the formation of two-meson and tetraquark states. On the other hand, the N_c-leading diagrams, such as those of Fig. 23, contribute to parts of the scattering amplitude that do not have s-channel singularities. One obtains the following large-N_c behaviors of the scattering amplitudes in channels $R1$ and $R2$ and the corresponding transition amplitudes through two-meson and tetraquark intermediate states, respectively:

$$A(M_{\bar{4}1}M_{\bar{2}3} \to M_{\bar{2}1}M_{\bar{4}3}) \sim A(M_{\bar{2}1}M_{\bar{4}3} \to M_{\bar{4}1}M_{\bar{2}3}) = O(N_c^{-1}), \tag{65}$$

$$A(M_{\bar{4}1}M_{\bar{2}3} \to MM \to M_{\bar{2}1}M_{\bar{4}3}) \sim A(M_{\bar{2}1}M_{\bar{4}3} \to MM \to M_{\bar{4}1}M_{\bar{2}3}) = O(N_c^{-3}), \tag{66}$$

$$A(M_{\bar{4}1}M_{\bar{2}3} \to T \to M_{\bar{2}1}M_{\bar{4}3}) \sim A(M_{\bar{2}1}M_{\bar{4}3} \to T \to M_{\bar{4}1}M_{\bar{2}3}) = O(N_c^{-3}). \tag{67}$$

One can analyze Eqs. (62) and (65) in terms of effective meson vertices. Four-meson vertices of the direct type appear as being of order N_c^{-2}, while those of the recombination type of order N_c^{-1} (Figs. 26a and 27a):

$$g(M_{\bar{2}1}M_{\bar{4}3}M_{\bar{2}1}M_{\bar{4}3}) \sim g(M_{\bar{4}1}M_{\bar{2}3}M_{\bar{4}1}M_{\bar{2}3}) = O(N_c^{-2}), \tag{68}$$

$$g(M_{\bar{4}1}M_{\bar{2}3}M_{\bar{2}1}M_{\bar{4}3}) = O(N_c^{-1}). \tag{69}$$

Four-meson contact terms are also accompanied by glueball-exchange and one-meson-exchange terms (Figs. 26b and 27b).

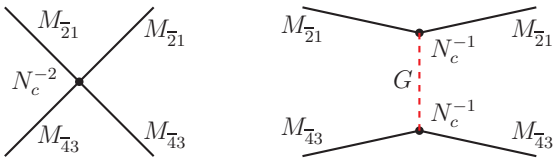

(a) $O(N_c^{-2})$ (b) $O(N_c^{-2})$

Figure 26: (a) Four-meson vertex in the direct channel $D1$ [Eq. (56)]. (b) Glueball exchange in the same channel. Similar diagrams also exist in the direct channel $D2$.

The determination of the behaviors of four-meson vertices, including contact terms and meson exchanges, allows us to evaluate the contributions of two-meson intermediate states in the above processes. They are summarized in Fig. 28, where we have kept, for simplicity, only contact-type interactions. They consistently reproduce the behaviors expected from Eqs. (63) and (66). Similar conclusions could also be obtained from the glueball- and one-meson-exchange diagrams.

The validity of the behaviors displayed in Fig. 28 can also be verified on individual Feynman diagrams with gluon exchanges, using the Landau equations and recognizing the type of intermediate state that can be obtained from the

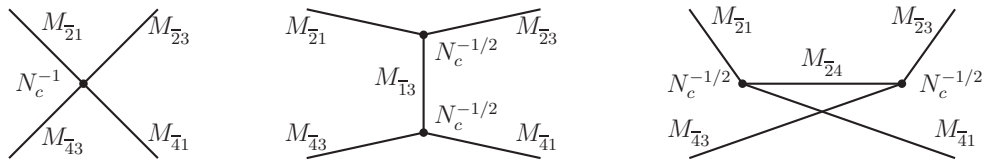

(a) $O(N_c^{-1})$ (b) $O(N_c^{-1})$ (c) $O(N_c^{-1})$

Figure 27: (a) Four-meson vertex in the recombination channel $R1$ [Eq. (57)]. (b,c) One-meson exchanges in the same channel. Similar diagrams also exist in the recombination channel $R2$.

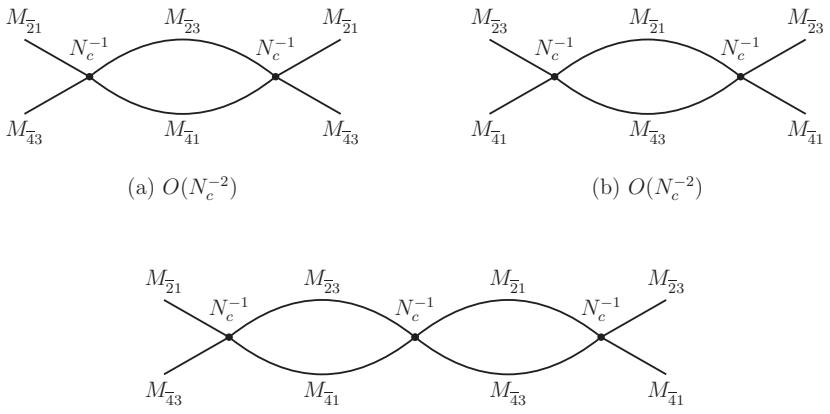

(a) $O(N_c^{-2})$ (b) $O(N_c^{-2})$

(c) $O(N_c^{-3})$

Figure 28: Leading-order contributions of two-meson intermediate states to the direct, (a) and (b), and recombination, (c), channels.

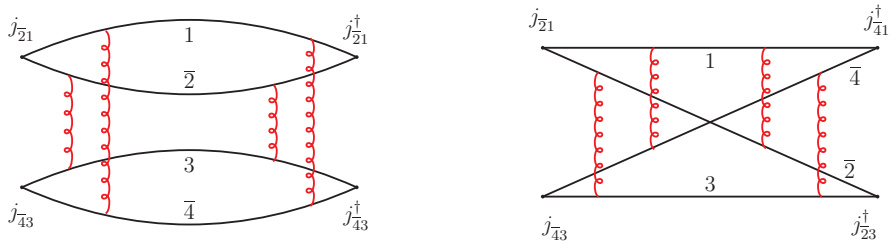

(a) $O(N_c^0)$ (b) $O(N_c^{-1})$

Figure 29: (a) Feynman diagram contributing to the reconstruction of the two-meson intermediate state $M_{\bar{4}1}M_{\bar{2}3}$ in the direct channel $D1$ [Fig. 28a]. (b) Feynman diagram contributing to the reconstruction of the two-meson intermediate states in the recombination channel $R1$ [Fig. 28c].

summation, with respect to multigluon exchanges, of such types of diagrams. Two examples are displayed in Fig. 29. In diagram (a), contributing to the direct channel $D1$, the intermediate state is manifestly the two-meson state $M_{\bar{4}1}M_{\bar{2}3}$, while the external mesons are $M_{\bar{2}1}M_{\bar{4}3}$. This corresponds to Fig. 28a. In diagram (b) of Fig. 29, contributing to the recombination channel $R1$, the intermediate state is composed of $M_{\bar{2}1}M_{\bar{4}3}$ on the right and of $M_{\bar{4}1}M_{\bar{2}3}$ on the left. This corresponds to Fig. 28c. (Also, one should not forget that in the right and left corners of the diagrams of Fig. 29, near the vertices of the currents j, one still has planar multigluon exchanges, whose infinite sum reconstitutes the external mesons.)

The properties of possibly existing tetraquark states can be extracted from Eqs. (64) and (67). One observes that a single tetraquark alone cannot satisfy these two equations. At least two different tetraquarks, which we designate by T_A and T_B, are needed to fulfill the conditions imposed by these equations. The results for tetraquark to two-meson-state transition amplitudes are the following (see Fig. 30):

$$A(T_A \to M_{\bar{2}1}M_{\bar{4}3}) \sim O(N_c^{-1}), \quad A(T_A \to M_{\bar{2}3}M_{\bar{4}1}) \sim O(N_c^{-2}), \tag{70}$$

$$A(T_B \to M_{\bar{2}3}M_{\bar{4}1}) \sim O(N_c^{-1}), \quad A(T_B \to M_{\bar{2}1}M_{\bar{4}3}) \sim O(N_c^{-2}). \tag{71}$$

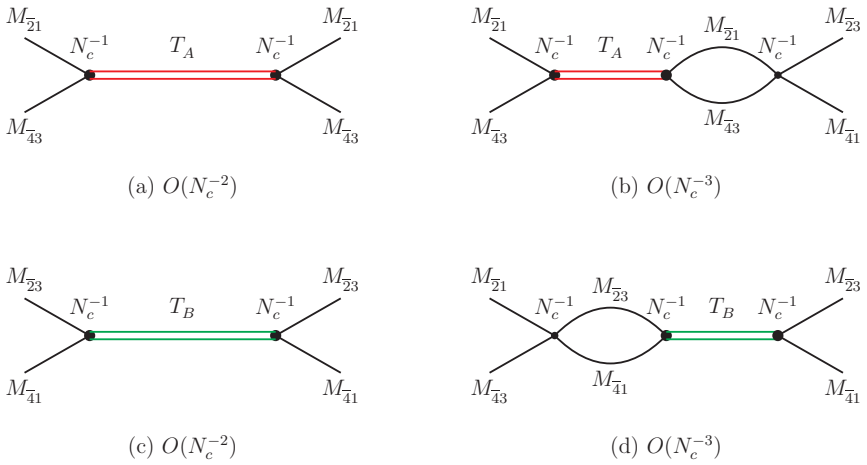

Figure 30: Leading-order contributions of tetraquarks T_A and T_B to the direct (a,c) and recombination (b,d) channels.

If the tetraquarks lie above the two-meson thresholds, the decay widths into two mesons are

$$\Gamma(T_A) \sim \Gamma(T_B) = O(N_c^{-2}), \tag{72}$$

which are smaller than those of the ordinary mesons [$\Gamma = O(N_c^{-1})$] by one power of N_c.

To have an insight into the internal structure of the two tetraquark candidates, one can transcribe the information about the four-meson couplings coming from Eqs. (68)–(69) into an effective Lagrangian, expressed through quark color-singlet bilinears:

$$\begin{aligned}\mathcal{L}_{\text{eff,int}} = & -\frac{\lambda_1}{N_c}[(\overline{q}_2 q_1)(\overline{q}_4 q_3)(\overline{q}_3 q_2)(\overline{q}_1 q_4) + (\overline{q}_4 q_1)(\overline{q}_2 q_3)(\overline{q}_3 q_4)(\overline{q}_1 q_2)] \\ & -\frac{\lambda_2}{N_c^2}[(\overline{q}_2 q_1)(\overline{q}_4 q_3)(\overline{q}_3 q_4)(\overline{q}_1 q_2) + (\overline{q}_2 q_3)(\overline{q}_4 q_1)(\overline{q}_1 q_4)(\overline{q}_3 q_2)],\end{aligned} \tag{73}$$

where we have explicitly factored out the N_c-dependence of the coupling constants. One then deduces from Eqs. (70) and (71) that the tetraquark fields T_A and T_B should have, at leading order at large N_c, the following structure in terms of the quark color-singlet bilinears:

$$T_A \sim (\overline{q}_2 q_3)(\overline{q}_4 q_1), \qquad T_B \sim (\overline{q}_2 q_1)(\overline{q}_4 q_3). \tag{74}$$

This result favors a color singlet-singlet structure of the tetraquarks in the exotic case. We notice that, according to Eqs. (70) and (71), the main decay channels of the tetraquarks are not of the dissociative type, but rather of the quark rearrangement type.

It is worth emphasizing here that the two-meson contributions, found in Eqs. (63) and (66) [Fig. 28], saturate by themselves, at large N_c, the singularity structure emerging from the Feynman diagrams. Contrary to the ordinary-meson case, they are in competition with the contributions of possibly existing tetraquarks. Therefore, the presence of the latter does not appear as mandatory for the saturation of the large-N_c equations. The results found above about the tetraquark couplings to two mesons and about their decay widths have, therefore, the meaning of upper bounds. Eventually, one might encounter an intermediate situation, where one of the tetraquarks, T_B, say, is absent from the spectrum for some dynamical reason. In that case, one tetraquark, T_A, would exist and, if it lies above the two-meson threshold, it would be observed through its preferred decay channel [Eq. (70)].

5.2. Cryptoexotic states

We next consider cryptoexotic channels, involving three different quark flavors, designated by 1, 2 and 3. As in Eqs. (56) and (57), we consider correlation functions describing two direct and two recombination channels:

$$\Gamma_{D1} \equiv \langle j_{\bar{2}\bar{3}}(x) j_{\bar{3}\bar{1}}(y) j^\dagger_{\bar{3}\bar{1}}(z) j^\dagger_{\bar{2}\bar{3}}(0)\rangle, \quad \Gamma_{D2} \equiv \langle j_{\bar{2}\bar{1}}(x) j_{\bar{3}\bar{3}}(y) j^\dagger_{\bar{3}\bar{3}}(z) j^\dagger_{\bar{2}\bar{1}}(0)\rangle, \tag{75}$$

$$\Gamma_{R1} \equiv \langle j_{\bar{2}\bar{3}}(x) j_{\bar{3}\bar{1}}(y) j^\dagger_{\bar{3}\bar{3}}(z) j^\dagger_{\bar{2}\bar{1}}(0)\rangle, \quad \Gamma_{R2} \equiv \langle j_{\bar{2}\bar{1}}(x) j_{\bar{3}\bar{3}}(y) j^\dagger_{\bar{3}\bar{1}}(z) j^\dagger_{\bar{2}\bar{3}}(0)\rangle. \tag{76}$$

Leading and subleading diagrams of the direct channel $D1$ are represented in Fig. 31.

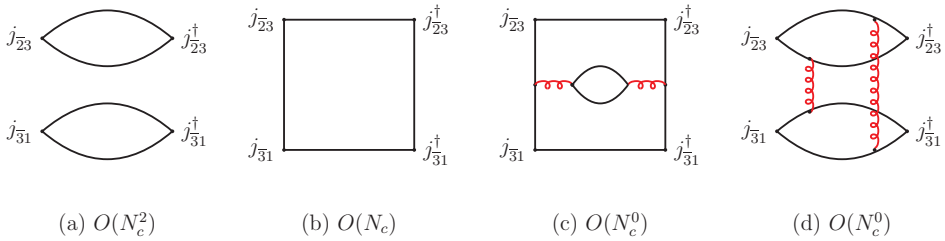

(a) $O(N_c^2)$ (b) $O(N_c)$ (c) $O(N_c^0)$ (d) $O(N_c^0)$

Figure 31: Leading- and subleading-order diagrams of the direct channel $D1$ of Eq. (75).

Diagram (b) of Fig. 31 corresponds to the leading-order contribution to the meson-meson scattering amplitude. It has only a two-quark singularity in the s-channel, which represents the contribution of a single-meson intermediate state. This diagram has also a t-channel one-meson singularity, as well as parts representing four-meson contact terms (cf. Figs. 34b and c); by iteration, they may generate poles in two-meson intermediate states. This type of mechanism of producing poles was previously advocated just before Sec. 5.1, to which we refer the reader. General aspects of it will be considered in Secs. 5.4 and 6. We are focusing in Secs. 5.1, 5.2 and 5.3 on the pole production mechanism that occurs in diagrams having the same N_c-leading behaviors.

Diagram (c) represents contributions from radiative corrections to the previous diagram. In the space of meson states, the first part of the intermediate states contributes to the formation of a single-meson state, which then emits two virtual mesons, or a tetraquark, and reabsorbs them later. This diagram may also describe a mixing between a single-meson state and a tetraquark state, having the same quantum numbers.

Diagram (d) represents a direct contribution of two-meson states and/or of a tetraquark state.

For the direct channel $D2$, the structure of the diagrams is similar to that of Fig. 22 and is represented in Fig. 32.

For the recombination channel $R1$ of Eq. (76), the main leading and subleading diagrams are shown in Fig. 33. Diagram (a) does not have s-channel singularities [cf. Fig. 23a and related comment], while diagrams (b) and (c) receive contributions from four-quark intermediate states in the s-channel. Similar conclusions also hold for the recombination channel $R2$.

From the previous results, one may obtain information about the various scattering and transition amplitudes and effective meson couplings, as in Eqs. (62)–(69). The effective meson-meson interactions at the vertex level are summarized in Fig. 34.

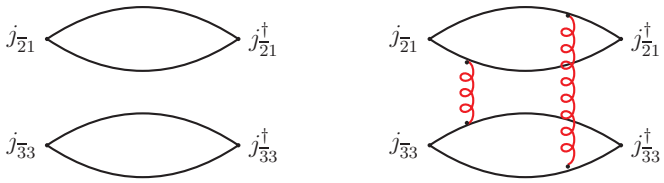

(a) $O(N_c^2)$ (b) $O(N_c^0)$

Figure 32: Leading- and subleading-order diagrams of the direct channel $D2$ of Eq. (75).

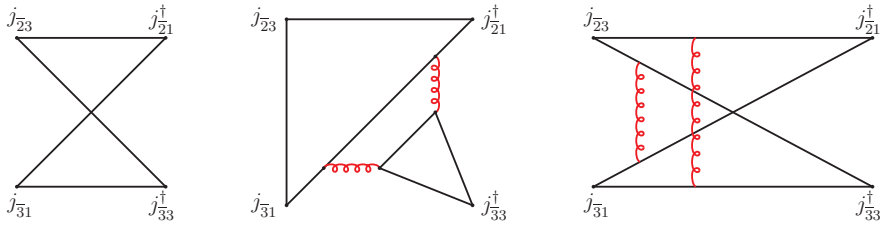

(a) $O(N_c)$ (b) $O(N_c^0)$ (c) $O(N_c^{-1})$

Figure 33: Leading- and typical subleading-order diagrams of the recombination channel $R1$ of Eq. (76). Similar diagrams also occur in the channel $R2$.

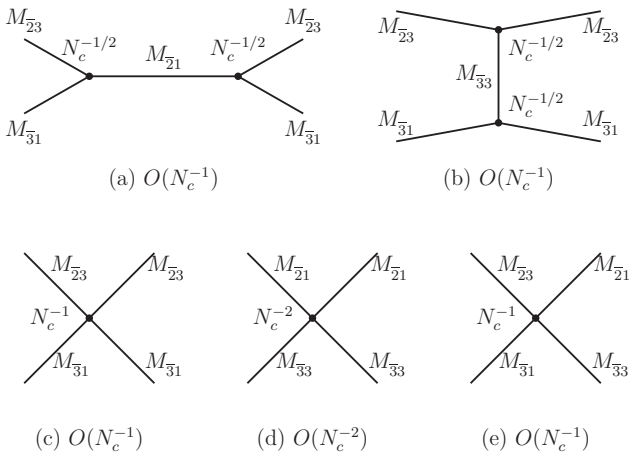

(a) $O(N_c^{-1})$ (b) $O(N_c^{-1})$

(c) $O(N_c^{-1})$ (d) $O(N_c^{-2})$ (e) $O(N_c^{-1})$

Figure 34: Tree-level vertex diagrams with meson propagators in the direct channel $D1$ (a,b,c), the direct channel $D2$ (d) and the recombination channel $R1$ (e). (u-channel analog of diagram (b) not drawn.)

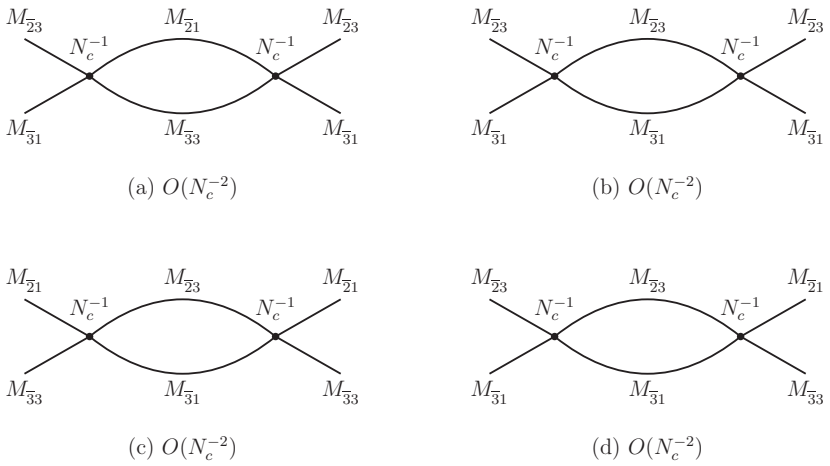

Figure 35: Two-meson intermediate-state contributions to the direct channel $D1$ (a,b), the direct channel $D2$ (c) and the recombination channel $R1$ (d).

The contributions of two-meson intermediate states are represented graphically in Fig. 35.

The tetraquark contributions are extracted in the same way as for the exotic channels. Because of the presence of the additional diagram (b) of Fig. 33, they are of the same order in all four channels and hence a single tetraquark T might accommodate all the corresponding constraints. However, a more detailed analysis of the mechanism of formation of two-meson and tetraquark intermediate states suggests that we again are in the presence of two different tetraquarks T_A and T_B, whose field structures, in terms of valence quarks and antiquarks, are

$$T_A \sim (\overline{q}_2 q_3)(\overline{q}_3 q_1), \qquad T_B \sim (\overline{q}_2 q_1)(\overline{q}_3 q_3). \tag{77}$$

This conclusion is based on calculations similar to those presented for the exotic case in Sec. 5.4, where, now, the cryptoexotic case gives rise to additional diagrams. The results are graphically summarized in Fig. 36. Actually, diagrams (a) and (d) of that figure may not exist, but could be represented by the mixing-mechanism diagrams (b) of Figs. 38 and 37, respectively (see below). This issue depends more sensitively on the formation mechanism of the tetraquarks.

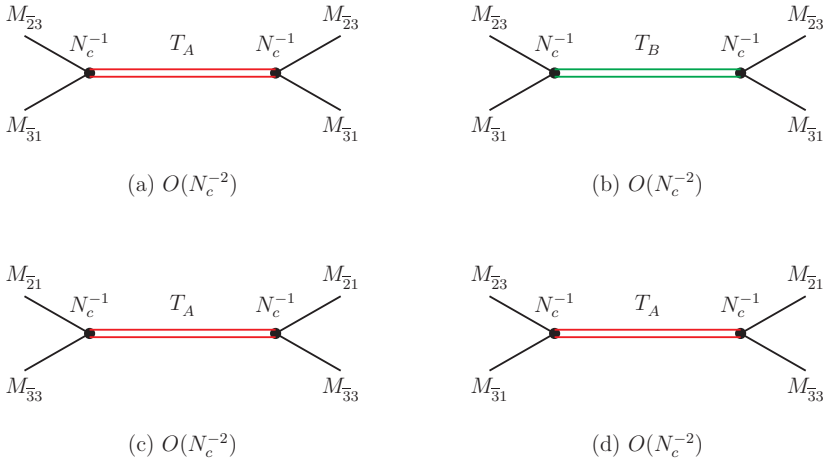

Figure 36: Tetraquark-state contributions to the direct channel $D1$, (a) and (b), the direct channel $D2$, (c), and the recombination channel $R1$, (d).

The decay widths of the tetraquarks into two mesons are again of order N_c^{-2} [Eq. (72)].

Diagram (b) of Fig. 33 may also describe mixings of two-meson or tetraquark states with a single-meson state that appears in the left part of the diagram. Figure 37 graphically describes this phenomenon.

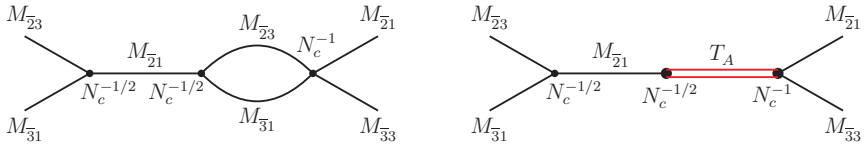

(a) $O(N_c^{-2})$ (b) $O(N_c^{-2})$

Figure 37: Mixings, in the recombination channel $R1$, of a single-meson state with two-meson (a) and tetraquark (b) states.

Mixings of a single-meson state with two-meson and tetraquark states also exist in the direct channel $D1$, as was previously mentioned, emerging from diagrams of the type of Fig. 31c. Since in the quark loop the quark and the antiquark can have any flavor, the resulting two-meson and tetraquark states may belong to another class of cryptoexotic states. Figure 38 graphically describes this phenomenon. Cryptoexotic tetraquarks may therefore decay

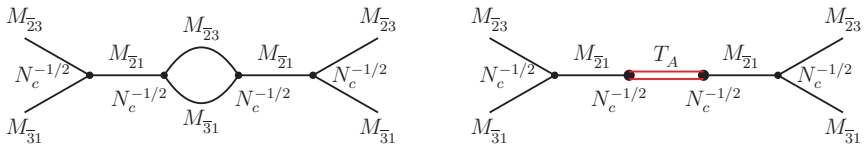

(a) $O(N_c^{-2})$ (b) $O(N_c^{-2})$

Figure 38: Mixings, in the direct channel $D1$, of a single-meson state with two-meson (a) and tetraquark (b) states.

into two mesons either through a direct coupling or through a mixing with single-meson states. In both cases, the transition amplitude is of order $O(N_c^{-1})$.

Cryptoexotic channels with two quark flavors can be treated in the same way as before. Here, the correlation functions to be considered are

$$\Gamma_{D1} \equiv \langle j_{\bar{2}\bar{1}}(x) j_{\bar{1}\bar{2}}(y) j^{\dagger}_{\bar{1}\bar{2}}(z) j^{\dagger}_{\bar{2}\bar{1}}(0)\rangle, \quad \Gamma_{D2} \equiv \langle j_{\bar{2}\bar{2}}(x) j_{\bar{1}\bar{1}}(y) j^{\dagger}_{\bar{1}\bar{1}}(z) j^{\dagger}_{\bar{2}\bar{2}}(0)\rangle, \tag{78}$$

$$\Gamma_{R1} \equiv \langle j_{\bar{2}\bar{1}}(x) j_{\bar{1}\bar{2}}(y) j^{\dagger}_{\bar{1}\bar{1}}(z) j^{\dagger}_{\bar{2}\bar{2}}(0)\rangle, \quad \Gamma_{R2} \equiv \langle j_{\bar{2}\bar{2}}(x) j_{\bar{1}\bar{1}}(y) j^{\dagger}_{\bar{1}\bar{2}}(z) j^{\dagger}_{\bar{2}\bar{1}}(0)\rangle. \tag{79}$$

Most of the leading and subleading diagrams are similar to those found in the three-flavor case. In addition, one finds, in the direct channel $D1$, annihilation-type diagrams involving at least two gluon lines, which produce, as intermediate states in the s-channel, glueballs (cf. Figs. 39 and 13). Mixings of tetraquarks with glueball states are of subleading order. Therefore, the main conclusions about tetraquark decay widths and two-meson intermediate states remain unchanged.

5.3. Open-flavor-type states

We now consider the case of an open flavor, where two quark fields have the same flavor. The corresponding four-point correlation function is

$$\Gamma \equiv \langle j_{\bar{2}\bar{3}}(x) j_{\bar{1}\bar{3}}(y) j^{\dagger}_{\bar{1}\bar{3}}(z) j^{\dagger}_{\bar{2}\bar{3}}(0)\rangle. \tag{80}$$

Here, the direct and the recombination channels are identical, with the common scattering process $M_{\bar{2}\bar{3}} M_{\bar{1}\bar{3}} \to M_{\bar{2}\bar{3}} M_{\bar{1}\bar{3}}$. The corresponding leading and main subleading diagrams are represented in Fig. 40.

The effective meson-meson interaction vertex, the two-meson intermediate-state contribution and the tetraquark state are graphically represented in Fig. 41. The decay width of the tetraquark into two mesons is of order N_c^{-2}. The tetraquark state couples to the local current $(\bar{q}_2 q_3)(\bar{q}_1 q_3)$, which should be antisymmetrized with respect to the quark field q_3, taking into account its spin degrees of freedom.

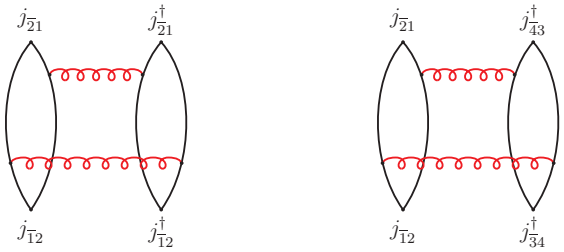

(a) $O(N_c^0)$ (b) $O(N_c^0)$

Figure 39: (a) Glueball appearance in the intermediate states of the s-channel of the scattering process $M_{\bar{2}1}M_{\bar{1}2} \to M_{\bar{2}1}M_{\bar{1}2}$. (b) Similar phenomenon in the scattering process $M_{\bar{4}3}M_{\bar{3}4} \to M_{\bar{2}1}M_{\bar{1}2}$. This diagram also contributes in the t-channel of the scattering process $M_{\bar{2}1}M_{\bar{4}3} \to M_{\bar{2}1}M_{\bar{4}3}$ (cf. Fig. 26b).

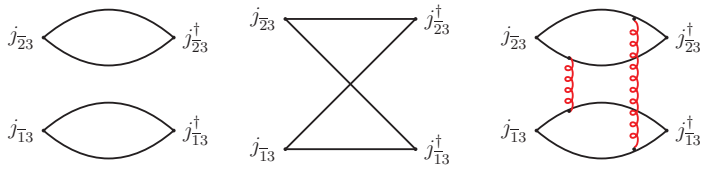

(a) $O(N_c^2)$ (b) $O(N_c)$ (c) $O(N_c^0)$

Figure 40: Leading and subleading diagrams in the open-flavor channel of the correlation function (80).

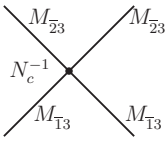

(a) $O(N_c^{-1})$

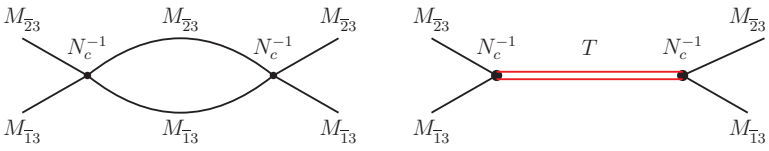

(b) $O(N_c^{-2})$ (c) $O(N_c^{-2})$

Figure 41: Four-meson effective vertex (a), two-meson intermediate states (b), and tetraquark intermediate state (c), corresponding to the open-flavor scattering process $M_{\bar{2}3}M_{\bar{1}3} \to M_{\bar{2}3}M_{\bar{1}3}$. (Meson-exchange diagrams, as in Fig. 27, are not represented.)

5.4. Are there tetraquarks at large N_c?

The fact that, in the exotic and cryptoexotic channels, the possibly existing tetraquarks should have, at N_c-leading order of the connected diagrams, an internal structure made of two mesonic clusters [Eqs. (74) and (77)] requires further clarification for the understanding of such a result. The main observation is that these solutions do not correspond to the expected diquark-antidiquark structure, which would result from a confining mechanism of the four-constituent system.

The reason for this can be traced back to the different behaviors of quark-antiquark and diquark systems at large N_c. In quark-antiquark systems, ladder-type gluon-exchange diagrams are planar and therefore the infinite number of such diagrams contributes with equal power of N_c to the whole sum (cf. Fig. 5). This is a necessary condition to possibly form, at that order of N_c, a bound-state pole in the corresponding scattering amplitude.

This is not the case for diquark (or antidiquark) systems. Ladder-type diagrams are damped by factors of N_c^{-1} at each inclusion of a gluon line (cf. Fig. 15). Here, it is the completely crossed diagrams which play the role of planar diagrams. However, the sum of such diagrams is of no help for the formation of bound states, since completely crossed diagrams do not have s-channel singularities and are parts of the definition of the irreducible kernel of any integral or bound-state equation. The formation of a bound state (or of a quasi-bound state) of a diquark necessitates the summation of ladder diagrams. One cannot obtain, with such type of summation, a bound state which would be stable with respect to a given order of N_c.

The above features can also be formulated in terms of the quark-antiquark and quark-quark scattering amplitudes, designated by $\mathcal{T}$, the first being in the color-singlet representation and the second in the antisymmetric representation. Designating by K the one-gluon-exchange kernel, wherein the coupling constant has been redefined according to 't Hooft's limit, Eq. (3), and from which color indices have been either factorized or summed together with nearby other color-tensor contributions, the two scattering amplitudes satisfy, after summation of all ladder diagrams, the integral equations

$$\mathcal{T}_{\bar{q}q} = \frac{1}{N_c} K + K * G_0 * \mathcal{T}_{\bar{q}q}, \tag{81}$$

$$\mathcal{T}_{qq} = \frac{1}{N_c} K + \frac{1}{N_c} K * G_0 * \mathcal{T}_{qq}, \tag{82}$$

where G_0 represents the two quark propagators, the star operation takes into account the eventual integrations with respect to the momenta, and the leading behaviors in N_c have been factorized.

In the quark-antiquark case, Eq. (81), a rescaling of $\mathcal{T}$ in the form $\mathcal{T}/N_c$ removes the factor $1/N_c$ from the equation and transforms the latter into an N_c-independent equation. If the latter equation is assumed, with an appropriate form of the gluon propagator, to be valid in the confining regime, then the resulting meson bound states will have, at leading order of N_c, N_c-independent masses, thus confirming the soft behavior of the latter under variations of N_c from infinity down to $N_c = 3$.

This is not the case for the diquark system. The previous rescaling of $\mathcal{T}$ does not remove the $1/N_c$ dependence of the kernel of the integral equation (82). To have a qualitative understanding of the consequences of the $1/N_c$ dependence of the kernel, which we assume being transmitted to the confining interaction, we consider the illustrative example of two heavy quarks, with reduced mass μ, satisfying the Schrödinger equation with a linearly confining potential:

$$\left[E - \frac{\mathbf{p}^2}{2\mu} - \frac{1}{N_c}\sigma r \right]\phi = 0, \tag{83}$$

where σ is the string tension and the $1/N_c$ dependence of the potential has been explicitly factorized. This equation leads to the formation of confined bound states, with bound state energies and mean spatial sizes scaling with respect to N_c in the following way:

$$E \sim \left(\frac{N_c\sqrt{\sigma}}{2\mu}\right)^{1/3} \frac{\sqrt{\sigma}}{N_c}, \qquad \langle r \rangle \sim \left(\frac{N_c\sqrt{\sigma}}{2\mu}\right)^{1/3} \frac{1}{\sqrt{\sigma}}. \tag{84}$$

At large N_c, the bound-state energies decrease and the diquark masses tend to the two-quark mass threshold. On the other hand, the mean spatial sizes of the diquarks increase, although weakly, with N_c and the diquarks cease to be

compact objects, in contradiction with the initial objective of finding diquark and antidiquark systems with compact sizes. In this situation, the system might easily switch to the N_c-dominant configuration made of two mesonic clusters.

The above example can be completed by considering, for the case of heavy quarks, instead of the confining potential, the color-Coulomb potential, which governs the dynamics at short distances and which is assumed to dominate for heavy-quark systems. Here, the interaction potential is $V(r) = -\lambda/(2N_c r)$, where λ is the redefined coupling constant squared at large N_c [Eq. (3)]. Then, when N_c increases, the bound-state spectrum shrinks rapidly, like $1/N_c^2$, to the two-quark threshold from below, while the mean spatial sizes of the bound states increase like N_c, much more rapidly than in the purely confining-potential example. In the present case, when the diquark system reaches the confining region, it already has ceased to be compact.

The above results can also be understood with the aid of the quadratic Casimirs of the various representations. Assuming that the confining interaction kernel has the same color-representation property as the gluon propagator, one can evaluate the relative strengths of the various two-body potentials (for more details, cf. Ref. [23], Appendix B). For the quark-antiquark system in the singlet representation, the potential is proportional to $-(N_c^2-1)/(2N_c)$, where the minus sign reflects the attractive nature of the potential. For the same system in the adjoint representation, it is proportional to $+1/(2N_c)$. For the diquark system in the antisymmetric representation [2] (Sec. 3.2), it is proportional to $-(N_c+1)/(2N_c)$, while in the symmetric representation [1, 1], it is proportional to $+(N_c-1)/(2N_c)$. We observe that, at large N_c, the ratio between the diquark potential in the antisymmetric representation and the quark-antiquark potential in the singlet representation decreases like $1/(N_c-1)$, displaying the dominance of the latter potential in the course of the formation of bound systems. For $N_c = 3$, however, the latter ratio is only 1/2, which might make possible the formation of diquark systems inside tetraquarks.

To remedy the above difficulties of the diquark scheme, several dynamical mechanisms have been advocated, either at the experimental production level [68, 215], or at the inner interaction level [216].

On theoretical grounds, an alternative viewpoint has been advocated in Ref. [211]. It was argued that the planar diagrams of the type of Figs. 22b and 29a do not represent, in spite of gluon exchanges and s-channel cuts, genuine interactions between mesons, but rather depict different ways of representing color or momentum flows in a system of two noninteracting mesons, and therefore tetraquark formation graphs should begin from nonplanar diagrams. This argument, if accepted, brings the contribution of the direct-channel $D1$ and $D2$ scattering amplitudes to order N_c^{-4}, instead of N_c^{-2}. However, one still has a discrepancy with the recombination channels, which remain at order N_c^{-3}. To remain at the end with one type of tetraquark, in the diquark-antidiquark antisymmetric representation, one is obliged to impose an additional selection rule, according to which tetraquarks may appear only in direct *or* recombination channels.

The main point of the above argument, the noninteracting feature of the two mesons, does not seem, however, well-founded. Diagrams of the types of Figs. 22b and 29a are representatives of an infinite set of planar diagrams containing at the right and left corners of the quark loops (near the currents j) planar gluons exchanged between antiquark 2 and quark 1, and between antiquark 4 and quark 3, which means that the initial and final parts of the diagrams already contain mesons $M_{\overline{2}1}$ and $M_{\overline{4}3}$; any gluon exchanged between these mesons represents a genuine interaction and not merely a color- or momentum-flow artifact. It is only these kinds of diagram that can describe two-meson-loop formation, as depicted in Fig. 28, which is of order N_c^{-2}. We shall describe below in more detail the mechanism of the two-meson interaction. The question as to whether the planar diagrams may produce by themselves tetraquark poles is more involved and requires further analysis, which we shall also present hereafter.

We come back to the N_c-dominant structure of the four-quark system, made of two mesonic clusters [Eqs. (74) and (77)]. The principal question that remains to be answered is whether such solutions are compatible with the formation of tetraquarks. Considering, for definiteness, the direct channel $D1$ of the flavor-exotic case [Eq. (56)], the candidate tetraquark would have, according to Eq. (74), the structure $T_A \sim (\overline{q}_2 q_3)(\overline{q}_4 q_1)$, which is generated by means of sums, with respect to ladder-gluon lines, of diagrams of the type of Fig. 29a. The gluon lines between quark 1 and antiquark 4 generate the scattering amplitude $\mathcal{T}_{\overline{4}1}$. Similarly, the gluon lines between antiquark 2 and quark 3 generate the scattering amplitude $\mathcal{T}_{\overline{2}3}$. The two scattering amplitudes are disconnected from each other. Nevertheless, they are embedded into the structure of the meson-meson scattering amplitude $\mathcal{T}_{[(\overline{2}1)(\overline{4}3),(\overline{2}1)(\overline{4}3)]} \equiv \mathcal{T}(M_{\overline{2}1}M_{\overline{4}3} \to M_{\overline{2}1}M_{\overline{4}3})$ and are subjected to additional loop integrations, providing a connected structure. A typical contribution is graphically represented in Fig. 42. Other contributions involve either $\mathcal{T}_{\overline{4}1}$ alone or $\mathcal{T}_{\overline{2}3}$ alone.

At leading order in N_c, the scattering amplitudes $\mathcal{T}_{\overline{q}q}$ are saturated by an infinite sum of stable mesons [Sec. 2.3],

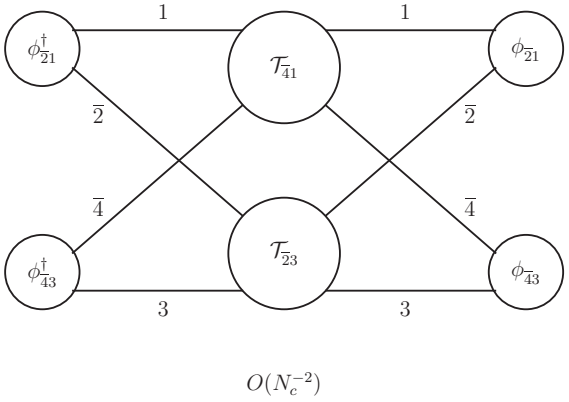

Figure 42: Typical contribution of the quark-antiquark scattering amplitudes $\mathcal{T}_{\overline{4}1}$ and $\mathcal{T}_{\overline{2}3}$ to the meson-meson scattering amplitude of the direct channel $D1$ [Eq. (56)]. Full lines represent quark propagators. $\phi_{\overline{2}1}$ and $\phi_{\overline{4}3}$ are the wave functions of the external mesons. Other contributions involve either $\mathcal{T}_{\overline{4}1}$ alone or $\mathcal{T}_{\overline{2}3}$ alone. The N_c-counting rules have been detailed in the text.

which we label by a global increasing index n, the value $n = 0$ corresponding to the ground state. They have then the following structure:

$$\mathcal{T}_{\overline{q}q}(P_{\overline{q}q}, \ldots) = \frac{1}{N_c} K - \frac{i}{N_c} \sum_{n=0}^{\infty} \frac{\phi_{\overline{q}q,n} \phi^\dagger_{\overline{q}q,n}}{P^2_{\overline{q}q} - P^2_n}, \tag{85}$$

where $P_{\overline{q}q}$ is the total momentum of the quark-antiquark system and P^2_n is the mass squared of the nth meson, with the $\phi_{\overline{q}q,n}$s being the corresponding wave functions[7]. The one-gluon-exchange contribution (or its equivalent one in a confining scheme) remains outside the sum, since it cannot contribute simultaneously to the product of the meson wave functions. An explicit realization of this structure is provided in two-dimensional QCD (cf. Eq. (18) of Ref. [113]).

The N_c-counting rules in diagrams of the type of Fig. 42 and of the next two figures (43 and 44) are the following: according to Eq. (85), each appearance of a scattering amplitude $\mathcal{T}_{\overline{q}q}$ is accompanied by a factor $1/N_c$, while the appearance of a meson wave function ϕ is accompanied by a factor $1/N_c^{1/2}$; every (four-dimensional) loop momentum integration is accompanied by a factor N_c.

The s-channel singularities of the object of Fig. 42 are governed by those coming from the product $\mathcal{T}_{\overline{4}1}\mathcal{T}_{\overline{2}3}$. Each of these scattering amplitudes has meson poles as singularities and hence behaves as a sum of effective meson propagators. The s-channel singularities that result from the integrations are therefore those of two-meson scattering amplitudes. They do not involve, however, any pole-type singularity which might signal the possible presence of a tetraquark state. It might, however, happen that the infinite sum of the two-meson contributions, which all have the same type of singularities but are located at different positions, produces a pole-type singularity through a divergence occurring in the vicinity of some particular point. Such a possibility, which closely depends on the behaviors of the various overlappings of wave functions, is the only one which might exist within the class of N_c-leading diagrams. It would no longer be the result of purely confining interactions, since the latter have been absorbed by the meson formations, but rather would be the result of a residual effect of them, coming from the existence of the tower of an infinite number of meson states. The possibility of such a mechanism needs, however, further detailed investigations.

In case the above mechanism does not produce a bound state, a second possibility of producing a tetraquark pole remains: an iteration mechanism of diagrams of the type of Fig. 42.

The effective iteration kernel is made of the succession of the recombination channels $R1$ and $R2$, examples of which are presented in Fig. 43, for the recombination channel $R1$, and in Fig. 44, for the direct channel $D1$. Because of the structure of the quark-antiquark scattering amplitude in terms of meson wave functions [Eq. (85)], the kernel of the

[7]The wave functions ϕ are equal, up to normalization factors, to the Bethe–Salpeter wave functions multiplied by the inverse of the two quark propagators.

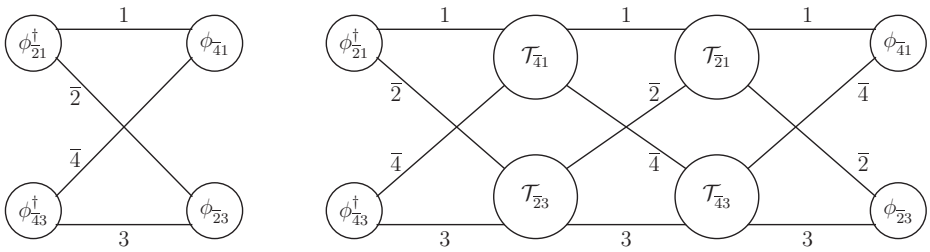

(a) $O(N_c^{-1})$ (b) $O(N_c^{-3})$

Figure 43: (a) The generic diagram corresponding to Fig. 23a, of the recombination channel $R1$ [Eq. (57)]. (b) First iteration with the contributions of the quark-antiquark scattering amplitudes $\mathcal{T}_{\bar{4}1}$ and $\mathcal{T}_{\bar{2}3}$, on the one hand, and $\mathcal{T}_{\bar{2}1}$ and $\mathcal{T}_{\bar{4}3}$, on the other, to the same scattering amplitude. Same notations as in Fig. 42. A typical Feynman diagram participating in this process is presented in Fig. 29b. Because of the structure of the quark-antiquark scattering amplitude (85) in terms of meson wave functions, this diagram involves the succession of the recombination channels $R1-R2-R1$. Insertion of the kernel of the above diagram, made of the product $R1-R2$, on the left of the kernel of the diagram of Fig. 42 generates the first iteration of the latter, introducing at the same time a factor of N_c^{-2}.

iterations in the recombination as well as in the direct channels has the structure of a product of the two recombination channels $R1$ and $R2$. An infinite series of such iterations, which act in convolution in momentum space, might generate, after summation, a tetraquark pole in the scattering amplitude. However, each iteration introduces here a factor of N_c^{-2}, which means that the effective interaction kernel of the possibly resulting integral equation is of order N_c^{-2} and hence vanishes when N_c tends to infinity.

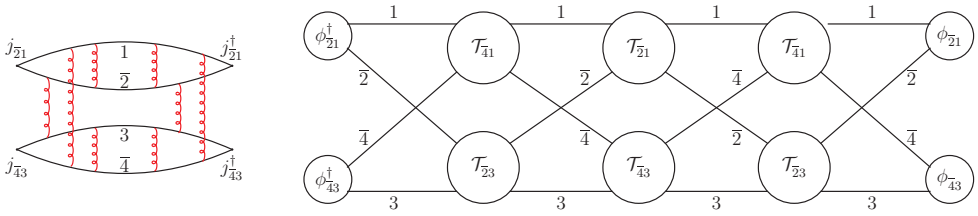

(a) $O(N_c^{-2})$ (b) $O(N_c^{-4})$

Figure 44: First iteration of the scattering amplitude of the direct channel $D1$ of Fig. 42 with the insertion of the product $R1-R2$ of the two recombination channels. Each insertion introduces a factor of N_c^{-2}. (a) Typical Feynman diagram of the first iteration. (b) General structure of the iteration, which involves the succession of the recombination channels $R1-R2-R1-R2$.

Since the confining interactions are explicitly absent between the meson clusters, one faces here two possibilities.

In the first one, the resulting interaction is of the residual long-range type (van der Waals, or another hidden mechanism). If it is globally attractive, then a bound state might exist, approaching the lowest two-meson threshold when N_c goes to infinity. However, the existence of such types of forces has not been observed up to now in the domain of light quarks. Whether they exist and are operative with heavy quarks remains a key issue of this mechanism.

Van der Waals forces have been considered in the realization of "hadrocharmonium" (or, more generally, of hadroquarkonium) states [217–219]. Here, one considers four-quark systems made of a heavy-quark $Q\bar{Q}$ pair and a light-quark pair. The heavy-quark pair will have the tendency to form a heavy quarkonium hadron, while the light quarks form a kind of hadron matter, interacting with the heavy-quark core by means of QCD gluon-exchange van der Waals forces. The possibility of global attractive forces and of existence of bound states has been shown. The difference of this system from conventional molecular states comes from the fact that the resulting bound state (or resonance) may lie relatively far from the two-meson threshold and can have distinctive decay channels.

In the second possibility, one rather is in the presence of effective short-range molecular-type interactions between mesons. The properties of these types of interaction will be considered in Sec. 6. The main property that concerns us here is that when the strength of the interaction tends to zero, and more generally becomes lower than a critical strength, no bound states exist, but resonances might appear; in the strength-vanishing limit, the resonance masses are

pushed towards infinity. Therefore, when N_c tends to infinity, no tetraquark bound states or low-mass resonances are expected to occur. It is only for finite (possibly large) values of N_c that tetraquark bound states might appear in the spectrum, in the vicinity of the two-meson threshold.

The detailed prediction of the above possibilities depends on the related integral equation that governs the pole production. The exact expression of the latter takes, however, a rather intricate form, since it actually involves, because of the infinite number of meson states, an infinite number of coupled equations, with off-mass-shell scattering amplitudes. This problem is not yet analyzed in the literature.

Bound-state equations for four-quark states, based on the Bethe–Salpeter and Dyson–Schwinger equations framework, have been considered in Refs. [220–223], where a detailed study of the various mechanisms of formation of tetraquark states has been undertaken. The results confirm the dominant role of meson clusters inside the tetraquark bound states.

The same mechanism as described above could also be applied to the other direct channel, $D2$, of the meson-meson scattering amplitude [Eq. (56)] by exchanging the roles of the antiquarks $\overline{2}$ and $\overline{4}$. Here, however, the quark flavors and masses having been changed, the structure of the kernel of the iteration is different from that of channel $D1$ and hence one should expect to find a tetraquark bound state different from that of the $D1$ channel. This is why the existence of two different direct channels might induce the existence of two different tetraquarks. Each of these, if they exist, would have a priviledged decay channel, according to the structure of their couplings to two-meson states.

The previous analysis could also be applied to the case of cryptoexotic channels, as discussed in Sec. 5.2, with appropriate adaptations, taking into account the additional diagrammatic possibilities, which are mainly related to mixing possibilities with ordinary mesons. One also encounters here two different structures in the iteration kernels, leading to two different tetraquarks, as was emphasized in Sec. 5.2. In the case of a molecular-type mechanism, an additional contribution comes from diagrams of the types of Figs. 34b, 34c and 34e, which, by iteration, may participate in the formation of the bound state; hence, the possible existence of diagrams 36a and 36d.

In conclusion, the tetraquark formation mechanism, as resulting from the large-N_c analysis of Feynman diagrams, seems to be dominated by the meson-meson interactions through a collaborative iteration of direct and recombination sectors[8]. From that viewpoint, we are rather close to a molecular-type structure, in which the role of confining interactions has been absorbed by the formation of mesons. However, residual long-range type interactions may still survive and contribute in a more specific way.

We shall come back, through another perspective, to the comparison of the diquark-formation and the mesonic-cluster-formation mechanisms in Sec. 7.

6. Molecular states

Molecular structure of exotic hadrons had been considered since the early days of the charmonium discovery [52–54]. Taking the analogy of the formation of atomic molecules or of nuclei, it is natural to consider the possibility of the existence of bound states or resonances resulting from the direct interaction of ordinary hadrons. Since the latter mutually interact by means of short-range forces, generated by meson exchanges, one is entitled to use effective field theories [73–80, 82–89, 91], adapted to the range of energies and masses that are involved [225–244]. In particular, the presence, in the exotic hadrons, of heavy quarks allows the use, at least partially, of a nonrelativistic formalism, which considerably facilitates the analysis of the problem.

6.1. Effective-theory matching

The main idea of the formulation of effective field theories is that the description of the dynamics of physical systems depends on the energy scale or the distance scale at which one evaluates physical observables. At low energies, or at large distances, the dynamics should be insensitive to the details of the dynamics at high energies or at short distances. It is then advantageous to integrate out the degrees of freedom that describe the short-distance dynamics and keep from them only overall effects, thus reducing the number of degrees of freedom needed for the description of the system at large distances. In this respect, a composite particle, which, at the microscopic level, is

[8] Quark recombination or interchange channels in meson-meson scattering have been considered in Ref. [224].

made of more elementary constituents, could be approximated, when observed from a sufficiently large distance, by a pointlike particle, with appropriate attributes.

The effective theory, resulting from the above reduction of degrees of freedom, should, however, reproduce the same results than the full, or microscopic, theory from which it is deduced. This is generally ensured by imposing matching conditions between the two theories concerning several observables, like the scattering amplitudes or form factors. The structure of the effective theory is organized according to counting rules involving the energy scale that validates its existence. In principle, the effective-theory Lagrangian should contain an infinite number of terms, ranked according to their dimensionality (in energy scale), the most important terms having the lowest dimensionality. Truncation of the series after the first few terms depends on the precision of the calculation that is required and on the energy scale to which one wishes to extend the predictions. The matching conditions allow the determination of the parameters of the effective theory in terms of quantities known from the full theory. It is worth emphasizing that, in general, the effective-theory reduction may involve several energy scales, for example, when the system contains particles with masses belonging to different energy scales, in which case the matching conditions become more involved.

Since most of the experimentally observed tetraquark candidates are located in the vicinity of two-meson thresholds, the issue of interest in the molecular scheme is the understanding of the conditions in which such a situation emerges, both in the effective-theory and in the full-theory frameworks.

In this respect, Luke and Manohar [245] have made, by means of a simplified model, which we briefly sketch below, a thorough analysis of the various aspects of the problem one meets. The model considers, as the full theory, a theory of nonrelativistic fermions with mass M, interacting by means of a Yukawa-type coupling with a scalar field of mass m and coupling constant g. The effective theory is obtained by integrating out the scalar field and keeping only the fermion field. In the latter theory, the leading-order interaction is represented by a four-fermion contact term, with coupling constant h. Nonleading interactions are represented by higher-dimensional operators. Matching conditions are implemented by considering the elastic (off-energy) two-fermion scattering amplitude. In the full theory, the most important contributions come from the series of ladder diagrams, while in the effective theory, the equivalent contributions come from the series of chains of bubble diagrams, generated by the four-fermion contact term. These diagrams are represented in Fig. 45, where the main parameters of the two theories are also displayed. This model has also direct connection with the evaluation of the nucleon-nucleon scattering amplitude at low energies, considered in [83–85].

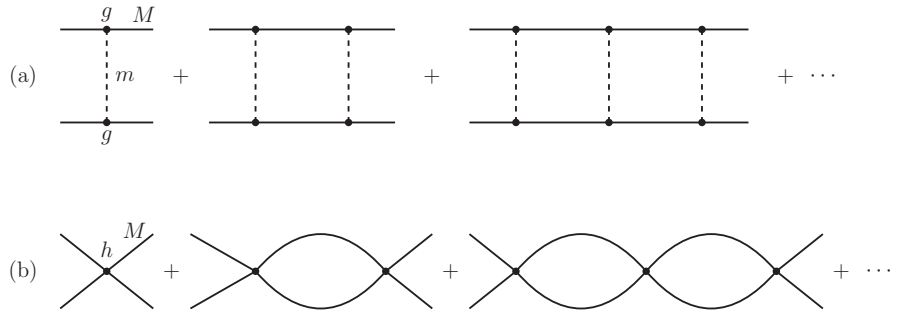

Figure 45: (a) The series of ladder diagrams in the full theory. (b) The series of chains of bubble diagrams in the effective theory. The masses and coupling constants are displayed.

In the full theory, the bound-state problem is governed by the Schrödinger equation with the (attractive) Yukawa potential. Bound states exist only when the coupling constant (squared) is greater than some critical value:

$$g^2 \geq g^2_{\text{cr.}} = 1.7 \times \left(\frac{4\pi m}{M}\right). \tag{86}$$

At the critical value, the bound state appears at the two-fermion threshold (zero binding energy) and when g^2 is gradually increased, the binding energy increases and the bound state goes down in the potential well. For higher values of g^2, new bound states may appear, representing excited states. When $g^2 < g^2_{\text{cr.}}$, the bound states disappear,

having been transformed into resonances. For values of g^2 approaching zero, the lowest-energy resonance has an energy (more precisely its real part) that increases up to infinity.

Nonrelativistic or semirelativistic theories are generally expanded in inverse powers of the heavy-fermion mass M. A kinematic quantity that is adequate for such expansions is the ratio of the c.m. momentum Q of the fermions to the mass M, Q/M. Introducing the velocity v of the fermions through the relation $Q = Mv$, the above expansion is therefore an expansion with respect to v; small velocities ensure rapid convergence of the corresponding series. In some cases, infrared singularities of loop diagrams are represented by negative powers of v and demand a separate treatment or isolation of such terms.

Considering now the effective theory, the matching condition with the full theory, up to some order in the loop counting, implies a redefinition of the effective coupling h. The latter then takes the following form:

$$h = \sum_{n=0}^{\infty} h^{(n)}, \tag{87}$$

where $h^{(n)}$ represents the contribution coming from the n-loop calculation. The calculations, up to two loops, provide the following expansion of h:

$$h = h^{(0)}\Big[\, 1 + \frac{1}{2}\Big(\frac{g^2 M}{4\pi m}\Big) + \ln\Big(\frac{4}{3}\Big)\Big(\frac{g^2 M}{4\pi m}\Big)^2 + \cdots \,\Big], \qquad h^{(0)} = \frac{g^2}{m^2}. \tag{88}$$

The chain diagrams of Fig. 45b can be summed using the full h as the effective coupling. The bubble diagram is ultraviolet divergent and requires renormalization. After the integration of the temporal component of the loop variable is done (the effective theory being formulated in the nonrelativistic regime), the three-dimensional part is regularized by dimensional regularization, in which case no subtraction is needed, the ultraviolet divergence being linear (odd power of the momentum). The series is simply a geometric series and is easily summed. One finds for the off-energy scattering amplitude

$$\mathcal{A} = \frac{h}{1 + hM^{3/2}(-E)^{1/2}/(4\pi)}, \tag{89}$$

where E is the total (nonrelativistic) energy of the two fermions. For h negative, there is a bound state with energy (cf. also [83])

$$E = -\frac{16\pi^2}{h^2 M^3}. \tag{90}$$

(The binding energy is $B = -E$.) When $|h| \to \infty$, the bound-state energy tends to zero and the bound state approaches the threshold. We have seen that in the full theory this situation occurs when g^2 tends to $g^2_{\text{cr.}}$ from above [Eq. (86)]. This means that the above limit of h occurs for a finite value of g^2, which is $g^2_{\text{cr.}}$; therefore, the series (87) diverges for that value of g^2, which signals the fact that the correspondence between the full and the effective theories is no longer perturbative. In this domain of the coupling constant, the higher-dimensional operators, which have been neglected in the above evaluations, become relevant to all orders and may signal the breakdown of the effective theory. On the other hand, when h tends to zero in its negative domain, the bound-state energy tends to $-\infty$ and the bound state disappears from the bottom of the energy domain. In the full theory, this happens when g^2 tends to $+\infty$. However, when g^2 gradually increases, new bound states appear in the spectrum of the full theory, representing excited states; these are not reproduced in the effective theory. In the domain of positive values of h, bound states do not exist. This, therefore, corresponds to the domain $0 \le g^2 \le g^2_{\text{cr.}}$; here, the full theory displays resonances, but in the effective theory they are absent. (The effective theory might display a resonance in the case of derivative-type couplings, a situation that occurs in chiral perturbation theory (cf. Sec. 6.3).) A perturbative matching between the full and the effective theories occurs only in the weak-coupling regime of the former, i.e., $g^2 \simeq 0$, which entails $h \simeq 0$ and $h > 0$.

From the above comparisons, one may deduce a schematic qualitative correspondence between the couplings of the full and the effective theories, which is represented in Fig. 46. The more singular behavior of the effective theory is a consequence of the fact that the bubble diagram is ultraviolet divergent, while the box diagram in the full theory is finite and therefore reflects smoothly the variations of the coupling constant. In x-space, the bound-state equation of the effective theory is governed by the three-dimensional δ-function potential, which requires renormalization of the coupling constant [246].

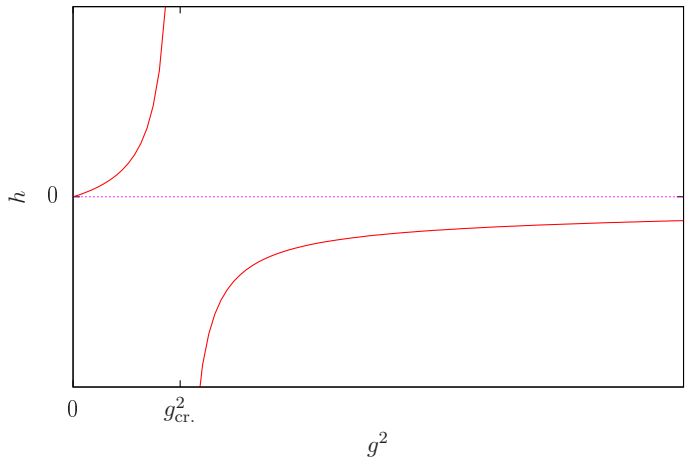

Figure 46: A schematic behavior of the effective-theory coupling constant h with respect to variations of the full-theory coupling constant squared g^2.

In spite of the breakdown of perturbation theory in the region $g^2 \sim g^2_{\rm cr.}$ and the lack of explicit correspondence between g^2 and h, it is possible to deduce further information through parameters that have direct connection with experimental measurements. These are the S-wave scattering length a and the effective range r_e. When the bound state approaches the threshold, the scattering length increases and tends to ∞ at threshold, while the effective range remains finite. It is then shown that h is related to the exact scattering length of the Yukawa theory [83, 85]:

$$h = -\frac{4\pi}{M}\, a, \tag{91}$$

whereas higher-dimensional derivative terms are suppressed by powers of $(4\pi r_e/a)$. Therefore, the bound-state energy (90) remains a valid result for large values of the scattering length. However, the radius of convergence of the effective theory is much reduced and is given by values of the momentum k of the order of $\sqrt{2/(ar_e)}$ and not by $r_e^{-1} \sim m$.

The above considerations allow us to foresee the implications of the large-N_c limit on the possibility of formation of bound states. Here, the full theory is QCD, while the effective theory is a meson theory, where mesons mutually interact either by meson exchanges, characterized by some effective generic coupling g^2, or by contact terms, characterized by an effective coupling h. We have seen in Sec. 2.3 that three-meson couplings and four-meson couplings generally scale like $1/N_c^{1/2}$ and $1/N_c$, respectively (cf. Figs. 10 and 12). Therefore, in the large-N_c limit, the meson-interaction couplings tend to zero and one reaches the situation where the mesons become free noninteracting particles. For large finite values of N_c, the effective theory is then in the weak-coupling regime, which corresponds to the phase $g^2 \simeq 0$, $h \simeq 0$ with $h > 0$. In this situation, one does not expect to find bound states. Rather, one should have resonances located far from the two-meson thresholds.

When N_c is decreased down to finite values, close to the physical value 3, two types of evolution might be expected, depending on the quark masses that are involved and also on the detailed quantum numbers of the system that is considered. For light quarks, the evolution probably remains in the phase $g^2 \leq g^2_{\rm cr.}$, $h > 0$, in which case the lowest-mass resonance approaches the two-meson threshold, but still remains sufficiently far from it. This is corroborated by results obtained within the framework of chiral perturbation theory (cf. Sec. 6.3). For systems involving heavy quarks, it seems that the evolution reaches the critical region of the vicinity of the two-meson threshold, characterized by $g^2 \sim g^2_{\rm cr.}$ and $|h| \sim \infty$, where a bound state or a resonance might appear. It is worth noticing that $g^2_{\rm cr.}$ is inversely proportional to the external-meson masses [Eq. (86)], which feel the heavy quark masses, and therefore has a smaller value for such systems, making easier the appearance of near-threshold structures. This is corroborated by the experimental observations of exotic hadrons involving heavy quarks. A similar conclusion has also been reached, from a different point of view, in Ref. [247]. The above descriptions, while remaining at the level of observations, require, however, more dynamical justifications at the QCD level.

6.2. Compositeness

The description of the internal structure of a bound state depends upon the scale at which the latter is probed. The mean size of the bound state is one of the criteria that can be used to distinguish two situations: (i) a large size, characterizing a loosely bound state, in which one may distinguish the existence of two or several clusters; (ii) a compact size, characterizing an undecomposable or elementary object. It is evident, however, that probing the latter object with higher precision, one may discover that, in turn, it is also decomposable into more elementary clusters. The most natural example of this situation comes from the nuclei, which, in first approximation, can be described as made of nucleons, considered as pointlike objects. However, observing the nucleons at shorter distances, one realizes that the latter are themselves made of more elementary particles, which are the quarks and the gluons.

The same criterion also applies to the case of exotic hadrons. Molecular-type exotic hadrons would be described as composed of clusters of ordinary hadrons, interacting by means of effective forces, while compact exotic hadrons would be described by the direct interactions of quarks and gluons, without leading to the appearance of hadronic clusters. The solution of bound-state equations and comparison of their predictions with experimental data would be sufficient to settle the question of the nature of a bound state; however, in many cases, the interactions that are at work have a nonperturbative character and do not allow for a deductive solution of the problem. In this case, the knowledge of external criteria, related to experimental data, could bring a complementary view to the efforts of understanding the problem.

In this respect, Weinberg proposed in the past, in the framework of nonrelativistic quantum mechanics, an independent criterion for the probe of compositeness of the deuteron, whose binding energy is much smaller than the scale of the strong interactions that govern nuclear physics [51, 248]. Defining Z as the probability of having the deuteron as an elementary particle ($0 \leq Z \leq 1$), the probability of having it as made of a proton and a neutron is $(1 - Z)$. The vicinity of the deuteron state to the two-nucleon threshold allows one to use, for the scattering phase shift δ of the two nucleons, the effective range expansion in terms of the scattering length a and the effective-range r_e

$$k \cot \delta \simeq -\frac{1}{a} + \frac{1}{2} r_e k^2, \tag{92}$$

and to relate the latter quantities to the binding energy and the parameter Z. Weinberg finds

$$a = [2(1 - Z)/(2 - Z)]\, R + O(m_\pi^{-1}), \quad r_e = [-Z/(1 - Z)]\, R + O(m_\pi^{-1}), \quad R = (2\mu B)^{-1/2}, \tag{93}$$

where B is the deuteron binding energy, $B = 2.22$ MeV, μ the proton-neutron reduced mass, m_π the pion mass, and R represents the deuteron radius. If the deuteron is composite, $Z \simeq 0$, a takes its maximum value, while $r_e \simeq 0$; in the opposite case, if the deuteron is elementary, $Z \simeq 1$, $a \simeq 0$ and $r_e \to -\infty$. Experimental data, $a = +5.41$ fm and $r_e = 1.75$ fm [51, 249], clearly favor the composite nature of the deuteron, made of a proton and a neutron. Notice that, for $Z \simeq 0$, the relationship between the binding energy and the scattering length of Eq. (93) reduces to Eq. (90), using (91).

Weinberg's criterion has been investigated by many authors and extended to a wider range of applicability, such as to resonances, multi-channel processes and relativistic cases [250–257]. Oller has proposed a new criterion for compositeness, based on the use of the number operators of free particles [258]. The compositeness criterion thus brings a complementary constraint for the analysis of the internal structure of bound states and resonances.

6.3. Resonances with light quarks

Molecular systems made of light quarks (u, d, s) need the use of a relativistic formalism. Since the hadronic clusters interact by means of short-range forces and the light quarks have a relativistic motion, one guesses that the mean forces experienced by the clusters are weaker than in the case of heavy quarks, which tend to stabilize the general motion. Therefore, the effective theory is expected here to be in its weak-coupling regime, where no bound states can be produced. Rather, one expects the appearance of resonances, generally located, mostly for the case of the quarks u and d, far from the two-hadron threshold.

The light-quark effective field theory which describes QCD at low energies is chiral perturbation theory (ChPT) [73–76]. The case of $SU(2)_L \times SU(2)_R$ chiral symmetry, involving pions, has been widely studied in the literature and precise experimental tests have confirmed its validity [259, 260].

The domain of validity of ChPT, concerning the meson momenta, extends over a few hundreds of MeV. Since the perturbative expansion is done polynomially (up to logarithms) in the momenta, it is not expected to find poles with the first few terms and to be able to probe directly the properties of resonances. To extend the domain of predictivity of ChPT, it has been combined with dispersion relations, using analyticity and crossing-symmetry properties [259, 260]. Extending the above setup to the complex plane, it has been shown that the $\pi\pi$ scattering amplitude in its partial S wave, with isospin 0, possesses a pole in the second Riemann sheet at the complex mass value $M = (441 - i272)$ MeV [261]. This solution has been identified with the $f_0(500)/\sigma$ meson, whose existence had been controversial for several decades, but which later had re-emerged through new experimental results as a wide resonance. Confirmation of the above result has been obtained in [262–264].

It had also been suggested that properties of resonances could be more directly probed by using elastic unitarity in its full form, by means of the inverse amplitude method [265–269]. A thorough study of the scalar resonance $f_0(500)/\sigma$, based on the combined frameworks of ChPT, dispersion relations and unitarization, has been undertaken by Peláez *et al.* [270–272]. Their analysis also leads to a pole position in the second Riemann sheet of the complex plane, at the mass value $M = (449 - i275)$ MeV, thus confirming the result of [261].

To appreciate the power of the unitarization scheme (cf. also [273–277]), one may consider the partial S-wave isospin-0 $\pi\pi$ scattering amplitude in its leading order, $O(p^2)$, of ChPT. The latter reads

$$t^{I=0}_{\ell=0}(s) \equiv t(s) = \frac{2s - M_\pi^2}{32\pi F_\pi^2}, \tag{94}$$

where s is the Mandelstam variable and F_π is the pion decay constant, defined as in Eq. (12) with an axial-vector current ($F_\pi \simeq 92.3$ MeV) and M_π is the pion mass. Notice that in ChPT the meson-meson interactions begin with derivative couplings, this is why an s-dependence appears at leading order. The elastic unitarity condition reads

$$\mathrm{Im}\, t(s) = \sigma(s)|t(s)|^2, \qquad \sigma(s) = \left(1 - 4M_\pi^2/s\right)^{1/2}. \tag{95}$$

This shows that the imaginary part of the scattering amplitude is of higher order, $O(p^4)$, than the real part. In terms of the inverse amplitude it takes the form

$$\mathrm{Im}\,\frac{1}{t(s)} = -\frac{\mathrm{Im}\, t(s)}{|t(s)|^2} = -\sigma(s). \tag{96}$$

Therefore, the imaginary part of the inverse of the amplitude is explicitly known and reduces to a kinematic factor. This allows one to complete expression (94), by incorporating in it information (96), and considering (94) as the real part of the amplitude:

$$t(s) = \frac{\mathrm{Re}\, t(s)}{1 - i\sigma(s)\mathrm{Re}\, t(s)}. \tag{97}$$

In searching for poles in the second Riemann sheet, one considers the complex conjugate of the amplitude of the first Riemann sheet. Expression (97) becomes

$$t^{\mathrm{II}}(s) = \frac{\mathrm{Re}\, t(s)}{1 + i\sigma^{\mathrm{II}}(s)\mathrm{Re}\, t(s)}. \tag{98}$$

Notice that this equation is the analog of Eq. (89), obtained by summing a series of bubble diagrams. In the lower s-plane, $\sigma(s)$ undergoes the change $\sigma^{\mathrm{II}}(s) = -(\sigma(s^*))^*$. The pole position is obtained from the zero of the denominator,

$$\sigma(s_\sigma)(2s_\sigma - M_\pi^2) = i32\pi F_\pi^2, \tag{99}$$

which gives $\sqrt{s_\sigma} = (493 - i441)$ MeV, of the same order of magnitude as the precise values obtained above. This means that the leading-order ChPT scattering amplitude, together with the unitarization condition, drags the solution to its exact value.

One of the advantages of the inverse amplitude method is that it displays more explicitly the large-N_c behavior of the various contributions. At large N_c, the pion mass remains unaffected at leading order, $M_\pi = O(N_c^0)$, while the decay constant scales like $N_c^{1/2}$, $F_\pi = O(N_c^{1/2})$ [Eq. (13)]. Taking into account these behaviors, one finds that Eq. (99) reduces to

$$\sqrt{s_\sigma} = (1 - i)\sqrt{8\pi} F_\pi = O(N_c^{1/2}), \tag{100}$$

which shows that the mass and width of the $f_0(500)/\sigma$ meson increase like $\sqrt{N_c}$ at large N_c. This is in accordance with the weak-coupling regime of molecular effective theories that we have met in Sec. 6.1. This shows that the $f_0(500)/\sigma$ meson is mainly made of two pions, rather than of a pair of quark and antiquark, in which case the mass should remain stable under changes of N_c and the width would decrease [270, 271] (cf. also [278, 279]). Nevertheless, because of mixing possibilities, the $f_0(500)/\sigma$ seems to have a small component of $\overline{q}q$ state.

The detailed analysis applied to the case of $f_0(500)/\sigma$ has also been applied to the case of the ρ meson, which appears as a resonance in the P wave. Here, however, the behaviors of the mass and the width under variations of N_c confirm the fact that the ρ meson is mainly made of a $\overline{q}q$ pair [270, 271].

In conclusion, the molecular scheme, considered as an effective theory, provides a systematic tool of investigation of the properties of many exotic-type states, either in the domain of heavy quarks, or that of light quarks.

7. The cluster reducibility problem

One salient feature of the multiquark currents, met in Secs. 3.1 and 3.2, is their decomposition property into combinations of products of meson and/or baryon currents, typical examples of which are Eqs. (32) and (36). This suggests that multiquark states are not color-irreducible, unlike ordinary hadrons, and, therefore, could not be put on the same footing as the latter states. The consequences of this fact are easily conceivable. If, within a multiquark state, clusters of ordinary hadrons may be formed, and since the mutual interactions of the latter are not confining, the multiquark state will have the tendancy to be dissociated into its hadronic components or to be transformed into a loosely bound state of hadrons.

One might still think that the above color-reducibility property concerns only couplings to local operators which involve a few moments of the corresponding bound state wave function. Actually, the property is very general and concerns also the couplings to multilocal operators [55].

7.1. Cluster reducibility of multilocal operators

We shall briefly sketch, in this subsection, the case of multilocal operators.

The proof of cluster reducibility of multilocal operators is based on two properties of the gauge links (50): they are elements of the gauge group SU(3) (and, more generally, of SU(N_c)), and have a determinant equal to 1. Hence, they satisfy the group composition law

$$U^a_{\ b}(C_{zy})U^b_{\ c}(C_{yx}) = U^a_{\ c}(C_{zyx}), \tag{101}$$

where C_{zyx} is the line composed of the union of the two lines C_{zy} and C_{yx}, with a junction point at y. The expression of the determinant of U is (cf. Ref. [143], Appendix C)

$$\det(U(C_{yx})) = 1 = \frac{1}{3!}\epsilon_{a_1a_2a_3}\epsilon^{b_1b_2b_3}U^{a_1}_{\ b_1}(C_{yx})U^{a_2}_{\ b_2}(C_{yx})U^{a_3}_{\ b_3}(C_{yx}). \tag{102}$$

Considering, for definiteness, the tetraquark operator of Fig. 17a, multiplying it with the determinant of the gauge link of the line C_{yx} and using the contraction property of two ϵ tensors,

$$\epsilon^{c_1c_2c_3}\epsilon_{d_1d_2d_3} = \delta^{c_1}_{\ d_1}\delta^{c_2}_{\ d_2}\delta^{c_3}_{\ d_3} + \sum_{k_i}(-1)^P\delta^{c_{k_1}}_{\ d_1}\delta^{c_{k_2}}_{\ d_2}\delta^{c_{k_3}}_{\ d_3}, \tag{103}$$

where the sum runs over all permutations of the indices k_i, with the sign of the parity of the permutation represented by $(-1)^P$, one ends up with a decomposition of the operator into a sum of products of two meson operators of the type (51), where the gauge link lines have a polygonal structure. Further simplification occurs, using the backtracking condition [146]

$$U^a_{\ b}(C_{yx})U^b_{\ c}(C_{xy}) = \delta^a_{\ c}, \tag{104}$$

which expresses the unitarity property of the parallel transport operation, leading to the decomposition displayed graphically in Fig. 47, which is the multilocal form of the first of Eqs. (32). The meson operators that appear on the right-hand side of the equation come out with polygonal phase-factor lines.

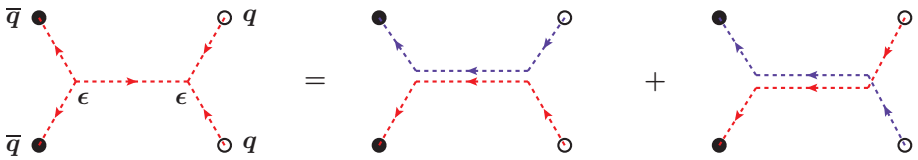

Figure 47: Decomposition of the tetraquark operator into a combination of products of two meson operators.

The same procedure can be applied to the cases of pentaquark and hexaquark operators. The pentaquark operator of Fig. 17b is decomposed into a combination of products of a mesonic and a baryonic operator (cf. Fig. 48).

The hexaquark operator of Fig. 17c is decomposed into a combination of products of two baryonic operators (cf. Fig. 49).

The cluster reducibility property remains also valid in the more general SU(N_c) case [55], by appropriately generalizing the ϵ-tensor properties [143]. Thus, for tetraquarks, the first operator in Fig. 19 decomposes into $(N_c - 1)!$ combinations of $(N_c - 1)$ mesonic operators. The last operator in that figure decomposes into combinations of two mesonic operators and of Wilson loops, according to the types of paths used between the two junction points. (In the case of straight lines, the Wilson loops disappear.) Similar decompositions occur for the other operators (not drawn) of that figure denoted by the ellipses and corresponding to intermediate-type representations.

For pentaquarks, the first operator in Fig. 20 decomposes into a combination of products of $(N_c - 2)$ mesonic operators and one baryonic operator. The last operator of the figure decomposes into a combination of products of one mesonic operator and one baryonic operator, and possibly of Wilson loops.

For hexaquarks, the first operator in Fig. 21 decomposes into a combination of $(N_c - 1)$ baryonic operators, while the last operator of that figure decomposes into a combination of products of two baryonic operators, and possibly of Wilson loops.

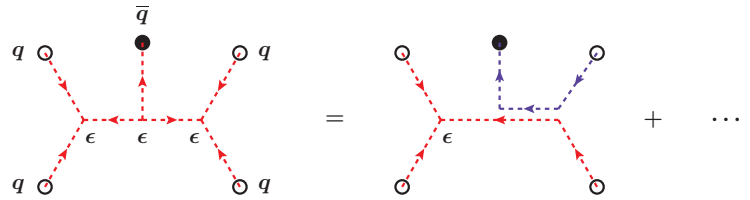

Figure 48: Decomposition of the pentaquark operator into a combination of products of a meson and a baryon operator. The ellipsis indicates the remaining three other products.

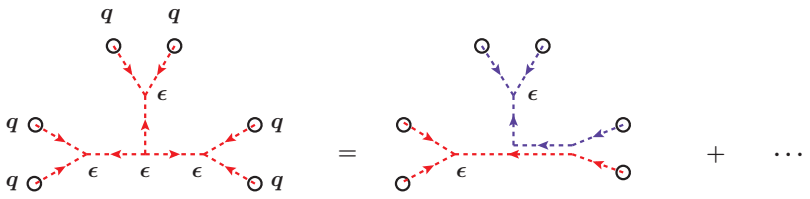

Figure 49: Decomposition of the hexaquark operator into a combination of products of two baryon operators. The ellipsis indicates the remaining other products.

7.2. Energy balance

The main question that remains to be clarified concerning the cluster reducibility property of multiquark operators is whether it survives in the quantized theory. This is not a trivial question, because the equivalence relations, which

were established on formal grounds between Y-shaped operators and combinations of products of ordinary hadronic operators, involve products of some phase factors along the same lines, but belonging to different global paths (cf. Figs. 47, 48 and 49, right-hand sides of the equalities). The disentanglement of such phase factors, in order to introduce them inside different hadronic states, corresponding to the clusters, might not be a neutral operation and might imply energy loss or gain. We shall show below, on simple examples, that this is indeed the case and that the result depends on the geometrical properties, in coordinate space, of the representations that are considered, favoring only one of the two sides of the equivalence relations.

General energy considerations are much more transparent in the case of static quarks, corresponding to the infinite mass limit of heavy quarks, kinematic effects of the motion of quarks being then suppressed; actually, the latter, for finite masses, do not affect the main property of confinement of the theory and introduce only nonleading terms in the confining regime. Therefore, the static limit is expected to provide, in the confining regime, the main qualitative properties that are searched for.

To extract the interaction energy properties of a static system, one generally considers correlation functions of appropriate operators having couplings to such systems. The calculation involves, among others, the propagators of the static quarks in the presence of gluon fields, which are essentially proportional to the gluon-field path-ordered phase factors along the time direction [49, 92, 131]. Considering in the correlation functions gauge-invariant multilocal operators, which involve in their definitions gluon-field phase factors, one ends up with the vacuum expectation value of an expression involving the color trace of phase factors along a closed contour (or traces along closed contours in the case of non-connected operators), which defines the vacuum average of the Wilson loop. On the other hand, inserting in the correlation function a complete set of intermediate hadronic states and taking the total evolution time T to infinity, one selects the ground-state hadron, which yields a factor e^{-iET}, where E is the corresponding interaction energy, the quark-mass contributions having been factorized. Then the comparison of this term with the Wilson-loop contribution allows for the determination of E.

We first consider the simplest example, corresponding to a mesonic operator [Eq. (51)] with a phase factor along a straight-line segment [Fig. 16a] of length R, taken in the three-dimensional space orthogonal to the time axis; R is equal to the distance between the quark and the antiquark, considered at equal times. The resulting Wilson-loop contour, for an evolution of the system during a time T, is a rectangle of length T and width R, represented in Fig. 50.

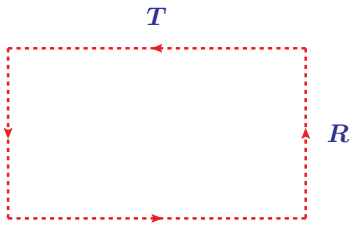

Figure 50: Wilson-loop contour resulting from the time evolution of a meson containing a static quark-antiquark pair.

The evaluation of the vacuum average of Wilson loops, in the absence of a completely analytic solution of QCD in its confining regime, can be numerically done in lattice gauge theory, where one works in Euclidean spacetime. Furthermore, making there the strong-coupling expansion leads to analytic predictions, which are generally confirmed by experimental data [48, 92, 131]. Generally, in the evaluation of the energy balance, one uses the fact that, in Euclidean space, the generating functional of Green's functions is dominated by field configurations which minimize the energy.

At leading order of the strong-coupling expansion, the Wilson-loop vacuum average is obtained by paving the minimal area enclosed by the contour with the lattice plaquettes. In the case of the rectangle above, the area is simply the product RT; the Wilson-loop vacuum average is then proportional to the factor $e^{-\sigma RT}$, where σ is the "string tension", here defined as $\sigma = \frac{1}{a^2}\ln(g^2)$, where a is the lattice spacing and g the QCD coupling constant. Upon comparing this factor with e^{-ET} (the Euclidean version of e^{-iET}), one obtains

$$E = \sigma R, \tag{105}$$

which means that the static quark-antiquark interaction energy increases linearly with the separation distance. This result analytically establishes the confinement of quarks. It has also been confirmed by direct numerical evaluations in lattice theory [280]. Corrections, coming from finite mass and spin effects, have been evaluated in Ref. [281].

We next examine the question of the possible influence on the energy of the state coming from a deformation of the phase-factor line in the definition of the mesonic operator (51). We choose, as a simple example, a rectangular line in position space, orthogonal to the time direction (Fig. 51a). The Wilson-loop contour, generated by this operator during a time evolution T, is represented in Fig. 51b by the dashed oriented line. The area mapped by the lattice plaquettes in the strong-coupling approximation is equal to $R(T + 2d)$. It is only the factor multiplying the variable T that contributes to the interaction energy; from this, one deduces the same relation as in Eq. (105), which shows that the phase-factor line deformation in the mesonic operator does not modify the energy of the state. The resulting change in the Wilson-loop vacuum average comes from the factor $e^{-\sigma 2dR}$, which is absorbed in the meson wave-function expressions. Also, line deformations having components on the time axis, with finite size Δt_0, say, cannot modify the energy of the state, since the size Δt_0 becomes negligible in front of T, when the latter goes to infinity.

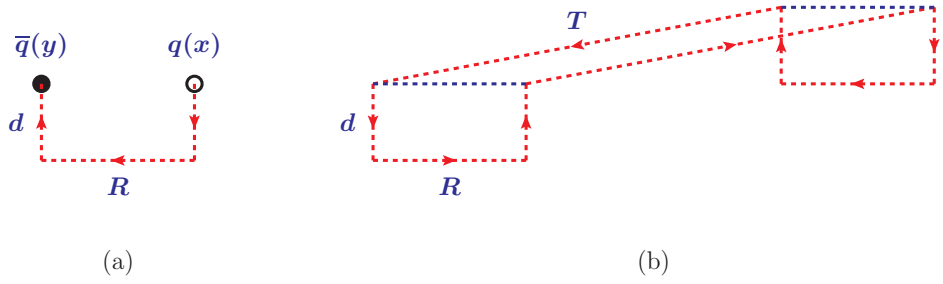

Figure 51: (a) A mesonic operator with a rectangular phase-factor line; (b) the Wilson-loop contour, generated after a time evolution T, represented by the dashed oriented line.

It is worth noticing that, in the continuum theory, it is expected that, for large contours, the Wilson-loop vacuum average is saturated by the minimal surface enclosed by the contour [48, 203, 204]. The minimal surface corresponding to the contour of Fig. 51b does not coincide with the union of the three rectangular areas delineated by the contour and paved by the plaquettes of the lattice. According to the defining equation of the minimal surfaces, it lies outside these areas [204]. However, when the limit $T \to \infty$ is taken, it shrinks to the above areas and thus provides the same result as that obtained on the lattice.

We now consider the problem of the tetraquark operator in the diquark-antidiquark antisymmetric representation together with its reduction into two mesonic operators, as represented in Fig. 47. As a consequence of the independence of the energy of a system of the types of phase-factor lines, as shown above, one can deform, in the mesonic operators of the right-hand side of the equality in Fig. 47, the phase-factor lines to transform them into straight line segments joining the quark to the antiquark. In the configuration adopted in that figure, the first diagram of the two-meson system involves smaller lengths for the distances between the quark and the antiquark inside the mesons with respect to the second diagram. According to Eq. (105), the energy of the first diagram being thus smaller than that of the second diagram, one can drop for the present study the contribution of the latter, which will give negligible contributions compared to the first one in the Wilson-loop evaluations. (We recall that the quarks are static.) Since we are interested in qualitative aspects, we make further simplifications in the geometric configurations of each representation. We choose equal distances ℓ between the quark and the antiquark in each meson. The two mesonic operators are placed in the same plane, along parallel directions, the two quarks and the two antiquarks being aligned along vertical lines, separated by a distance d (see Fig. 52a, top). The same configuration of the quarks and the antiquarks is also chosen for the tetraquark operator (Fig. 52b, top).

The evolution of the two systems during a time T generates Wilson loops whose contours are represented in Fig. 52. The system of two mesons generates two independent factorized Wilson loops, each with a rectangular contour. (In the continuum theory, factorization of Wilson loops occurs at leading order of large N_c [115]; nonfactorizable contributions are of the OZI-rule violating type, cf. Fig. 13.) The total area enclosed by the contours is $2\ell T$. The tetraquark operator generates a single Wilson loop, whose contour is composed of a central rectangle of width ℓ and

of four wings, each having a width equal to $d/2$. The total area enclosed in the contour is $(\ell + 2d)T$. One then obtains for the two-meson system and for the tetraquark system the following interaction energies:

$$E_{\text{2mes.}} = \sigma(2\ell), \qquad E_{\text{tetrq.}} = \sigma(\ell + 2d). \tag{106}$$

The two energies are not equal. The system which will dominate in the generating functional of Green's functions is the one that has the smallest energy. A fair dominance of the tetraquark system thus requires

$$\sigma(\ell + 2d) \ll \sigma(2\ell) \quad \Longrightarrow \quad d \ll \ell/2. \tag{107}$$

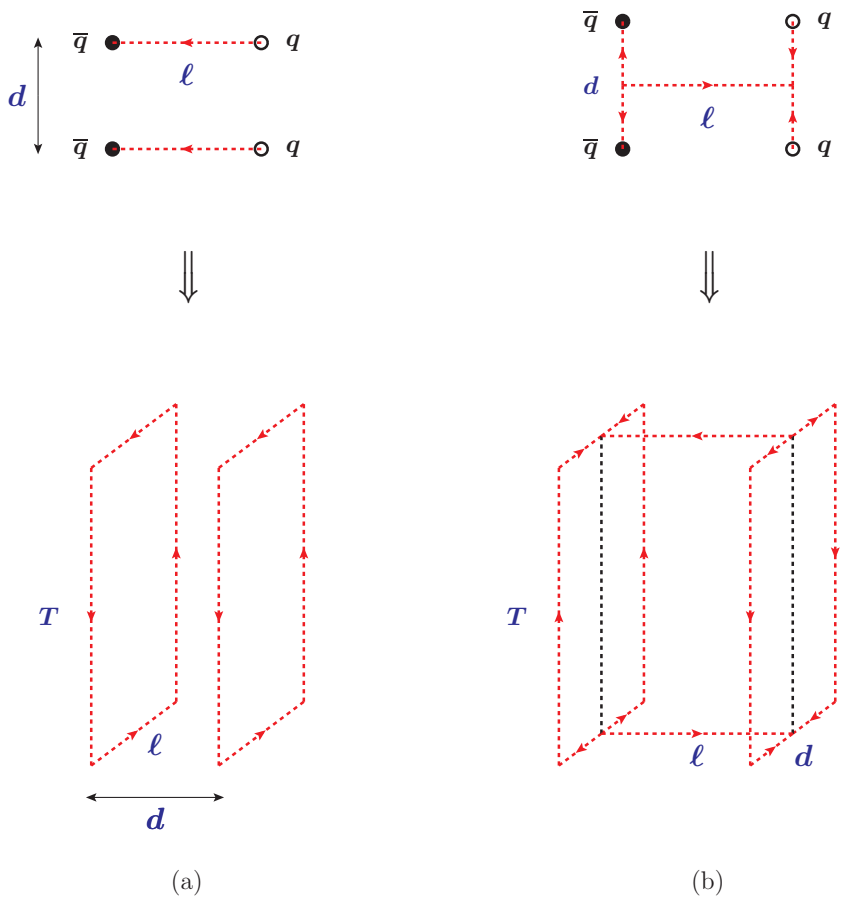

Figure 52: (a) Two mesonic operators and the Wilson loop contours generated after a time evolution T. (b) Tetraquark operator in the diquark-antidiquark antisymmetric representation and the Wilson-loop contour generated after a time evolution T, represented by the dashed oriented lines.

The meaning of Eq. (107) is that, when the distance between the two mesons is much smaller compared to their mean size, the tetraquark operator may be considered as the representative of the system. More generally, one might also have situations where the two mesons are overlapping each other. Therefore, condition (107) depicts situations where the two quark-antiquark pairs are located in a small volume, in which the two mesons are not sufficiently separated from each other. When a clear separation of the two mesons is realized, such that $d \gg \ell/2$, then the latter system becomes the dominant one.

The analysis presented above can easily be extended to the case of the general group SU(N_c). We consider here the two extreme cases of Fig. 19. For the left diagram, one obtains, in similar geometric configurations as before,

$E_{\text{tetrq.}} = \sigma(\ell + (N_c - 1)d)$ and $E_{(N_c-1)\text{mes.}} = \sigma(N_c - 1)\ell$. At large N_c, the dominance of the tetraquark system occurs when $d \ll \ell$, a condition that is qualitatively similar to Eq. (107). For the right diagram of Fig. 19, one obtains[9] $E_{\text{tetrq.}} = \sigma((N_c - 2)\ell + 2d)$ and $E_{2\text{mes.}} = \sigma(2\ell)$. At large N_c, the two-meson system is dominant for any situation; this is a corollary to a similar property arising from the comparison of the quadratic Casimirs of the diquark and quark-antiquark systems (Sec. 5.4).

The previous analyses can also be applied to other multiquark systems, like pentaquarks and hexaquarks, reaching similar conclusions: the multiquark operator, constructed in the diquark-type antisymmetric representation (or, equivalently, in the string-junction-type or Y-shaped-type representations) is representative of the system only when all quarks and antiquarks are positioned in a small volume of space, where the mesonic or baryonic clusters are overlapping each other or are very close to each other; outside such a volume, the mesonic and baryonic clusters become more faithful representatives of the system under study.

It is evident that when the static approximation is relaxed, the energy spectrum of the four-quark system will be determined from the solution of the corresponding bound-state equation with its energy eigenvalues, which implicitly takes into account the underlying gauge-field configurations and the probabilities of their realization in the corresponding dynamical situation. The quantum-mechanical outcome of the previous analysis is the sharp dominance of the two-meson description for the tetraquark case, which is corroborated by the analysis based on the comparison of the quadratic Casimirs of the diquark and quark-antiquark systems (Sec. 5.4; cf. also Refs. [220–223] and Sec. 7.3).

The strong-coupling approximation in lattice gauge theories for four-quark systems has been first considered by Dosch [282]. The results presented above have been confirmed by direct numerical calculations on the lattice for the SU(3) case [101, 283–287].

In conclusion, the cluster separability property of multiquark operators, obtained on formal grounds, has a weaker significance when energy balance is considered in the static limit, where the quarks stand at fixed spatial positions. Although the string-junction-type representation does not survive in all space, it may still dominate in small volumes, from which it may influence, by continuity on the frontier of the volume, the properties of the system in the external volume. Nevertheless, for the general case of moving quarks, one should expect a stronger dominance of the mesonic or baryonic clusters. We shall study, in the next subsection, in more detail, the contributions of each type of description to the interaction energy of the system.

7.3. Geometric partitioning

A general feature of the static interaction energies is that they continue representing the dragging guide of the system under consideration even when the constituents are in motion, after, of course, taking into account the kinematic modifications. We shall now consider the case of moving quarks and antiquarks in the nonrelativistic approximation, corresponding, in practice, to heavy quarks and antiquarks. This generalization is sufficient to deduce the essential qualitative aspects of the problem.

We denote henceforth the interaction energies by V. The system that is considered is the tetraquark system in its Y-shaped representation (Fig. 53a) and in its mesonic-cluster-type representations (Figs. 53b and c), as deduced from the cluster reducibility relation of Fig. 47. The two quarks are designated by 1 and 3, the antiquarks by $\overline{2}$ and $\overline{4}$, and the two junction points of the Y-shaped representation by k and ℓ. The quarks and antiquarks being in motion, the lengths of the various segments of Fig. 53 are now variables of the problem. On the other hand, the positions of the junction points k and ℓ are not predetermined; they are obtained after a minimization of the interaction energy V of the Y-shaped representation with respect to these points. The latter are called "Steiner points" in the literature. In general, for a configuration of the type of Fig. 53a, the point k corresponds to the position from which the pairs of points $(1, 3)$, $(3, \ell)$ and $(\ell, 1)$ are seen under 120° and similarly for the point ℓ. In principle, the minimization program should be applied continuously for every configuration of the quark and antiquark positions; this, however, is a lengthy time consuming task and generally one is satisfied with simple geometric configurations, which are proved as introducing only tiny quantitative errors.

The interaction or potential energy of the two-mesonic clusters is composed of the contributions of Figs. 53b and c. According to Eq. (105), they are, respectively,

$$V_{\overline{2}1,\overline{4}3} = \sigma(r_{\overline{2}1} + r_{\overline{4}3}), \qquad V_{\overline{4}1,\overline{2}3} = \sigma(r_{\overline{4}1} + r_{\overline{2}3}), \tag{108}$$

[9] For the tetraquark system, one has $(N_c - 2)$ independent Wilson lines.

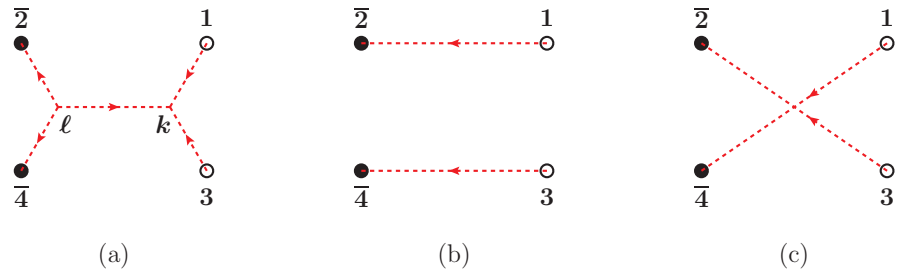

Figure 53: The tetraquark system in (a) the Y-shaped representation, (b) and (c) two-mesonic cluster representations.

where we have designated by r_{ij} the three-dimensional distance between positions i and j.

According to the positions of the quarks and antiquarks, the interaction energy that prevails is the one that is minimal:

$$V_{\text{2mes.}} = \min(V_{\overline{2}1,\overline{4}3}, V_{\overline{4}1,\overline{2}3}), \tag{109}$$

which can also be rewritten as

$$\begin{aligned} V_{\text{2mes.}} \;=\; & \sigma(r_{\overline{2}1} + r_{\overline{4}3})\,\theta((r_{\overline{4}1} + r_{\overline{2}3}) - (r_{\overline{2}1} + r_{\overline{4}3})) \\ & + \sigma(r_{\overline{4}1} + r_{\overline{2}3})\,\theta((r_{\overline{2}1} + r_{\overline{4}3}) - (r_{\overline{4}1} + r_{\overline{2}3})). \end{aligned} \tag{110}$$

On the other hand, the Y-shaped potential takes the form

$$V_Y = \sigma(r_{k1} + r_{k3} + r_{\overline{2}\ell} + r_{\overline{4}\ell} + r_{k\ell}). \tag{111}$$

The final potential is then the minimum of $V_{\text{2mes.}}$ and V_Y:

$$V_{\text{tetrq.}} = \min(V_Y, V_{\text{2mes.}}), \tag{112}$$

which is explicitly dependent on the positions of the quarks and the antiquarks. The Y-shaped potential will dominate in small volumes, where the quarks and the antiquarks are close to each other, while the two-meson potential will dominate when the two mesonic clusters are well separated.

The two-meson potential (110), which is composed of the contributions of two different clusters, exclusive to each other, is based on the quark rearrangement mechanism when two quarks or two antiquarks come close to each other. This potential is known in the literature under the name of "flip-flop" [288–300]. One of its features is that it is free of long-range van der Waals-type forces, which unavoidably occur in additive quark models with confining potentials [301–305]. Actually, Ref. [289] adopted it just on the basis of the latter property. It also introduced the concept of "configuration-space partitioning", due to the appearance of different potentials according to the positions of the quarks and the antiquarks. However, one should be aware that potential (110) is not a mere model proposition, but is the outcome of QCD lattice calculations in the strong-coupling limit, and is verified in full numerical calculations [101, 282–286]. In the continuum theory, it has support from Wilson-loop calculations in the large-N_c limit [203, 204].

In calculations with potential (112), one is interested in the possible existence of tetraquark bound states, which would be stable under strong interactions and would thus provide a clear experimental signal. This would happen if the bound state is located below the two-meson thresholds. Narrow resonance-type states, which would be located above two-meson thresholds, might also give signals about the existence of quasi-stable tetraquark states. Detailed calculations have been done in Refs. [294–300]. In particular, Ref. [294] provides instructive details about the contributions of the various forces. Ignoring spin degrees of freedom, systems made of quarks with two different flavors, of the types $QQ\bar{q}\bar{q}$ and $Qq\overline{Q}\overline{q}$, have been considered. It turns out that, for the existence of a bound state, the Y-shaped potential plays a minor role; the main role is played by the flip-flop potential. Thus the system $QQ\bar{q}\bar{q}$ has always a bound state for any value of the ratio of the quark masses, with a binding energy rather small compared to the strong-interaction energy scale. The system $Qq\overline{Q}\overline{q}$ has bound states only for comparable masses of the two quarks.

It may seem puzzling how the flip-flop potential, where the two clusters do not directly interact, can produce a bound state. Actually, the interaction is hidden in the quark rearrangement mechanism, since the flip-flop potential involves transitions between the quark configurations $(\bar{2}1)(\bar{4}3)$ and $(\bar{4}1)(\bar{2}3)$. The dynamical mechanism that realizes such transitions at the level of scattering amplitudes and Feynman diagrams is based on the quark rearrangement channels $R1$ and $R2$, the role of which, as a possible kernel in iteration series of bound-state emergence, was stressed in Sec. 5.4.

The existence of a stable tetraquark bound state with the structure $QQ\bar{q}\bar{q}$ had also been predicted by Manohar and Wise [306] on the basis of the heavy-quark limit. In this limit, the interaction between the two heavy quarks is well described by the short-range component of the confining potential and, because of its attractive nature, it produces a deeply bound diquark state, which behaves like an almost pointlike color-antitriplet heavy antiquark, which then forms with the two light antiquarks an antibaryon-like bound state. This mechanism has also been advocated in recent studies, together with the heavy-quark symmetry, to predict, on quantitative grounds, the tetraquark bound-state masses [307–309].

Although the predictions about the existence of tetraquark bound states of the type $QQ\bar{q}\bar{q}$ seem to be similar in the two approaches based on the geometric partitioning, on one hand, and on the heavy-quark symmetry, on the other, the lines of approach do not seem to have common features. In the heavy-quark symmetry approach, the heavy diquark system is reduced to a pointlike antiquark, while in the geometric partitioning approach it is just the contrary that is used, that is, the cluster reducibility of the system into mesonic clusters and their mutual interaction through the quark rearrangement mechanism.

Coming back to the geometric partitioning idea, it seems to provide a refined analysis of the conditions under which the reducibility of the multiquark operators and states occurs. The string-junction or Y-shaped junction-type description of multiquark states seems to survive only in small volumes of space, leaving the rest of space to the description based on the mesonic or baryonic clusters, which continue interacting by means of the quark exchange mechanism, producing, in turn, weakly bound multiquark states.

Nevertheless, the qualitative, as well as quantitative, conclusions reached up to now by means of the latter descriptions cannot be considered as definitive. The main reason of this is related to the fact that a complete description of a multiquark state necessitates, even in the nonrelativistic limit, the use of a multichannel interacting system, relating the independent basis states, the number of which is not limited to one. Taking the example of the tetraquark, we have seen, in Sec. 3.1, that there are two independent basis states or sectors, which could be taken to be the sectors $(\overline{2}1)(\overline{4}3)$ and $(\overline{4}1)(\overline{2}3)$ in their color-singlet-singlet representation, respectively, or the sector $(\overline{2}1)(\overline{4}3)$ in its singlet-singlet and octet-octet representations, or the diquark-antidiquark sectors in their antisymmetric and symmetric representations. Usually, the diquark-antidiquark sector in its symmetric representation, as well as the octet-octet sector, are discarded on the basis that their internal interaction is repulsive and could not lead to the formation of diquark or antidiquark or quark-antiquark intermediate bound states. However, one should also take into account the fact that the mutual interaction between these clusters to form a color-singlet state is still attractive with a strength at least twice greater than the conventional quark-antiquark interaction forming a color singlet. The existence of such forces might still substantially modify the predictions obtained up to now. Therefore, complementary studies are still needed in this approach to reach a definitive conclusion.

As a last remark, geometric partitioning, which has been formulated in a nonrelativistic framework, cannot be considered, in general, as an instantaneous phenomenon. It is the result of a transition process from an energetically favorable configuration to another one. This transition involves the quark rearrangement or interchange mechanism. Therefore, it might be that geometric partitioning is actually a simplified description of the more complicated quark rearrangement mechanism, which involves, in its generality, many Feynman diagrams.

8. Summary and concluding remarks

The extension of the color gauge group SU(3) to SU(N_c), with large N_c, as had been proposed by 't Hooft, has been revealed to form an efficient tool for the investigation of the nonperturbative regime of QCD. Without solving the theory, it has clarified many theoretical questions that had been raised with the emergence of QCD, some of which having already appeared with the early days of the quark model.

It is in the large-N_c limit that the notion of confinement takes its idealized formulation. In this limit, quark-pair creation being suppressed, mesons appear as made of a pair of quark and antiquark, therefore providing to the notion

of valence quarks a precise meaning. The $1/N_c$ expansion method, starting from leading terms, provides a systematic tool for a qualitative understanding of the order of magnitude of physical processes and observables. However, in this limit, baryons undergo a huge transition, since the number of their constituents increases with N_c and they tend to have a solitonic structure, necessitating a treatment different from that of mesons.

It is then natural to apply the large-N_c analysis to the case of exotic hadrons, which, in the language of valence quarks, are states containing more quarks and antiquarks than the ordinary hadrons. Many newly experimentally discovered or observed particles fall into this category, since their quantum numbers or decay modes do not fit into the scheme of the ordinary quark model.

The main theoretical question that arises at this level is whether such states are color irreducible, like ordinary hadrons. The latter, at the valence-quark level, cannot be decomposed into simpler color-singlet states. The answer, for the exotic states, is negative. They are decomposable into combinations of products of ordinary hadrons. This property is true not only for local interpolating currents, but also for multilocal operators involving gauge links. This means that exotic states are not natural extensions of ordinary hadrons and could not be solutions resulting from fully confining forces, with a spectroscopy made of towers of bound states with increasing masses. Such a situation might be reached only with the existence of hidden fine-tuning mechanisms that could favor the confining forces to take place, without being destabilized by cluster decomposition.

In passing to the gauge group SU(N_c), new technical complications arise. It turns out that exotic states can be probed or described by several inequivalent representations, each containing different numbers of valence quarks. Thus, tetraquarks, which in the case of SU(3) are described as made of two pairs of valence quarks and antiquarks, have now $(N_c - 2)$ different representations, a generic representation having J pairs of quarks and antiquarks, J taking values from 2 to $(N_c - 1)$. Similar generalizations occur also for pentaquarks and hexaquarks. Concerning tetraquarks, the interpolating operators that contain two pairs of quarks and antiquarks are the most convenient ones, since they remain closest to the SU(3) case and allow easy recognition of experimental outcomes. It is the latter representation which has been adopted throughout the present work.

Since tetraquarks are expected to decay or to couple to two-meson states, it is natural to analyze their properties by means of meson-meson scattering amplitudes. The case of fully exotic tetraquarks, containing four different quark flavors, is the simplest one, for there mixing channels with ordinary mesons are avoided. One is then in the presence of a coupled-channel problem, where the contributions of all channels shoud be taken into account. It turns out that, at large N_c, the diagonal channels (or direct channels) are dominant, while the off-diagonal channels (or quark-rearrangement or quark-interchanging channels) are subdominant. This has as a consequence that if there are tetraquark states, they are two in number, each one corresponding to the diagonal-channel solution, and each of them having a dominant coupling with the two mesons of that channel, of the order of $1/N_c$. In case of a possibility of decay, the corresponding decay width would be of the order of $1/N_c^2$. This solution does not favor the diquark scheme, which, because of the confinement constraint, is built on a single antisymmetric representation and thus predicts a single tetraquark, having equal couplings with the two mesons of each channel (spin quantum numbers having been ignored, as not being essential for these analyses).

It should be stressed that, contrary to the case of ordinary hadrons, the large-N_c analysis does not imply the existence of tetraquarks. These are in competition with contributions of two-meson intermediate states, which consistently can saturate the various equations. Tetraquarks, if they exist, are additonal contributions to the intermediate states. Therefore, predictions obtained about tetraquarks at large N_c should be considered as upper bounds for the related quantities.

The large-N_c analysis also allows the study of the formation mechanism of tetraquark states. At leading order, it is the two-meson clusters that provide the main contributions and these are expected not to mutually interact by means of confining forces. In that scheme, the main formation mechanism is generated by the internal contributions of quark-rearrangement (quark-interchange) processes. These sum up and might produce tetraquark poles in the meson-meson scattering amplitudes. There are two possible interpretations of the global outcome of this mechanism: (i) The whole summation is reduced to an effective meson-meson interaction, producing molecular-type tetraquarks. (ii) The interaction between the meson clusters, even if not confining, is of the residual type of confining interactions, not reducible to meson exchanges or contact terms. Only a more detailed investigation of the corresponding dynamics might provide a clarification of that issue.

For cryptoexotic states, with three or two quark flavors, mixing diagrams, involving ordinary mesons as intermediate states, complicate the extraction of the tetraquark properties. Nevertheless, the existence of four-channel processes

and the fact that the quark-rearrangement mechanism is still at work, imply, in general, the possibility of the existence of two different tetraquarks, eventually having privileged couplings with the mesons of the diagonal-type channels.

Finally, the idea of geometric partitioning, which takes into account the energy balance of meson-cluster- and string-junction-type configurations, has provided further clarification about the dominant configurations which might produce tetraquark states. Except in small volumes, where the four quarks are located, most of space is dominated by two-meson-cluster configurations. The transition from one of these configurations to the other implies again the quark-rearrangement mechanism.

The mechanism of formation of tetraquarks is not yet fully understood, due to the complexity of experimental data and the lack of explicit theoretical solutions. However, the large-N_c approach provides a complementary view to the problem by establishing a hierarchy among the various types of contributions. The general outcome that emerges from that approach is that the tetraquark formation is mainly dominated by the quark-rearrangement mechanism, which operates at the internal level of the processes.

The problem of exotic hadrons still remains a challenge for all theoretical approaches.

Acknowledgements

D. M. acknowledges support from the Austrian Science Fund (FWF), Grant No. P29028. H. S. acknowledges support from the EU research and innovation programme Horizon 2020, under Grant agreement No. 824093. D. M. and H. S. are grateful for support under joint CNRS/RFBR Grant No. PRC Russia/19-52-15022. The figures (except Fig. 46) were drawn with the aid of the package Axodraw2 [310].

References

[1] M. Gell-Mann, A schematic model of baryons and mesons, Phys. Lett. 8 (1964) 214. doi:10.1016/S0031-9163(64)92001-3.

[2] G. Zweig, An SU(3) model for strong interaction symmetry and its breaking. Version 2, in: D. Lichtenberg, S. P. Rosen (Eds.), Developments in the quark theory of hadrons, vol. 1. 1964 - 1978, 1964, p. 22.
URL `http://inspirehep.net/record/4674/files/cern-th-412.pdf`

[3] H. Fritzsch, M. Gell-Mann, H. Leutwyler, Advantages of the color octet gluon picture, Phys. Lett. B 47 (1973) 365. doi:10.1016/0370-2693(73)90625-4.

[4] D. J. Gross, F. Wilczek, Ultraviolet behavior of non-Abelian gauge theories, Phys. Rev. Lett. 30 (1973) 1343. doi:10.1103/PhysRevLett.30.1343.

[5] H. Politzer, Reliable perturbative results for strong interactions?, Phys. Rev. Lett. 30 (1973) 1346. doi:10.1103/PhysRevLett.30.1346.

[6] R. L. Jaffe, Multi-quark hadrons. 1. The phenomenology of $Q^2\overline{Q}^2$ mesons, Phys. Rev. D 15 (1977) 267. doi:10.1103/PhysRevD.15.267.

[7] R. L. Jaffe, Multi-quark hadrons. 2. Methods, Phys. Rev. D 15 (1977) 281. doi:10.1103/PhysRevD.15.281.

[8] S. Choi, et al., Observation of a narrow charmonium-like state in exclusive $B^{\pm} \to K^{\pm}\pi^{+}\pi^{-}J/\psi$ decays, Phys. Rev. Lett. 91 (2003) 262001. arXiv:hep-ex/0309032, doi:10.1103/PhysRevLett.91.262001.

[9] B. Aubert, et al., Observation of a narrow meson decaying to $D_s^{+}\pi^{0}$ at a mass of 2.32 GeV/c^2, Phys. Rev. Lett. 90 (2003) 242001. arXiv:hep-ex/0304021, doi:10.1103/PhysRevLett.90.242001.

[10] D. Besson, et al., Observation of a narrow resonance of mass 2.46 GeV/c^2 decaying to $D_s^{*+}\pi^{0}$ and confirmation of the $D_{sJ}^{*}(2317)$ state, Phys. Rev. D 68 (2003) 032002, [Erratum: Phys. Rev. D 75 (2007) 119908]. arXiv:hep-ex/0305100, doi:10.1103/PhysRevD.68.032002.

[11] B. Aubert, et al., Observation of a broad structure in the $\pi^{+}\pi^{-}J/\psi$ mass spectrum around 4.26 GeV/c^2, Phys. Rev. Lett. 95 (2005) 142001. arXiv:hep-ex/0506081, doi:10.1103/PhysRevLett.95.142001.

[12] M. Ablikim, et al., Observation of a charged charmoniumlike structure in $e^{+}e^{-} \to \pi^{+}\pi^{-}J/\psi$ at $\sqrt{s}$ = 4.26 GeV, Phys. Rev. Lett. 110 (2013) 252001. arXiv:1303.5949, doi:10.1103/PhysRevLett.110.252001.

[13] Z. Liu, et al., Study of $e^{+}e^{-} \to \pi^{+}\pi^{-}J/\psi$ and observation of a charged charmoniumlike state at Belle, Phys. Rev. Lett. 110 (2013) 252002, [Erratum: Phys. Rev. Lett. 111 (2013) 019901]. arXiv:1304.0121, doi:10.1103/PhysRevLett.110.252002.

[14] M. Ablikim, et al., Observation of a charged charmoniumlike structure $Z_c(4020)$ and search for the $Z_c(3900)$ in $e^{+}e^{-} \to \pi^{+}\pi^{-}h_c$, Phys. Rev. Lett. 111 (2013) 242001. arXiv:1309.1896, doi:10.1103/PhysRevLett.111.242001.

[15] R. Aaij, et al., Observation of the resonant character of the $Z(4430)^{-}$ state, Phys. Rev. Lett. 112 (2014) 222002. arXiv:1404.1903, doi:10.1103/PhysRevLett.112.222002.

[16] R. Aaij, et al., Observation of $J/\psi p$ resonances consistent with pentaquark states in $\Lambda_b^0 \to J/\psi K^{-} p$ decays, Phys. Rev. Lett. 115 (2015) 072001. arXiv:1507.03414, doi:10.1103/PhysRevLett.115.072001.

[17] R. Aaij, et al., Observation of structure in the J/ψ-pair mass spectrum, Sci. Bull. 65 (2020) 1983. arXiv:2006.16957, doi:10.1016/j.scib.2020.08.032.

[18] R. Aaij, et al., Amplitude analysis of the $B^{+} \to D^{+}D^{-}K^{+}$ decay, Phys. Rev. D 102 (2020) 112003. arXiv:2009.00026, doi:10.1103/PhysRevD.102.112003.

[19] L. Wu, Recent XYZ results at BESIII (2020). arXiv:2012.15473.

[20] H.-X. Chen, W. Chen, X. Liu, S.-L. Zhu, The hidden-charm pentaquark and tetraquark states, Phys. Rep. 639 (2016) 1. arXiv:1601.02092, doi:10.1016/j.physrep.2016.05.004.

[21] A. Hosaka, T. Iijima, K. Miyabayashi, Y. Sakai, S. Yasui, Exotic hadrons with heavy flavors: X, Y, Z, and related states, PTEP 2016 (2016) 062C01. arXiv:1603.09229, doi:10.1093/ptep/ptw045.
[22] R. F. Lebed, R. E. Mitchell, E. S. Swanson, Heavy-quark QCD exotica, Prog. Part. Nucl. Phys. 93 (2017) 143. arXiv:1610.04528, doi:10.1016/j.ppnp.2016.11.003.
[23] A. Esposito, A. Pilloni, A. D. Polosa, Multiquark resonances, Phys. Rep. 668 (2017) 1. arXiv:1611.07920, doi:10.1016/j.physrep.2016.11.002.
[24] A. Ali, J. S. Lange, S. Stone, Exotics: heavy pentaquarks and tetraquarks, Prog. Part. Nucl. Phys. 97 (2017) 123. arXiv:1706.00610, doi:10.1016/j.ppnp.2017.08.003.
[25] F.-K. Guo, C. Hanhart, U.-G. Meissner, Q. Wang, Q. Zhao, B.-S. Zou, Hadronic molecules, Rev. Mod. Phys. 90 (2018) 015004. arXiv:1705.00141, doi:10.1103/RevModPhys.90.015004.
[26] S. L. Olsen, T. Skwarnicki, D. Zieminska, Non-standard heavy mesons and baryons: Experimental evidence, Rev. Mod. Phys. 90 (2018) 015003. arXiv:1708.04012, doi:10.1103/RevModPhys.90.015003.
[27] M. Karliner, J. L. Rosner, T. Skwarnicki, Multiquark states, Ann. Rev. Nucl. Part. Sci. 68 (2018) 17. arXiv:1711.10626, doi:10.1146/annurev-nucl-101917-020902.
[28] R. M. Albuquerque, J. M. Dias, K. Khemchandani, A. Martínez Torres, F. S. Navarra, M. Nielsen, C. M. Zanetti, QCD sum rules approach to the X, Y and Z states, J. Phys. G 46 (2019) 093002. arXiv:1812.08207, doi:10.1088/1361-6471/ab2678.
[29] Y.-R. Liu, H.-X. Chen, W. Chen, X. Liu, S.-L. Zhu, Pentaquark and tetraquark states, Prog. Part. Nucl. Phys. 107 (2019) 237. arXiv:1903.11976, doi:10.1016/j.ppnp.2019.04.003.
[30] A. Ali, L. Maiani, A. D. Polosa, Multiquark Hadrons, Cambridge University Press, 2019. doi:10.1017/9781316761465.
[31] N. Brambilla, S. Eidelman, C. Hanhart, A. Nefediev, C.-P. Shen, C. E. Thomas, A. Vairo, C.-Z. Yuan, The XYZ states: experimental and theoretical status and perspectives, Phys. Rep. 873 (2020) 1. arXiv:1907.07583.
[32] A. Chodos, R. Jaffe, K. Johnson, C. B. Thorn, V. Weisskopf, A new extended model of hadrons, Phys. Rev. D 9 (1974) 3471. doi:10.1103/PhysRevD.9.3471.
[33] A. Chodos, R. Jaffe, K. Johnson, C. B. Thorn, Baryon structure in the bag theory, Phys. Rev. D 10 (1974) 2599. doi:10.1103/PhysRevD.10.2599.
[34] T. A. DeGrand, R. Jaffe, K. Johnson, J. Kiskis, Masses and other parameters of the light hadrons, Phys. Rev. D 12 (1975) 2060. doi:10.1103/PhysRevD.12.2060.
[35] A. De Rújula, H. Georgi, S. Glashow, Hadron masses in a gauge theory, Phys. Rev. D 12 (1975) 147. doi:10.1103/PhysRevD.12.147.
[36] T. Appelquist, H. D. Politzer, Heavy quarks and long-lived hadrons, Phys. Rev. D 12 (1975) 1404. doi:10.1103/PhysRevD.12.1404.
[37] E. Eichten, K. Gottfried, T. Kinoshita, K. Lane, T.-M. Yan, Charmonium: the model, Phys. Rev. D 17 (1978) 3090, [Erratum: Phys. Rev. D 21 (1980) 313]. doi:10.1103/PhysRevD.17.3090.
[38] E. Eichten, K. Gottfried, T. Kinoshita, K. Lane, T.-M. Yan, Charmonium: comparison with experiment, Phys. Rev. D 21 (1980) 203. doi:10.1103/PhysRevD.21.203.
[39] N. Isgur, G. Karl, P-wave baryons in the quark model, Phys. Rev. D 18 (1978) 4187. doi:10.1103/PhysRevD.18.4187.
[40] S. Godfrey, N. Isgur, Mesons in a relativized quark model with chromodynamics, Phys. Rev. D 32 (1985) 189. doi:10.1103/PhysRevD.32.189.
[41] A. Le Yaouanc, L. Oliver, S. Ono, O. Pene, J.-C. Raynal, A quark model of light mesons with dynamically broken chiral symmetry, Phys. Rev. D 31 (1985) 137. doi:10.1103/PhysRevD.31.137.
[42] W. Lucha, F. F. Schöberl, D. Gromes, Bound states of quarks, Phys. Rep. 200 (1991) 127. doi:10.1016/0370-1573(91)90001-3.
[43] T. Regge, Introduction to complex orbital momenta, Nuovo Cim. 14 (1959) 951. doi:10.1007/BF02728177.
[44] T. Regge, Bound states, shadow states and Mandelstam representation, Nuovo Cim. 18 (1960) 947. doi:10.1007/BF02733035.
[45] G. Veneziano, Construction of a crossing-symmetric, Regge-behaved amplitude for linearly rising trajectories, Nuovo Cim. A 57 (1968) 190. doi:10.1007/BF02824451.
[46] R. J. Eden, Regge poles and elementary particles, Rep. Prog. Phys. 34 (1971) 995. doi:10.1088/0034-4885/34/3/304.
[47] V. N. Gribov, Strong Interactions of Hadrons at High Energies: Gribov Lectures on Theoretical Physics, Cambridge University Press, 2008. doi:10.1017/CBO9780511534942.
[48] K. G. Wilson, Confinement of quarks, Phys. Rev. D 10 (1974) 2445. doi:10.1103/PhysRevD.10.2445.
[49] L. S. Brown, W. I. Weisberger, Remarks on the static potential in quantum chromodynamics, Phys. Rev. D 20 (1979) 3239. doi:10.1103/PhysRevD.20.3239.
[50] R. L. Jaffe, Two types of hadrons, Nucl. Phys. A 804 (2008) 25. doi:10.1016/j.nuclphysa.2008.01.009.
[51] S. Weinberg, Evidence that the deuteron is not an elementary particle, Phys. Rev. 137 (1965) B672. doi:10.1103/PhysRev.137.B672.
[52] M. B. Voloshin, L. B. Okun, Hadron molecules and charmonium atom, JETP Lett. 23 (1976) 333, [Pisma Zh. Eksp. Teor. Fiz. 23, 369 (1976)].
[53] A. De Rújula, H. Georgi, S. L. Glashow, Molecular charmonium: a new spectroscopy?, Phys. Rev. Lett. 38 (1977) 317. doi:10.1103/PhysRevLett.38.317.
[54] N. A. Törnqvist, From the deuteron to deusons, an analysis of deuteronlike meson-meson bound states, Z. Phys. C 61 (1994) 525. arXiv:hep-ph/9310247, doi:10.1007/BF01413192.
[55] W. Lucha, D. Melikhov, H. Sazdjian, Cluster reducibility of multiquark operators, Phys. Rev. D 100 (2019) 094017. arXiv:1908.10164, doi:10.1103/PhysRevD.100.094017.
[56] M. Anselmino, E. Predazzi, S. Ekelin, S. Fredriksson, D. Lichtenberg, Diquarks, Rev. Mod. Phys. 65 (1993) 1199. doi:10.1103/RevModPhys.65.1199.
[57] D. B. Lichtenberg, W. Namgung, E. Predazzi, J. G. Wills, Baryon masses in a relativistic quark-diquark model, Phys. Rev. Lett. 48 (1982) 1653. doi:10.1103/PhysRevLett.48.1653.
[58] S. Fleck, B. Silvestre-Brac, J.-M. Richard, Search for diquark clustering in baryons, Phys. Rev. D 38 (1988) 1519. doi:10.1103/PhysRevD.38.1519.

[59] T. Schäfer, E. V. Shuryak, J. J. M. Verbaarschot, Baryonic correlators in the random instanton vacuum, Nucl. Phys. B 412 (1994) 143. arXiv:hep-ph/9306220, doi:10.1016/0550-3213(94)90497-9.
[60] R. Jaffe, F. Wilczek, Diquarks and exotic spectroscopy, Phys. Rev. Lett. 91 (2003) 232003. arXiv:hep-ph/0307341, doi:10.1103/PhysRevLett.91.232003.
[61] E. Shuryak, I. Zahed, A schematic model for pentaquarks using diquarks, Phys. Lett. B 589 (2004) 21. arXiv:hep-ph/0310270, doi:10.1016/j.physletb.2004.03.019.
[62] L. Maiani, F. Piccinini, A. D. Polosa, V. Riquer, Diquark-antidiquarks with hidden or open charm and the nature of X(3872), Phys. Rev. D 71 (2005) 014028. arXiv:hep-ph/0412098, doi:10.1103/PhysRevD.71.014028.
[63] L. Maiani, V. Riquer, F. Piccinini, A. D. Polosa, Four quark interpretation of Y(4260), Phys. Rev. D 72 (2005) 031502. arXiv:hep-ph/0507062, doi:10.1103/PhysRevD.72.031502.
[64] D. Ebert, R. N. Faustov, V. O. Galkin, W. Lucha, Masses of tetraquarks with two heavy quarks in the relativistic quark model, Phys. Rev. D 76 (2007) 114015. arXiv:0706.3853, doi:10.1103/PhysRevD.76.114015.
[65] D. Ebert, R. N. Faustov, V. O. Galkin, Masses of tetraquarks with open charm and bottom, Phys. Lett. B 696 (2011) 241. arXiv:1011.2677, doi:10.1016/j.physletb.2010.12.033.
[66] L. Maiani, A. D. Polosa, V. Riquer, The new pentaquarks in the diquark model, Phys. Lett. B 749 (2015) 289. arXiv:1507.04980, doi:10.1016/j.physletb.2015.08.008.
[67] J. Wu, Y.-R. Liu, K. Chen, X. Liu, S.-L. Zhu, Heavy-flavored tetraquark states with the $QQ\bar{Q}\bar{Q}$ configuration, Phys. Rev. D 97 (2018) 094015. arXiv:1605.01134, doi:10.1103/PhysRevD.97.094015.
[68] R. F. Lebed, Spectroscopy of exotic hadrons formed from dynamical diquarks, Phys. Rev. D 96 (2017) 116003. arXiv:1709.06097, doi:10.1103/PhysRevD.96.116003.
[69] A. Ali, L. Maiani, A. V. Borisov, I. Ahmed, M. Jamil Aslam, A. Y. Parkhomenko, A. D. Polosa, A. Rehman, A new look at the Y tetraquarks and Ω_c baryons in the diquark model, Eur. Phys. J. C 78 (2018) 29. arXiv:1708.04650, doi:10.1140/epjc/s10052-017-5501-6.
[70] A. Ali, I. Ahmed, M. J. Aslam, A. Y. Parkhomenko, A. Rehman, Mass spectrum of the hidden-charm pentaquarks in the compact diquark model, JHEP 10 (2019) 256. arXiv:1907.06507, doi:10.1007/JHEP10(2019)256.
[71] J. F. Giron, R. F. Lebed, Simple spectrum of $c\bar{c}c\bar{c}$ states in the dynamical diquark model, Phys. Rev. D 102 (2020) 074003. arXiv:2008.01631, doi:10.1103/PhysRevD.102.074003.
[72] R. N. Faustov, V. O. Galkin, E. M. Savchenko, Masses of the $QQ\bar{Q}\bar{Q}$ tetraquarks in the relativistic diquark–antidiquark picture, Phys. Rev. D 102 (2020) 114030. arXiv:2009.13237, doi:10.1103/PhysRevD.102.114030.
[73] S. Weinberg, Phenomenological Lagrangians, Physica A 96 (1979) 327. doi:10.1016/0378-4371(79)90223-1.
[74] J. Gasser, H. Leutwyler, Chiral perturbation theory to one loop, Annals Phys. 158 (1984) 142. doi:10.1016/0003-4916(84)90242-2.
[75] J. Gasser, H. Leutwyler, Chiral perturbation theory: Expansions in the mass of the strange quark, Nucl. Phys. B 250 (1985) 465. doi:10.1016/0550-3213(85)90492-4.
[76] A. V. Manohar, Effective field theories, Lect. Notes Phys. 479 (1997) 311. arXiv:hep-ph/9606222, doi:10.1007/BFb0104294.
[77] H. Georgi, An effective field theory for heavy quarks at low energies, Phys. Lett. B 240 (1990) 447. doi:10.1016/0370-2693(90)91128-X.
[78] N. Isgur, M. B. Wise, Spectroscopy with heavy-quark symmetry, Phys. Rev. Lett. 66 (1991) 1130. doi:10.1103/PhysRevLett.66.1130.
[79] M. B. Wise, Chiral perturbation theory for hadrons containing a heavy quark, Phys. Rev. D 45 (1992) R2188. doi:10.1103/PhysRevD.45.R2188.
[80] M. Neubert, Heavy quark symmetry, Phys. Rep. 245 (1994) 259. arXiv:hep-ph/9306320, doi:10.1016/0370-1573(94)90091-4.
[81] R. Casalbuoni, A. Deandrea, N. Di Bartolomeo, R. Gatto, F. Feruglio, G. Nardulli, Phenomenology of heavy meson chiral Lagrangians, Phys. Rep. 281 (1997) 145. arXiv:hep-ph/9605342, doi:10.1016/S0370-1573(96)00027-0.
[82] J. Gasser, M. Sainio, A. Svarc, Nucleons with chiral loops, Nucl. Phys. B 307 (1988) 779. doi:10.1016/0550-3213(88)90108-3.
[83] S. Weinberg, Effective chiral Lagrangians for nucleon–pion interactions and nuclear forces, Nucl. Phys. B 363 (1991) 3. doi:10.1016/0550-3213(91)90231-L.
[84] C. Ordóñez, L. Ray, U. van Kolck, Two-nucleon potential from chiral Lagrangians, Phys. Rev. C 53 (1996) 2086. arXiv:hep-ph/9511380, doi:10.1103/PhysRevC.53.2086.
[85] D. B. Kaplan, M. J. Savage, M. B. Wise, Nucleon–nucleon scattering from effective field theory, Nucl. Phys. B 478 (1996) 629. arXiv:nucl-th/9605002, doi:10.1016/0550-3213(96)00357-4.
[86] E. Epelbaum, W. Glöckle, U.-G. Meissner, Nuclear forces from chiral Lagrangians using the method of unitary transformation. 1. Formalism, Nucl. Phys. A 637 (1998) 107. arXiv:nucl-th/9801064, doi:10.1016/S0375-9474(98)00220-6.
[87] E. Epelbaum, W. Glöckle, U.-G. Meissner, Nuclear forces from chiral Lagrangians using the method of unitary transformation. 2. The two nucleon system, Nucl. Phys. A 671 (2000) 295. arXiv:nucl-th/9910064, doi:10.1016/S0375-9474(99)00821-0.
[88] P. F. Bedaque, U. van Kolck, Effective field theory for few-nucleon systems, Ann. Rev. Nucl. Part. Sci. 52 (2002) 339. arXiv:nucl-th/0203055, doi:10.1146/annurev.nucl.52.050102.090637.
[89] H.-W. Hammer, S. König, U. van Kolck, Nuclear effective field theory: status and perspectives, Rev. Mod. Phys. 92 (2020) 025004. arXiv:1906.12122, doi:10.1103/RevModPhys.92.025004.
[90] W. E. Caswell, G. P. Lepage, Effective Lagrangians for bound state problems in QED, QCD, and other field theories, Phys. Lett. B 167 (1986) 437. doi:10.1016/0370-2693(86)91297-9.
[91] N. Brambilla, A. Pineda, J. Soto, A. Vairo, Effective field theories for heavy quarkonium, Rev. Mod. Phys. 77 (2005) 1423. arXiv:hep-ph/0410047, doi:10.1103/RevModPhys.77.1423.
[92] J. B. Kogut, Lattice gauge theory approach to quantum chromodynamics, Rev. Mod. Phys. 55 (1983) 775. doi:10.1103/RevModPhys.55.775.
[93] M. Lüscher, Two-particle states on a torus and their relation to the scattering matrix, Nucl. Phys. B 354 (1991) 531. doi:10.1016/0550-3213(91)90366-6.
[94] R. A. Briceno, J. J. Dudek, R. D. Young, Scattering processes and resonances from lattice QCD, Rev. Mod. Phys. 90 (2018) 025001. arXiv:1706.06223, doi:10.1103/RevModPhys.90.025001.
[95] S. Prelovsek, L. Leskovec, Evidence for $X(3872)$ from DD^* scattering on the lattice, Phys. Rev. Lett. 111 (2013) 192001. arXiv:1307.5172,

doi:10.1103/PhysRevLett.111.192001.
[96] S. Prelovsek, C. B. Lang, L. Leskovec, D. Mohler, Study of the Z_c^+ channel using lattice QCD, Phys. Rev. D 91 (2015) 014504. arXiv:1405.7623, doi:10.1103/PhysRevD.91.014504.
[97] Y. Ikeda, B. Charron, S. Aoki, T. Doi, T. Hatsuda, T. Inoue, N. Ishii, K. Murano, H. Nemura, K. Sasaki, Charmed tetraquarks T_{cc} and T_{cs} from dynamical lattice QCD simulations, Phys. Lett. B 729 (2014) 85. arXiv:1311.6214, doi:10.1016/j.physletb.2014.01.002.
[98] Y. Ikeda, S. Aoki, T. Doi, S. Gongyo, T. Hatsuda, T. Inoue, T. Iritani, N. Ishii, K. Murano, K. Sasaki, Fate of the tetraquark candidate $Z_c(3900)$ from lattice QCD, Phys. Rev. Lett. 117 (2016) 242001. arXiv:1602.03465, doi:10.1103/PhysRevLett.117.242001.
[99] M. Padmanath, C. B. Lang, S. Prelovsek, X(3872) and Y(4140) using diquark-antidiquark operators with lattice QCD, Phys. Rev. D 92 (2015) 034501. arXiv:1503.03257, doi:10.1103/PhysRevD.92.034501.
[100] P. Bicudo, K. Cichy, A. Peters, B. Wagenbach, M. Wagner, Evidence for the existence of $ud\bar{b}\bar{b}$ and the non-existence of $ss\bar{b}\bar{b}$ and $cc\bar{b}\bar{b}$ tetraquarks from lattice QCD, Phys. Rev. D 92 (2015) 014507. arXiv:1505.00613, doi:10.1103/PhysRevD.92.014507.
[101] P. Bicudo, M. Cardoso, O. Oliveira, P. J. Silva, Lattice QCD static potentials of the meson-meson and tetraquark systems computed with both quenched and full QCD, Phys. Rev. D 96 (2017) 074508. arXiv:1702.07789, doi:10.1103/PhysRevD.96.074508.
[102] P. Bicudo, M. Cardoso, A. Peters, M. Pflaumer, M. Wagner, $ud\bar{b}\bar{b}$ tetraquark resonances with lattice QCD potentials and the Born-Oppenheimer approximation, Phys. Rev. D 96 (2017) 054510. arXiv:1704.02383, doi:10.1103/PhysRevD.96.054510.
[103] A. Francis, R. J. Hudspith, R. Lewis, K. Maltman, Lattice prediction for deeply bound doubly heavy tetraquarks, Phys. Rev. Lett. 118 (2017) 142001. arXiv:1607.05214, doi:10.1103/PhysRevLett.118.142001.
[104] A. Francis, R. J. Hudspith, R. Lewis, K. Maltman, Evidence for charm-bottom tetraquarks and the mass dependence of heavy-light tetraquark states from lattice QCD, Phys. Rev. D 99 (2019) 054505. arXiv:1810.10550, doi:10.1103/PhysRevD.99.054505.
[105] G. K. C. Cheung, C. E. Thomas, J. J. Dudek, R. G. Edwards, Tetraquark operators in lattice QCD and exotic flavour states in the charm sector, JHEP 11 (2017) 033. arXiv:1709.01417, doi:10.1007/JHEP11(2017)033.
[106] C. Hughes, E. Eichten, C. T. H. Davies, Searching for beauty-fully bound tetraquarks using lattice nonrelativistic QCD, Phys. Rev. D 97 (2018) 054505. arXiv:1710.03236, doi:10.1103/PhysRevD.97.054505.
[107] P. Junnarkar, N. Mathur, M. Padmanath, Study of doubly heavy tetraquarks in lattice QCD, Phys. Rev. D 99 (2019) 034507. arXiv:1810.12285, doi:10.1103/PhysRevD.99.034507.
[108] L. Liu, K. Orginos, F.-K. Guo, C. Hanhart, U.-G. Meissner, Interactions of charmed mesons with light pseudoscalar mesons from lattice QCD and implications on the nature of the $D_{s0}^*(2317)$, Phys. Rev. D 87 (2013) 014508. arXiv:1208.4535, doi:10.1103/PhysRevD.87.014508.
[109] C. B. Lang, L. Leskovec, D. Mohler, S. Prelovsek, R. M. Woloshyn, D_s mesons with DK and D^*K scattering near threshold, Phys. Rev. D 90 (2014) 034510. arXiv:1403.8103, doi:10.1103/PhysRevD.90.034510.
[110] F.-K. Guo, L. Liu, U.-G. Meissner, P. Wang, Tetraquarks, hadronic molecules, meson-meson scattering and disconnected contributions in lattice QCD, Phys. Rev. D 88 (2013) 074506. arXiv:1308.2545, doi:10.1103/PhysRevD.88.074506.
[111] G. 't Hooft, A planar diagram theory for strong interactions, Nucl. Phys. B 72 (1974) 461. doi:10.1016/0550-3213(74)90154-0.
[112] G. 't Hooft, A two-dimensional model for mesons, Nucl. Phys. B 75 (1974) 461. doi:10.1016/0550-3213(74)90088-1.
[113] C. G. Callan, Jr., N. Coote, D. J. Gross, Two-dimensional Yang-Mills theory: a model of quark confinement, Phys. Rev. D 13 (1976) 1649. doi:10.1103/PhysRevD.13.1649.
[114] E. Witten, Baryons in the $1/N$ expansion, Nucl. Phys. B 160 (1979) 57. doi:10.1016/0550-3213(79)90232-3.
[115] E. Witten, The $1/N$ expansion in atomic and particle physics, NATO Sci. Ser. B 59 (1980) 403. doi:10.1007/978-1-4684-7571-5-21.
[116] S. Okubo, φ-meson and unitary symmetry model, Phys. Lett. 5 (1963) 165. doi:10.1016/S0375-9601(63)92548-9.
[117] J. Iizuka, Systematics and phenomenology of meson family, Prog. Theor. Phys. Suppl. 37 (1966) 21. doi:10.1143/PTPS.37.21.
[118] J. M. Maldacena, The large N limit of superconformal field theories and supergravity, Adv. Theor. Math. Phys. 2 (1998) 231. arXiv:hep-th/9711200, doi:10.4310/ATMP.1998.v2.n2.a1.
[119] J. M. Maldacena, Wilson loops in large N field theories, Phys. Rev. Lett. 80 (1998) 4859. arXiv:hep-th/9803002, doi:10.1103/PhysRevLett.80.4859.
[120] E. Witten, Anti-de Sitter space and holography, Adv. Theor. Math. Phys. 2 (1998) 253. arXiv:hep-th/9802150, doi:10.4310/ATMP.1998.v2.n2.a2.
[121] E. Witten, Anti-de Sitter space, thermal phase transition, and confinement in gauge theories, Adv. Theor. Math. Phys. 2 (1998) 505. arXiv:hep-th/9803131, doi:10.4310/ATMP.1998.v2.n3.a3.
[122] S. S. Gubser, I. R. Klebanov, A. M. Polyakov, Gauge theory correlators from non-critical string theory, Phys. Lett. B 428 (1998) 105. arXiv:hep-th/9802109, doi:10.1016/S0370-2693(98)00377-3.
[123] O. Aharony, S. S. Gubser, J. M. Maldacena, H. Ooguri, Y. Oz, Large N field theories, string theory and gravity, Phys. Rep. 323 (2000) 183. arXiv:hep-th/9905111, doi:10.1016/S0370-1573(99)00083-6.
[124] J. M. Maldacena, Gravity, particle physics and their unification, Int. J. Mod. Phys. A 15S1B (2000) 840. arXiv:hep-ph/0002092, doi:10.1142/S0217751X00005449.
[125] L. D. Landau, On analytic properties of vertex parts in quantum field theory, Nucl. Phys. 13 (1959) 181. doi:10.1016/0029-5582(59)90154-3.
[126] R. J. Eden, P. V. Landshoff, D. I. Olive, J. C. Polkinghorne, The Analytic S-Matrix, Cambridge Univ. Press, Cambridge, 1966.
[127] C. Itzykson, J.-B. Zuber, Quantum Field Theory, International Series in Pure and Applied Physics, McGraw-Hill, New York, 1980.
[128] L. D. Faddeev, V. N. Popov, Feynman diagrams for the Yang-Mills field, Phys. Lett. B 25 (1967) 29. doi:10.1016/0370-2693(67)90067-6.
[129] E. S. Abers, B. W. Lee, Gauge theories, Phys. Rep. 9 (1973) 1. doi:10.1016/0370-1573(73)90027-6.
[130] T. Cheng, L. Li, Gauge Theory of Elementary Particle Physics, Oxford Science Publications, Oxford, UK, 1984.
[131] M. Kaku, Quantum Field Theory: A Modern Introduction, Oxford University Press, New York, 1993.
[132] A. Buras, E. Floratos, D. Ross, C. T. Sachrajda, Asymptotic freedom beyond the leading order, Nucl. Phys. B 131 (1977) 308. doi:10.1016/0550-3213(77)90375-3.
[133] P. A. Zyla, et al., Review of Particle Physics, PTEP 2020 (2020) 083C01. doi:10.1093/ptep/ptaa104.
[134] H. B. Nielsen, P. Olesen, Vortex-line models for dual strings, Nucl. Phys. B 61 (1973) 45. doi:10.1016/0550-3213(73)90350-7.
[135] H. D. Politzer, Asymptotic freedom: An approach to strong interactions, Phys. Rep. 14 (1974) 129. doi:10.1016/0370-1573(74)90014-3.

[136] D. J. Gross, Applications of the renormalization group to high-energy physics, Conf. Proc. C 7507281 (1975) 141.
[137] G. Veneziano, Some aspects of a unified approach to gauge, dual and Gribov theories, Nucl. Phys. B 117 (1976) 519. doi:10.1016/0550-3213(76)90412-0.
[138] E. Corrigan, P. Ramond, A note on the quark content of large color groups, Phys. Lett. B 87 (1979) 73. doi:10.1016/0370-2693(79)90022-4.
[139] A. Armoni, M. Shifman, G. Veneziano, SUSY relics in one-flavor QCD from a new $1/N$ expansion, Phys. Rev. Lett. 91 (2003) 191601. arXiv:hep-th/0307097, doi:10.1103/PhysRevLett.91.191601.
[140] A. Armoni, M. Shifman, G. Veneziano, From super-Yang-Mills theory to QCD: Planar equivalence and its implications, in: From fields to strings: Circumnavigating theoretical physics. Ian Kogan memorial collection, World Scientific, 2005, p. 353. arXiv:hep-th/0403071, doi:10.1142/9789812775344_0013.
[141] A. Cherman, T. D. Cohen, The Skyrmion strikes back: Baryons and a new large N_c limit, JHEP 12 (2006) 035. arXiv:hep-th/0607028, doi:10.1088/1126-6708/2006/12/035.
[142] S. Coleman, Aspects of Symmetry, Chap. 8, Cambridge University Press, Cambridge, U.K., 1985. doi:10.1017/CBO9780511565045.
[143] A. A. Migdal, Loop equations and 1/N expansion, Phys. Rep. 102 (1983) 199. doi:10.1016/0370-1573(83)90076-5.
[144] A. V. Manohar, Large N QCD, in: Les Houches Summer School in Theoretical Physics, Session 68: Probing the Standard Model of Particle Interactions, 1998, p. 1091. arXiv:hep-ph/9802419.
[145] R. F. Lebed, Phenomenology of large N_c QCD, Czech. J. Phys. 49 (1999) 1273. arXiv:nucl-th/9810080, doi:10.1023/A:1022820227262.
[146] Y. Makeenko, Large-N gauge theories, NATO Sci. Ser. C 556 (2000) 285. arXiv:hep-th/0001047, doi:10.1007/978-94-011-4303-5-7.
[147] E. Jenkins, Large-N_c QCD, PoS EFT09 (2009) 044. arXiv:0905.1061, doi:10.22323/1.069.0044.
[148] B. Lucini, M. Panero, SU(N) gauge theories at large N, Phys. Rep. 526 (2013) 93. arXiv:1210.4997, doi:10.1016/j.physrep.2013.01.001.
[149] B. Lucini, M. Panero, Introductory lectures to large-N QCD phenomenology and lattice results, Prog. Part. Nucl. Phys. 75 (2014) 1. arXiv:1309.3638, doi:10.1016/j.ppnp.2014.01.001.
[150] P. Hernández, F. Romero-López, The large N_c limit of QCD on the lattice, Eur. Phys. J. A 57 (2021) 52. arXiv:2012.03331, doi:10.1140/epja/s10050-021-00374-2.
[151] G. 't Hooft, How instantons solve the U(1) problem, Phys. Rep. 142 (1986) 357. doi:10.1016/0370-1573(86)90117-1.
[152] M. Knecht, E. de Rafael, Patterns of spontaneous chiral symmetry breaking in the large-N_c limit of QCD-like theories, Phys. Lett. B 424 (1998) 335. arXiv:hep-ph/9712457, doi:10.1016/S0370-2693(98)00223-8.
[153] S. Peris, M. Perrottet, E. de Rafael, Matching long and short distances in large-N_c QCD, JHEP 05 (1998) 011. arXiv:hep-ph/9805442, doi:10.1088/1126-6708/1998/05/011.
[154] M. Knecht, S. Peris, M. Perrottet, E. de Rafael, Decay of pseudoscalars into lepton pairs and large-N_c QCD, Phys. Rev. Lett. 83 (1999) 5230. arXiv:hep-ph/9908283, doi:10.1103/PhysRevLett.83.5230.
[155] V. Cirigliano, G. Ecker, H. Neufeld, A. Pich, Meson resonances, large N_c and chiral symmetry, JHEP 06 (2003) 012. arXiv:hep-ph/0305311, doi:10.1088/1126-6708/2003/06/012.
[156] A. Pich, I. Rosell, J. J. Sanz-Cillero, Form-factors and current correlators: Chiral couplings $L_{10}^r(\mu)$ and $C_{87}^r(\mu)$ at NLO in $1/N_c$, JHEP 07 (2008) 014. arXiv:0803.1567, doi:10.1088/1126-6708/2008/07/014.
[157] I. Rosell, P. Ruiz-Femenía, J. J. Sanz-Cillero, Resonance saturation of the chiral couplings at NLO in $1/N_c$, Phys. Rev. D 79 (2009) 076009. arXiv:0903.2440, doi:10.1103/PhysRevD.79.076009.
[158] G. S. Bali, F. Bursa, L. Castagnini, S. Collins, L. Del Debbio, B. Lucini, M. Panero, Mesons in large-N QCD, JHEP 06 (2013) 071. arXiv:1304.4437, doi:10.1007/JHEP06(2013)071.
[159] G. 't Hooft, Magnetic monopoles in unified gauge theories, Nucl. Phys. B 79 (1974) 276. doi:10.1016/0550-3213(74)90486-6.
[160] A. M. Polyakov, Particle spectrum in the quantum field theory, JETP Lett. 20 (1974) 194.
[161] A. M. Polyakov, Isometric states of quantum fields, JETP 41 (1976) 988.
[162] L. Faddeev, V. Korepin, Quantum theory of solitons, Phys. Rep. 42 (1978) 1. doi:10.1016/0370-1573(78)90058-3.
[163] R. Dashen, E. Jenkins, A. V. Manohar, The $1/N_c$ expansion for baryons, Phys. Rev. D 49 (1994) 4713, [Erratum: Phys. Rev. D 51 (1995) 2489]. arXiv:hep-ph/9310379, doi:10.1103/PhysRevD.51.2489.
[164] R. F. Dashen, E. Jenkins, A. V. Manohar, Spin-flavor structure of large-N_c baryons, Phys. Rev. D 51 (1995) 3697. arXiv:hep-ph/9411234, doi:10.1103/PhysRevD.51.3697.
[165] E. Jenkins, Baryon hyperfine mass splittings in large-N QCD, Phys. Lett. B 315 (1993) 441. arXiv:hep-ph/9307244, doi:10.1016/0370-2693(93)91638-4.
[166] R. Dashen, A. V. Manohar, Baryon–pion couplings from large-N_c QCD, Phys. Lett. B 315 (1993) 425. arXiv:hep-ph/9307241, doi:10.1016/0370-2693(93)91635-Z.
[167] D. B. Kaplan, A. V. Manohar, The nucleon–nucleon potential in the $1/N_c$ expansion, Phys. Rev. C 56 (1997) 76. arXiv:nucl-th/9612021, doi:10.1103/PhysRevC.56.76.
[168] D. Pirjol, T.-M. Yan, $1/N_c$ expansion for excited baryons, Phys. Rev. D 57 (1998) 1449. arXiv:hep-ph/9707485, doi:10.1103/PhysRevD.57.1449.
[169] D. Pirjol, T.-M. Yan, Excited baryons phenomenology from large-N_c QCD, Phys. Rev. D 57 (1998) 5434. arXiv:hep-ph/9711201, doi:10.1103/PhysRevD.57.5434.
[170] J. L. Goity, C. L. Schat, N. N. Scoccola, Negative parity 70-plet baryon masses in the $1/N_c$ expansion, Phys. Rev. D 66 (2002) 114014. arXiv:hep-ph/0209174, doi:10.1103/PhysRevD.66.114014.
[171] T. D. Cohen, N. Kumar, K. K. Ndousse, Baryons and baryonic matter in the large N_c and heavy quark limits, Phys. Rev. C 84 (2011) 015204. arXiv:1102.2197, doi:10.1103/PhysRevC.84.015204.
[172] T. D. Cohen, B. A. Gelman, Total nucleon-nucleon cross sections in large N_c QCD, Phys. Rev. C 85 (2012) 024001. arXiv:1111.4465, doi:10.1103/PhysRevC.85.024001.
[173] N. Matagne, F. Stancu, Baryon resonances in large N_c QCD, Rev. Mod. Phys. 87 (2015) 211. arXiv:1406.1791, doi:10.1103/RevModPhys.87.211.
[174] A. J. Buchmann, R. F. Lebed, Large N_c, constituent quarks, and N, Δ charge radii, Phys. Rev. D 62 (2000) 096005. arXiv:hep-ph/0003167,

doi:10.1103/PhysRevD.62.096005.
[175] J. Scherk, An introduction to the theory of dual models and strings, Rev. Mod. Phys. 47 (1975) 123. doi:10.1103/RevModPhys.47.123.
[176] M. B. Green, J. Schwarz, E. Witten, Superstring Theory. Vol. 1: Introduction, Cambridge Monographs on Mathematical Physics, Cambridge University Press, 1988.
[177] M. B. Green, J. Schwarz, E. Witten, Superstring Theory. Vol. 2: Loop Amplitudes, Anomalies and Phenomenology, Cambridge Monographs on Mathematical Physics, Cambridge University Press, 1988.
[178] J. Polchinski, String theory. Vol. 1: An Introduction to the Bosonic String, Cambridge Monographs on Mathematical Physics, Cambridge University Press, 2007. doi:10.1017/CBO9780511816079.
[179] J. Polchinski, String theory. Vol. 2: Superstring Theory and Beyond, Cambridge Monographs on Mathematical Physics, Cambridge University Press, 2007. doi:10.1017/CBO9780511618123.
[180] M. Lüscher, Symmetry breaking aspects of the roughening transition in gauge theories, Nucl. Phys. B 180 (1981) 317. doi:10.1016/0550-3213(81)90423-5.
[181] J. Polchinski, A. Strominger, Effective string theory, Phys. Rev. Lett. 67 (1991) 1681. doi:10.1103/PhysRevLett.67.1681.
[182] Y. Makeenko, QCD string as an effective string, in: Low dimensional physics and gauge principles, 2011. arXiv:1206.0922, doi:10.1142/9789814440349_0018.
[183] J. Polchinski, Dirichlet branes and Ramond-Ramond charges, Phys. Rev. Lett. 75 (1995) 4724. arXiv:hep-th/9510017, doi:10.1103/PhysRevLett.75.4724.
[184] G. 't Hooft, Dimensional reduction in quantum gravity, Conf. Proc. C 930308 (1993) 284. arXiv:gr-qc/9310026.
[185] C. B. Thorn, Reformulating string theory with the $1/N$ expansion, in: The First International A. D. Sakharov Conference on Physics, Vol. 1, 1991, p. 447. arXiv:hep-th/9405069.
[186] L. Susskind, The world as a hologram, J. Math. Phys. 36 (1995) 6377. arXiv:hep-th/9409089, doi:10.1063/1.531249.
[187] J. D. Brown, M. Henneaux, Central charges in the canonical realization of asymptotic symmetries: An example from three-dimensional gravity, Commun. Math. Phys. 104 (1986) 207. doi:10.1007/BF01211590.
[188] A. Karch, E. Katz, D. T. Son, M. A. Stephanov, Linear confinement and AdS/QCD, Phys. Rev. D 74 (2006) 015005. arXiv:hep-ph/0602229, doi:10.1103/PhysRevD.74.015005.
[189] O. Andreev, V. I. Zakharov, Heavy-quark potentials and AdS/QCD, Phys. Rev. D 74 (2006) 025023. arXiv:hep-ph/0604204, doi:10.1103/PhysRevD.74.025023.
[190] J. Erdmenger, N. Evans, I. Kirsch, E. Threlfall, Mesons in gauge/gravity duals – A review, Eur. Phys. J. A 35 (2008) 81. arXiv:0711.4467, doi:10.1140/epja/i2007-10540-1.
[191] S. J. Brodsky, G. F. de Téramond, AdS/CFT and light-front QCD, Subnucl. Ser. 45 (2009) 139. arXiv:0802.0514, doi:10.1142/9789814293242_0008.
[192] W. de Paula, T. Frederico, H. Forkel, M. Beyer, Dynamical AdS/QCD with area-law confinement and linear Regge trajectories, Phys. Rev. D 79 (2009) 075019. arXiv:0806.3830, doi:10.1103/PhysRevD.79.075019.
[193] P. Colangelo, F. De Fazio, F. Giannuzzi, F. Jugeau, S. Nicotri, Light scalar mesons in the soft-wall model of AdS/QCD, Phys. Rev. D 78 (2008) 055009. arXiv:0807.1054, doi:10.1103/PhysRevD.78.055009.
[194] H. Georgi, Lie algebras in particle physics. From isospin to unified theories, Vol. 54 of Frontiers in Physics, Lecture Note Series, Addison-Wesley, Redwood City, 1982.
[195] S. Weinberg, Tetraquark mesons in large-N quantum chromodynamics, Phys. Rev. Lett. 110 (2013) 261601. arXiv:1303.0342, doi:10.1103/PhysRevLett.110.261601.
[196] T. Cohen, F. J. Llanes-Estrada, J. R. Peláez, J. Ruiz de Elvira, Non-ordinary light meson couplings and the $1/N_c$ expansion, Phys. Rev. D 90 (2014) 036003. arXiv:1405.4831, doi:10.1103/PhysRevD.90.036003.
[197] L. Maiani, V. Riquer, W. Wang, Tetraquarks, pentaquarks and dibaryons in the large N QCD, Eur. Phys. J. C 78 (2018) 1011. arXiv:1810.07848, doi:10.1140/epjc/s10052-018-6486-5.
[198] S. Mandelstam, Quantum electrodynamics without potentials, Annals Phys. 19 (1962) 1. doi:10.1016/0003-4916(62)90232-4.
[199] I. Bialynicki-Birula, Gauge invariant variables in the Yang-Mills theory, Bull. Acad. Polon. Sci., Sér. Sci. Math., Astr. et Phys. 11 (1963) 135.
[200] S. Mandelstam, Feynman rules for electromagnetic and Yang-Mills fields from the gauge-independent field-theoretic formalism, Phys. Rev. 175 (1968) 1580. doi:10.1103/PhysRev.175.1580.
[201] Y. Nambu, QCD and the string model, Phys. Lett. B 80 (1979) 372. doi:10.1016/0370-2693(79)91193-6.
[202] E. Corrigan, B. Hasslacher, A functional equation for exponential loop integrals in gauge theories, Phys. Lett. B 81 (1979) 181. doi:10.1016/0370-2693(79)90518-5.
[203] Yu. M. Makeenko, A. A. Migdal, Self-consistent area law in QCD, Phys. Lett. B 97 (1980) 253. doi:10.1016/0370-2693(80)90595-X.
[204] F. Jugeau, H. Sazdjian, Bound state equation in the Wilson loop approach with minimal surfaces, Nucl. Phys. B 670 (2003) 221. arXiv:hep-ph/0305021, doi:10.1016/j.nuclphysb.2003.07.018.
[205] G. C. Rossi, G. Veneziano, A possible description of baryon dynamics in dual and gauge theories, Nucl. Phys. B 123 (1977) 507. doi:10.1016/0550-3213(77)90178-X.
[206] G. C. Rossi, G. Veneziano, The string-junction picture of multiquark states: an update, JHEP 06 (2016) 041. arXiv:1603.05830, doi:10.1007/JHEP06(2016)041.
[207] T. D. Cohen, R. F. Lebed, Are there tetraquarks at large N_c in QCD(F)?, Phys. Rev. D 90 (2014) 016001. arXiv:1403.8090, doi:10.1103/PhysRevD.90.016001.
[208] W. Lucha, D. Melikhov, H. Sazdjian, Tetraquark and two-meson states at large N_c, Eur. Phys. J. C 77 (2017) 866. arXiv:1710.08316, doi:10.1140/epjc/s10052-017-5437-x.
[209] M. Knecht, S. Peris, Narrow tetraquarks at large N, Phys. Rev. D 88 (2013) 036016. arXiv:1307.1273, doi:10.1103/PhysRevD.88.036016.
[210] L. Maiani, A. D. Polosa, V. Riquer, Tetraquarks in the 1/N expansion and meson-meson resonances, JHEP 1606 (2016) 160. arXiv:1605.04839, doi:10.1007/JHEP06(2016)160.

[211] L. Maiani, A. D. Polosa, V. Riquer, Tetraquarks in the $1/N$ expansion: a new appraisal, Phys. Rev. D 98 (2018) 054023. arXiv:1803.06883, doi:10.1103/PhysRevD.98.054023.
[212] W. Lucha, D. Melikhov, H. Sazdjian, Narrow exotic tetraquark mesons in large-N_c QCD, Phys. Rev. D 96 (2017) 014022. arXiv:1706.06003, doi:10.1103/PhysRevD.96.014022.
[213] W. Lucha, D. Melikhov, H. Sazdjian, Are there narrow flavor-exotic tetraquarks in large-N_c QCD?, Phys. Rev. D 98 (2018) 094011. arXiv:1810.09986, doi:10.1103/PhysRevD.98.094011.
[214] W. Lucha, D. Melikhov, H. Sazdjian, OPE and quark-hadron duality for two-point functions of tetraquark currents in the $1/N_c$ expansion, Phys. Rev. D 103 (2021) 014012. arXiv:2012.03894, doi:10.1103/PhysRevD.103.014012.
[215] S. J. Brodsky, D. S. Hwang, R. F. Lebed, Dynamical picture for the formation and decay of the exotic XYZ mesons, Phys. Rev. Lett. 113 (2014) 112001. arXiv:1406.7281, doi:10.1103/PhysRevLett.113.112001.
[216] L. Maiani, A. D. Polosa, V. Riquer, A theory of X and Z multiquark resonances, Phys. Lett. B 778 (2018) 247. arXiv:1712.05296, doi:10.1016/j.physletb.2018.01.039.
[217] S. Dubynskiy, M. B. Voloshin, Hadro-charmonium, Phys. Lett. B 666 (2008) 344. arXiv:0803.2224, doi:10.1016/j.physletb.2008.07.086.
[218] M. B. Voloshin, Charmonium, Prog. Part. Nucl. Phys. 61 (2008) 455. arXiv:0711.4556, doi:10.1016/j.ppnp.2008.02.001.
[219] M. B. Voloshin, $Z_c(4100)$ and $Z_c(4200)$ as hadrocharmonium, Phys. Rev. D 98 (2018) 094028. arXiv:1810.08146, doi:10.1103/PhysRevD.98.094028.
[220] W. Heupel, G. Eichmann, C. S. Fischer, Tetraquark bound states in a Bethe-Salpeter approach, Phys. Lett. B 718 (2012) 545. arXiv:1206.5129, doi:10.1016/j.physletb.2012.11.009.
[221] G. Eichmann, C. S. Fischer, W. Heupel, The light scalar mesons as tetraquarks, Phys. Lett. B 753 (2016) 282. arXiv:1508.07178, doi:10.1016/j.physletb.2015.12.036.
[222] P. C. Wallbott, G. Eichmann, C. S. Fischer, $X(3872)$ as a four-quark state in a Dyson-Schwinger/Bethe-Salpeter approach, Phys. Rev. D 100 (2019) 014033. arXiv:1905.02615, doi:10.1103/PhysRevD.100.014033.
[223] G. Eichmann, C. S. Fischer, W. Heupel, N. Santowsky, P. C. Wallbott, Four-quark states from functional methods, Few Body Syst. 61 (2020) 38. arXiv:2008.10240, doi:10.1007/s00601-020-01571-3.
[224] T. Barnes, E. Swanson, A diagrammatic approach to meson-meson scattering in the nonrelativistic quark potential model, Phys. Rev. D 46 (1992) 131. doi:10.1103/PhysRevD.46.131.
[225] F. E. Close, P. R. Page, The $D^{*0}\overline{D}^{0}$ threshold resonance, Phys. Lett. B 578 (2004) 119. arXiv:hep-ph/0309253, doi:10.1016/j.physletb.2003.10.032.
[226] C.-Y. Wong, Molecular states of heavy quark mesons, Phys. Rev. C 69 (2004) 055202. arXiv:hep-ph/0311088, doi:10.1103/PhysRevC.69.055202.
[227] E. S. Swanson, Short range structure in the X(3872), Phys. Lett. B 588 (2004) 189. arXiv:hep-ph/0311229, doi:10.1016/j.physletb.2004.03.033.
[228] C. Amsler, N. A. Törnqvist, Mesons beyond the naive quark model, Phys. Rep. 389 (2004) 61. doi:10.1016/j.physrep.2003.09.003.
[229] N. A. Törnqvist, Isospin breaking of the narrow charmonium state of Belle at 3872 MeV as a deuson, Phys. Lett. B 590 (2004) 209. arXiv:hep-ph/0402237, doi:10.1016/j.physletb.2004.03.077.
[230] M. T. AlFiky, F. Gabbiani, A. A. Petrov, X(3872): Hadronic molecules in effective field theory, Phys. Lett. B 640 (2006) 238. arXiv:hep-ph/0506141, doi:10.1016/j.physletb.2006.07.069.
[231] S. Fleming, M. Kusunoki, T. Mehen, U. van Kolck, Pion interactions in the $X(3872)$, Phys. Rev. D 76 (2007) 034006. arXiv:hep-ph/0703168, doi:10.1103/PhysRevD.76.034006.
[232] Y. Dong, A. Faessler, T. Gutsche, S. Kovalenko, V. E. Lyubovitskij, X(3872) as a hadronic molecule and its decays to charmonium states and pions, Phys. Rev. D 79 (2009) 094013. arXiv:0903.5416, doi:10.1103/PhysRevD.79.094013.
[233] T. Gutsche, T. Branz, A. Faessler, I. W. Lee, V. E. Lyubovitskij, Hadron molecules, Chin. Phys. C 34 (2010) 1185. arXiv:1001.1870, doi:10.1088/1674-1137/34/9/007.
[234] R. Molina, T. Branz, E. Oset, A new interpretation for the $D^*_{s2}(2573)$ and the prediction of novel exotic charmed mesons, Phys. Rev. D 82 (2010) 014010. arXiv:1005.0335, doi:10.1103/PhysRevD.82.014010.
[235] F. Aceti, R. Molina, E. Oset, The $X(3872) \to J/\psi\gamma$ decay in the $D\bar{D}^*$ molecular picture, Phys. Rev. D 86 (2012) 113007. arXiv:1207.2832, doi:10.1103/PhysRevD.86.113007.
[236] M. Pavon Valderrama, Power counting and perturbative one pion exchange in heavy meson molecules, Phys. Rev. D 85 (2012) 114037. arXiv:1204.2400, doi:10.1103/PhysRevD.85.114037.
[237] M. Karliner, J. L. Rosner, Exotic resonances due to η exchange, Nucl. Phys. A 954 (2016) 365. arXiv:1601.00565, doi:10.1016/j.nuclphysa.2016.03.057.
[238] S. Sakai, L. Roca, E. Oset, Charm-beauty meson bound states from $B(B^*)D(D^*)$ and $B(B^*)\bar{D}(\bar{D}^*)$ interaction, Phys. Rev. D 96 (2017) 054023. arXiv:1704.02196, doi:10.1103/PhysRevD.96.054023.
[239] V. Baru, E. Epelbaum, J. Gegelia, C. Hanhart, U. G. Meissner, A. V. Nefediev, Remarks on the heavy-quark flavour symmetry for doubly heavy hadronic molecules, Eur. Phys. J. C 79 (2019) 46. arXiv:1810.06921, doi:10.1140/epjc/s10052-019-6560-7.
[240] Y. S. Kalashnikova, A. V. Nefediev, $X(3872)$ in the molecular model, Phys. Usp. 62 (2019) 568. arXiv:1811.01324, doi:10.3367/UFNe.2018.08.038411.
[241] M. Pavon Valderrama, Heavy hadron molecules in effective field theory: the emergence of exotic nuclear landscapes, Eur. Phys. J. A 56 (2020) 109. arXiv:1906.06491, doi:10.1140/epja/s10050-020-00099-8.
[242] J. Habashi, S. Fleming, U. van Kolck, Nonrelativistic effective field theory with a resonance field (2020). arXiv:2012.14995.
[243] X.-K. Dong, F.-K. Guo, B.-S. Zou, A survey of heavy-antiheavy hadronic molecules, Progr. Phys. 41 (2021) 65. arXiv:2101.01021, doi:10.13725/j.cnki.pip.2021.02.001.
[244] H.-X. Chen, Hadronic molecules in B decays (2021). arXiv:2103.08586.
[245] M. E. Luke, A. V. Manohar, Bound states and power counting in effective field theories, Phys. Rev. D 55 (1997) 4129. arXiv:hep-ph/9610534, doi:10.1103/PhysRevD.55.4129.

[246] R. Jackiw, Delta-function potentials in two- and three-dimensional quantum mechanics, in: M. A. B. Bég Memorial Volume, World Scientific, Singapore, 1991, p. 25.
[247] X.-K. Dong, F.-K. Guo, B.-S. Zou, Explaining the many threshold structures in the heavy-quark hadron spectrum, Phys. Rev. Lett. 126 (2021) 152001. arXiv:2011.14517, doi:10.1103/PhysRevLett.126.152001.
[248] S. Weinberg, Elementary particle theory of composite particles, Phys. Rev. 130 (1963) 776. doi:10.1103/PhysRev.130.776.
[249] V. G. J. Stoks, P. C. van Campen, W. Spit, J. J. de Swart, Determination of the residue at the deuteron pole in an np phase-shift analysis, Phys. Rev. Lett. 60 (1988) 1932. doi:10.1103/PhysRevLett.60.1932.
[250] V. Baru, J. Haidenbauer, C. Hanhart, Y. Kalashnikova, A. E. Kudryavtsev, Evidence that the $a_0(980)$ and $f_0(980)$ are not elementary particles, Phys. Lett. B 586 (2004) 53. arXiv:hep-ph/0308129, doi:10.1016/j.physletb.2004.01.088.
[251] M. Cleven, F.-K. Guo, C. Hanhart, U.-G. Meissner, Bound state nature of the exotic Z_b states, Eur. Phys. J. A 47 (2011) 120. arXiv:1107.0254, doi:10.1140/epja/i2011-11120-6.
[252] C. Hanhart, Y. S. Kalashnikova, A. V. Nefediev, Interplay of quark and meson degrees of freedom in a near-threshold resonance: multichannel case, Eur. Phys. J. A 47 (2011) 101. arXiv:1106.1185, doi:10.1140/epja/i2011-11101-9.
[253] T. Hyodo, D. Jido, A. Hosaka, Compositeness of dynamically generated states in a chiral unitary approach, Phys. Rev. C 85 (2012) 015201. arXiv:1108.5524, doi:10.1103/PhysRevC.85.015201.
[254] T. Sekihara, T. Hyodo, D. Jido, Comprehensive analysis of the wave function of a hadronic resonance and its compositeness, PTEP 2015 (2015) 063D04. arXiv:1411.2308, doi:10.1093/ptep/ptv081.
[255] Z.-H. Guo, J. A. Oller, Probabilistic interpretation of compositeness relation for resonances, Phys. Rev. D 93 (2016) 096001. arXiv:1508.06400, doi:10.1103/PhysRevD.93.096001.
[256] U.-G. Meissner, J. A. Oller, Testing the $\chi_{c1}\,p$ composite nature of the $P_c(4450)$, Phys. Lett. B 751 (2015) 59. arXiv:1507.07478, doi:10.1016/j.physletb.2015.10.015.
[257] Z.-H. Guo, J. A. Oller, A unified description of the hidden-charm tetraquark states $Z_{cs}(3985)$, $Z_c(3900)$ and $X(4020)$ (2020). arXiv:2012.11904.
[258] J. A. Oller, New results from a number operator interpretation of the compositeness of bound and resonant states, Annals Phys. 396 (2018) 429. arXiv:1710.00991, doi:10.1016/j.aop.2018.07.023.
[259] G. Colangelo, J. Gasser, H. Leutwyler, $\pi\pi$ scattering, Nucl. Phys. B 603 (2001) 125. arXiv:hep-ph/0103088, doi:10.1016/S0550-3213(01)00147-X.
[260] B. Ananthanarayan, G. Colangelo, J. Gasser, H. Leutwyler, Roy equation analysis of $\pi\pi$ scattering, Phys. Rep. 353 (2001) 207. arXiv:hep-ph/0005297, doi:10.1016/S0370-1573(01)00009-6.
[261] I. Caprini, G. Colangelo, H. Leutwyler, Mass and width of the lowest resonance in QCD, Phys. Rev. Lett. 96 (2006) 132001. arXiv:hep-ph/0512364, doi:10.1103/PhysRevLett.96.132001.
[262] G. Mennessier, S. Narison, X. G. Wang, The σ and $f_0(980)$ from $Ke4 \bigoplus \pi\pi$ scatterings data, Phys. Lett. B 688 (2010) 59. arXiv:1002.1402, doi:10.1016/j.physletb.2010.03.031.
[263] R. Garcia-Martin, R. Kamiński, J. R. Peláez, J. Ruiz de Elvira, Precise determination of the $f_0(600)$ and $f_0(980)$ pole parameters from a dispersive data analysis, Phys. Rev. Lett. 107 (2011) 072001. arXiv:1107.1635, doi:10.1103/PhysRevLett.107.072001.
[264] B. Moussallam, Couplings of light $I = 0$ scalar mesons to simple operators in the complex plane, Eur. Phys. J. C 71 (2011) 1814. arXiv:1110.6074, doi:10.1140/epjc/s10052-011-1814-z.
[265] T. N. Truong, Chiral perturbation theory and final-state theorem, Phys. Rev. Lett. 61 (1988) 2526. doi:10.1103/PhysRevLett.61.2526.
[266] A. Dobado, M. J. Herrero, T. N. Truong, Unitarized chiral perturbation theory for elastic pion-pion scattering, Phys. Lett. B 235 (1990) 134. doi:10.1016/0370-2693(90)90109-J.
[267] A. Dobado, J. R. Peláez, The inverse amplitude method in chiral perturbation theory, Phys. Rev. D 56 (1997) 3057. arXiv:hep-ph/9604416, doi:10.1103/PhysRevD.56.3057.
[268] M. Boglione, M. R. Pennington, Chiral poles and zeros and the role of the left hand cut, Z. Phys. C 75 (1997) 113. arXiv:hep-ph/9607266, doi:10.1007/s002880050452.
[269] J. Nieves, E. Ruiz Arriola, Bethe–Salpeter approach for unitarized chiral perturbation theory, Nucl. Phys. A 679 (2000) 57. arXiv:hep-ph/9907469, doi:10.1016/S0375-9474(00)00321-3.
[270] J. R. Peláez, G. Rios, Nature of the $f_0(600)$ from its N_c dependence at two loops in unitarized chiral perturbation theory, Phys. Rev. Lett. 97 (2006) 242002. arXiv:hep-ph/0610397, doi:10.1103/PhysRevLett.97.242002.
[271] J. R. Peláez, From controversy to precision on the sigma meson: a review on the status of the non-ordinary $f_0(500)$ resonance, Phys. Rep. 658 (2016) 1. arXiv:1510.00653, doi:10.1016/j.physrep.2016.09.001.
[272] J. R. Peláez, A. Rodas, J. Ruiz de Elvira, Precision dispersive approaches versus unitarized chiral perturbation theory for the lightest scalar resonances $\sigma/f_0(500)$ and $\kappa/K_0^*(700)$ (2021). arXiv:2101.06506.
[273] J. A. Oller, E. Oset, Chiral symmetry amplitudes in the S wave isoscalar and isovector channels and the σ, $f_0(980)$, $a_0(980)$ scalar mesons, Nucl. Phys. A 620 (1997) 438, [Erratum: Nucl. Phys. A 652, 407 (1999)]. arXiv:hep-ph/9702314, doi:10.1016/S0375-9474(97)00160-7.
[274] J. A. Oller, E. Oset, J. Peláez, Nonperturbative approach to effective chiral Lagrangians and meson interactions, Phys. Rev. Lett. 80 (1998) 3452. arXiv:hep-ph/9803242, doi:10.1103/PhysRevLett.80.3452.
[275] J. A. Oller, Coupled-channel approach in hadron–hadron scattering, Prog. Part. Nucl. Phys. 110 (2020) 103728. arXiv:1909.00370, doi:10.1016/j.ppnp.2019.103728.
[276] J. A. Oller, Unitarization technics in hadron physics with historical remarks, Symmetry 12 (2020) 1114. arXiv:2005.14417, doi:10.3390/sym12071114.
[277] D.-L. Yao, L.-Y. Dai, H.-Q. Zheng, Z.-Y. Zhou, A review on partial-wave dynamics with chiral effective field theory and dispersion relation (2020). arXiv:2009.13495.
[278] Z. X. Sun, L. Y. Xiao, Z. Xiao, H. Q. Zheng, Model dependent analyses on the N_c dependence of the σ pole trajectory, Mod. Phys. Lett. A 22 (2007) 711. arXiv:hep-ph/0503195, doi:10.1142/S0217732307023304.
[279] J. Nieves, A. Pich, E. Ruiz Arriola, Large-N_c properties of the ρ and $f_0(600)$ mesons from unitary resonance chiral dynamics, Phys. Rev. D

84 (2011) 096002. arXiv:1107.3247, doi:10.1103/PhysRevD.84.096002.
[280] G. S. Bali, QCD forces and heavy quark bound states, Phys. Rep. 343 (2001) 1. arXiv:hep-ph/0001312, doi:10.1016/S0370-1573(00)00079-X.
[281] E. Eichten, F. Feinberg, Spin-dependent forces in QCD, Phys. Rev. D 23 (1981) 2724. doi:10.1103/PhysRevD.23.2724.
[282] H. G. Dosch, Multi-quark interactions in strong coupling expansion of lattice gauge theories, Phys. Rev. D 28 (1983) 412. doi:10.1103/PhysRevD.28.412.
[283] C. Alexandrou, G. Koutsou, The static tetraquark and pentaquark potentials, Phys. Rev. D 71 (2005) 014504. arXiv:hep-lat/0407005, doi:10.1103/PhysRevD.71.014504.
[284] F. Okiharu, H. Suganuma, T. T. Takahashi, First study for the pentaquark potential in SU(3) lattice QCD, Phys. Rev. Lett. 94 (2005) 192001. arXiv:hep-lat/0407001, doi:10.1103/PhysRevLett.94.192001.
[285] F. Okiharu, H. Suganuma, T. T. Takahashi, Detailed analysis of the tetraquark potential and flip-flop in SU(3) lattice QCD, Phys. Rev. D 72 (2005) 014505. arXiv:hep-lat/0412012, doi:10.1103/PhysRevD.72.014505.
[286] H. Suganuma, T. Iritani, F. Okiharu, T. T. Takahashi, A. Yamamoto, Lattice QCD study for confinement in hadrons, AIP Conf. Proc. 1388 (2011) 195. arXiv:1103.4015, doi:10.1063/1.3647373.
[287] N. Cardoso, M. Cardoso, P. Bicudo, Colour fields computed in SU(3) lattice QCD for the static tetraquark system, Phys. Rev. D 84 (2011) 054508. arXiv:1107.1355, doi:10.1103/PhysRevD.84.054508.
[288] H. Miyazawa, Reconnection of strings and quark matter, Phys. Rev. D 20 (1979) 2953. doi:10.1103/PhysRevD.20.2953.
[289] F. Lenz, J. T. Londergan, E. J. Moniz, R. Rosenfelder, M. Stingl, K. Yazaki, Quark confinement and hadronic interactions, Annals Phys. 170 (1986) 65. doi:10.1016/0003-4916(86)90088-6.
[290] M. Oka, Hadron-hadron interaction in a string-flip model of quark confinement. I. Meson-meson interaction, Phys. Rev. D 31 (1985) 2274. doi:10.1103/PhysRevD.31.2274.
[291] M. Oka, C. Horowitz, Hadron-hadron interaction in a string-flip model of quark confinement. II. Nucleon-nucleon interaction, Phys. Rev. D 31 (1985) 2773. doi:10.1103/PhysRevD.31.2773.
[292] J. Carlson, V. R. Pandharipande, Absence of exotic hadrons in flux tube-quark models, Phys. Rev. D 43 (1991) 1652. doi:10.1103/PhysRevD.43.1652.
[293] G. Martens, C. Greiner, S. Leupold, U. Mosel, Interactions of multi-quark states in the chromodielectric model, Phys. Rev. D 73 (2006) 096004. arXiv:hep-ph/0603100, doi:10.1103/PhysRevD.73.096004.
[294] J. Vijande, A. Valcarce, J.-M. Richard, Stability of multiquarks in a simple string model, Phys. Rev. D 76 (2007) 114013. arXiv:0707.3996, doi:10.1103/PhysRevD.76.114013.
[295] J.-M. Richard, Stability of the pentaquark in a naive string model, Phys. Rev. C 81 (2010) 015205. arXiv:0908.2944, doi:10.1103/PhysRevC.81.015205.
[296] C. Ay, J.-M. Richard, J. H. Rubinstein, Stability of asymmetric tetraquarks in the minimal-path linear potential, Phys. Lett. B 674 (2009) 227. arXiv:0901.3022, doi:10.1016/j.physletb.2009.03.018.
[297] J. Vijande, A. Valcarce, J.-M. Richard, Stability of hexaquarks in the string limit of confinement, Phys. Rev. D 85 (2012) 014019. arXiv:1111.5921, doi:10.1103/PhysRevD.85.014019.
[298] P. Bicudo, M. Cardoso, Decays of tetraquark resonances in a two-variable approximation to the triple flip-flop potential, Phys. Rev. D 83 (2011) 094010. arXiv:1010.0281, doi:10.1103/PhysRevD.83.094010.
[299] P. Bicudo, M. Cardoso, Tetraquark bound states and resonances in a unitary microscopic quark model: A case study of bound states of two light quarks and two heavy antiquarks, Phys. Rev. D 94 (2016) 094032. arXiv:1509.04943, doi:10.1103/PhysRevD.94.094032.
[300] P. Bicudo, K. Cichy, A. Peters, M. Wagner, BB interactions with static bottom quarks from lattice QCD, Phys. Rev. D 93 (2016) 034501. arXiv:1510.03441, doi:10.1103/PhysRevD.93.034501.
[301] P. M. Fishbane, M. T. Grisaru, Consequences of a color-induced Van der Waals force between hadrons, Phys. Lett. B 74 (1978) 98. doi:10.1016/0370-2693(78)90069-2.
[302] T. Appelquist, W. Fischler, Some remarks on van der Waals forces in QCD, Phys. Lett. B 77 (1978) 405. doi:10.1016/0370-2693(78)90587-7.
[303] R. S. Willey, Quark van der Waals forces, Phys. Rev. D 18 (1978) 270. doi:10.1103/PhysRevD.18.270.
[304] S. Matsuyama, H. Miyazawa, Long range forces between hadrons, Prog. Theor. Phys. 61 (1979) 942. doi:10.1143/PTP.61.942.
[305] M. B. Gavela, A. Le Yaouanc, L. Oliver, O. Pène, J. C. Raynal, S. Sood, Van der Waals-like forces between hadrons induced by color confining potentials, Phys. Lett. B 82 (1979) 431. doi:10.1016/0370-2693(79)90260-0.
[306] A. V. Manohar, M. B. Wise, Exotic $QQ\overline{qq}$ states in QCD, Nucl. Phys. B 399 (1993) 17. arXiv:hep-ph/9212236, doi:10.1016/0550-3213(93)90614-U.
[307] M. Karliner, J. L. Rosner, Discovery of doubly-charmed Ξ_{cc} baryon implies a stable ($bb\bar{u}\bar{d}$) tetraquark, Phys. Rev. Lett. 119 (2017) 202001. arXiv:1707.07666, doi:10.1103/PhysRevLett.119.202001.
[308] E. J. Eichten, C. Quigg, Heavy-quark symmetry implies stable heavy tetraquark mesons $Q_iQ_j\bar{q}_k\bar{q}_l$, Phys. Rev. Lett. 119 (2017) 202002. arXiv:1707.09575, doi:10.1103/PhysRevLett.119.202002.
[309] C. Quigg, Stable tetraquarks, in: 53d Rencontres de Moriond on QCD and High Energy Interactions, 2018, p. 127. arXiv:1804.04929.
[310] J. C. Collins, J. A. M. Vermaseren, Axodraw version 2 (2016). arXiv:1606.01177.